The Utilization of Boron-doped Diamond Electrode for CO_2 Electrochemical Reduction: Exploring the Production of Value-added Chemicals

July 2019

JIWANTI, Prastika Krisma

Thesis for the Degree of Ph.D. in Science

The Utilization of Boron-doped Diamond Electrode for CO_2 Electrochemical Reduction: Exploring the Production of Value-added Chemicals

July 2019

Graduate School of Science and Technology
Keio University

JIWANTI, Prastika Krisma

Contents

Chapter 1 General Introduction

Chapter 2 Electrochemical reduction of CO_2 on boron-doped diamond electrodes in aqueous ammonia solution

Chapter 3 Electrochemical reduction of CO_2 on copper-modified boron-doped diamond electrodes

Chapter 4 Electrochemical reduction of CO_2 on palladium modified boron-doped diamond electrodes

Chapter 5 CO_2 electrochemical reduction on metal-oxide modified BDD electrode: Study on Ni and Ir based metal

1

Chapter

General Introduction

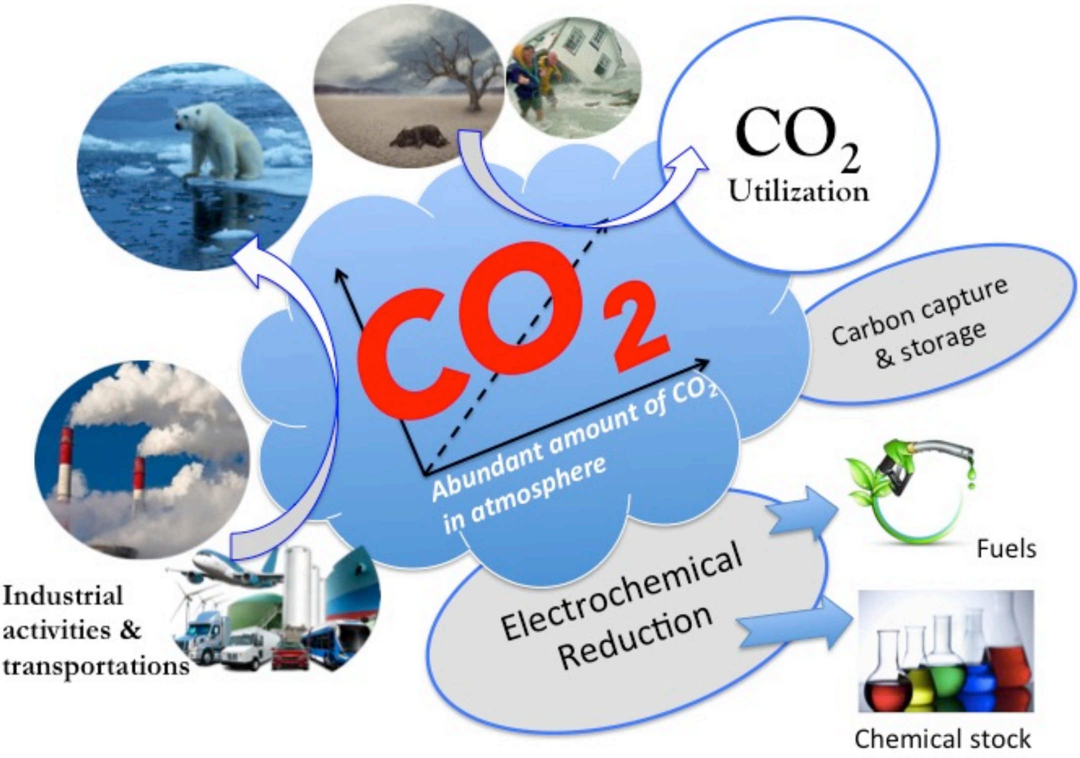

1. The status quo of global greenhouse effect and carbon cycle

The earth atmosphere contains of nitrogen (78.1%), oxygen (20.9%), argon (0.9%), and 0.43% small portion of greenhouse gases. These trace amount of gasses may cause the warming of the earth surface and atmosphere since they able to absorb infrared range wavelength, emitted by earth. In normal condition, it has the advantage to block the living organisms. However, one of the greenhouse gas, that is carbon dioxide (CO_2) has increased the concentration up to 38% (as of 2009) since preindustrial time, and therefore contributes the most of the greenhouse effect that could bring to the unwanted impact.

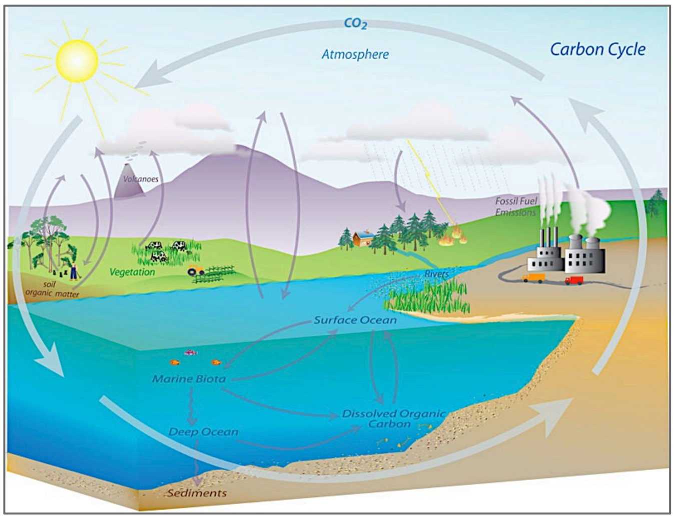

Figure 1. Carbon cycle [2]

CO_2 gas itself is involved in the process called carbon cycle [1], where the carbon moves between many different natural reservoirs, by photosynthesis, respiration, decomposition, etc. Since industrial revolution in the 1800s, human have been burning fossil fuels, and releasing the carbon as CO_2 gas to the atmosphere. On the other hand, the rate of fossil fuel formation and its rate of the human activities are not equal, furthermore even the biomass process also a climate impact [3]. Those are resulting in the large amount of CO_2 gas in the atmosphere and it still increases every year (Figure 2). Unfortunately, it goes beyond the environmental stability toward the dangerous effect. There have been numerous studies, measuring the CO_2 concentration in atmosphere [2-5], in order to estimate and prevent the worst effects.

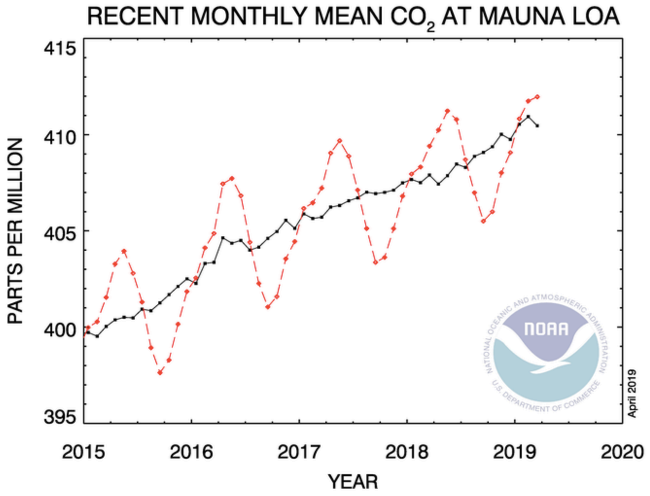

Figure 2. Recent global monthly CO_2 concentration [2]

2. The reduction of CO_2 emissions

Since then, many attempts have been developed to reduce the CO_2 emissions from atmosphere. Many countries have been trying several ways, such as promoting energy conservation, using low carbon fuels, deploying renewable energy, and by carbon sequestration [6], such as carbon capture and storage (CCS) technology [7]. Among those ways, CCS can reduce up to 85-90% CO_2 emission from large point emission sources. On the other hand, despite of this promising way, CO_2 gas as a high abundant and cheap gas available in atmosphere is also very attractive to be utilized to improve the value and more broadly to support the environment protection issue. CO_2 conversion with the support of catalysts, through wet chemistry, electrochemistry, or the combination between renewable energy and electrochemistry method have been widely developed and reported in these decades.

2.1 Carbon capture and storage (CCS)

The CCS technology has been known as an amine scrubbing from the year of 1930,[8] in which CO_2 gas is separated from natural gas and hydrogen. The technology began in 1930 was the basic process where CO_2 is absorbed from the fuel gas or combustion gas near ambient temperature into amine solution that has a low volatility (Figure 3). Monoethanolamine (MEA), diglycolamine (DGA) [9], diisopropanolamine (DIPA) [10], methyldiethanolamine (MDEA) [11] and diethanolamine (DEA) [12] are the solutions that have been known as the absorber for CO_2 sequestration [13]. Among many alkanolamines solution, MEA solution is known as the most efficient one for CO_2 absorber with the efficiency over 90%. In addition, ammonia (NH_3) solution is also known as a strong absorber and high capacity for CO_2 scrubbing (3 times higher than MEA) [14]. Ammonia solution has also been known as a strong CO_2 absorber that does not have a degradation problem that used to be occurred in amine solution, and thus, this behavior may decrease the material cost. However, the regeneration of ammonia solution, in which, separating the ammonia and the CO_2 gas itself still require high energy consumption. Nevertheless, in this thesis, we researched and reported, an NH_3 aqueous solution as electrolyte for CO_2 electrochemical reduction, considering about its degradation difficulties, and thus, simplify the products analysis [15].

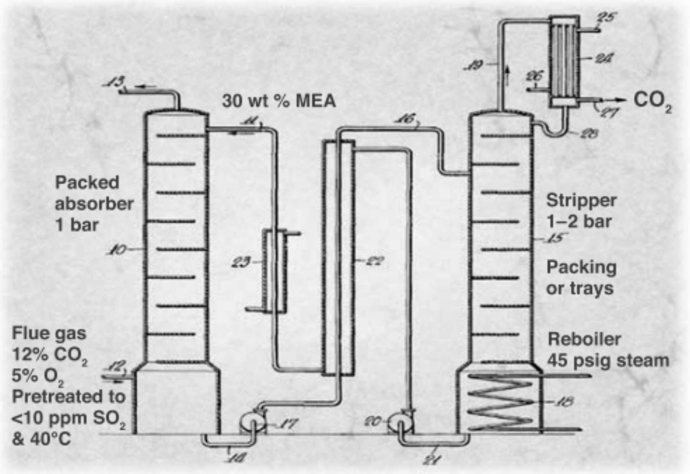

Figure 3. Process of amine scrubbing reported by Bottoms in 1930. Reprinted with permission from reference [8]. Copyright (2009) American Association for the Advancement of Science.

2.2 CO_2 conversion

On the other hand, other solutions have been proposed and researched to add the value of this cheap and abundant gas in atmosphere, by converting CO_2 gas to useful chemical stocks, or even more to convert it back to fuel, as what will this thesis describes about. Many methods have been reported in numerous articles, such as:

2.2.1 Chemical process

There have been many studies using chemical process, converting CO_2 to value-added chemicals by hydrogenation of CO_2 gas [16]. For example, a mixture of pure H_2 and CO_2 gas to produce hydrocarbon by using Fischer–Tropsch process [17,18]. In addition, the production of urea by combining ammonia and CO_2 gas, so called, Bosch–Meiser method, methane production through Sabatier reaction or other catalysis attempt [19,20]. Others are synthesis of dimethyl carbonate [21], polyurethane [22], methane [23], and many chemicals of ethers, esters, and acids. Those productions have been studied and developed in mass-production by using particular heterogeneous or homogeneous catalyst. In summary, chemical process has a greater potential and even some of the reactions have been applied in large scale. On the other hand, a reaction of so called Fischer–Tropsch process needs clean H_2 (which requires an expensive process), otherwise the by-products can be an obstacle. Beside that, the process is known to be exothermic, that might be lead to uncontrollable condition.

2.2.2 Bio-chemical process

The CO_2 conversion by utilizing the living organism is also promising. The used of photosynthetic and non-photosynthetic microorganisms have been utilized and some of the methods have been commercially available [24,25]. For example, a photosynthetic prokaryotic microorganism, *Synechocystis* sp. PCC 6803 has been used for the production of ethanol [26]. Bio-chemical process has a merit since it uses living organism, in conversely, maintaining the existence of organism is mandatory.

2.2.3 Electrochemical process

The method can be described as a CO_2 conversion using an external energy, that is, electricity, to drive a direct or indirect conversion of CO_2 to value-added chemicals. CO_2 electrochemical reduction requires a high overpotential reduction, for direct electron transfer to the CO_2 molecule (eqn. (1)):

$$CO_2 + e^- \rightarrow CO_2^{\bullet -} \qquad E_0 = -1.9\ \text{V}\ \textit{vs}.\ \text{NHE} \qquad (1)$$

The standard potential for CO_2 reduction to several compounds are listed as followed (Table 1) [27]:

Table 1. Standard potential for CO_2 reduction and hydrogen evolution reaction

Reaction	E^0 [V vs. (SHE)] at pH 7
$2H^{+}_{(aq)} + 2e^{-} \rightarrow H_{2(g)}$	−0.414
$CO_{2(g)} + e^{-} \rightarrow CO_2^{-}{}_{(aq)}$	−1.85
$CO_{2(g)} + H_2O_{(aq)} + 2e^{-} \rightarrow CO_{(g)} + 2OH^{-}{}_{(aq)}$	−0.52
$CO_{2(g)} + H_2O_{(aq)} + 2e^{-} \rightarrow HCOO^{-}{}_{(aq)} + OH^{-}$	−0.67
$CO_{2(g)} + 5H_2O_{(aq)} + 6e^{-} \rightarrow CH_3OH_{(l)} + 6OH^{-}{}_{(aq)}$	−0.40
$2CO_{2(g)} + 9H_2O_{(aq)} + 12e^{-} \rightarrow C_2H_5OH_{(l)} + 12OH^{-}{}_{(aq)}$	−0.33

The electrochemical process has advantage of its customizable behavior, in which, the selectivity of the products can be adjusted. Under mild condition, the process is moderate and controllable. Beside that, the electricity that is used for the process can be attained from the renewable energy. Apart from that, it has a demerit since CO_2 gas has low solubility in water, in which, water can be a proton source to convert CO_2 to more valuable compound. This lack somehow can be solved by the use or organic solvent.

Numerous results have been reported [28-31], regarding to the effort to generate products with the required-energy as minimum as possible. As in electrochemical technique, a suitable electrode is one of the most important parts for the optimum system. Many electrodes have been carried out whether on carbon-based electrode [32,27] or metal electrode [33]. Moreover, gas diffusion electrode is also one of the well-known systems to be used for CO_2 reduction (Figure 4). Meanwhile, Cu is one of the best-known metal to be used as an electrode, which is possible to convert CO_2 to hydrocarbon or oxygenated species [34-36]. Recently, a quite new study of CO_2 reduction on boron doped diamond BDD electrode as a carbon-based electrode has been reported, and several contributions on it will be described in this thesis.

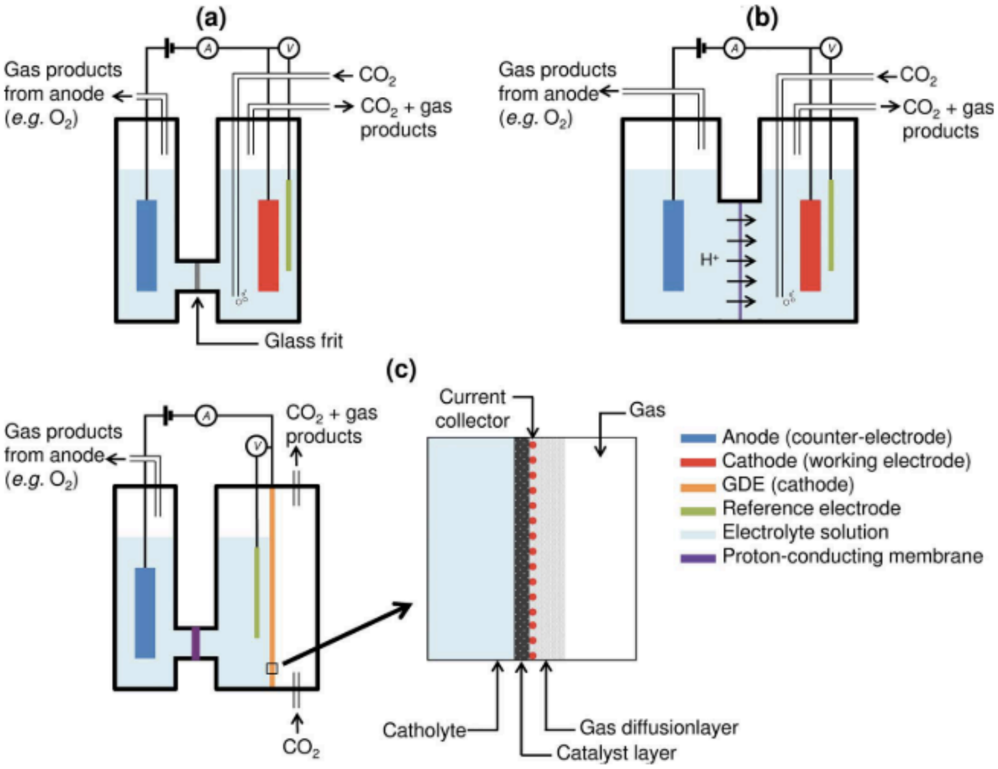

Figure 4. Gas diffusion electrode set up for the electrochemical reduction of CO_2. Reprinted with permission from reference [37]. Copyright (2013) The Royal Society of Chemistry

2.2.4 Photochemical process

A photochemical process for CO_2 conversion is a way to reduce CO_2 gas by the assistance of light or renewable solar energy. From the years of 1980s to 2013, the development of photochemical process for CO_2 electrochemical reduction was insignificantly improved. Most of the catalyst used in the process was also focusing on TiO_2 [37]. However, recently, the development using this process is growing and attracts much attention, as it is a step forward to build an artificial photosynthesis.

The method of photocatalytic process is divided into three categories, those are, photoreduction using molecular catalyst, using semiconducting photocathode, and using electrochemical reduction with photovoltaic devices [38]. The examples of the study on Photochemical CO_2 reduction are the use of p-GaP electrode in aqueous solution [39], a supramolecular photocatalyst using visible light [40], photoelectrochemical conversion using Ag loaded on BDD electrode [41], and many more. The photochemical process is lacking of low efficiency up to this moment and still need the improvement for several order of magnitude to be available for practical usability.

2.3 BDD electrode for CO_2 electrochemical reduction application

BDD electrode has been studied in many years since its beginning utilization on photoelectrochemistry by Russian scientist, Plescov, in the year 1987 that leads to other works around the world using diamond electrode. Since then, many works was done, numerous applications have been reported, for sensor and also synthesis applications [42-44]. Meanwhile, as has been mentioned above, a quite new study of CO_2 electrochemical reduction on BDD electrode has been reported. The wide potential window of BDD electrode that suggested being able for H_2 evolution suppressing, has attracted attention, since H_2 evolution mostly competes the CO_2 reduction itself (Figure 5). The study on bare BDD electrode in alkali metal cation based aqueous solution has been known to produce HCOOH with efficiency for more than 90% using circulation flow cell [45]. Since then, the detailed study on this, such as, the boron concentration [46], and also electrolyte effect [47,48] have been reported. Beside, methanol was produced as the ammonia solution was used as the electrolyte [15].

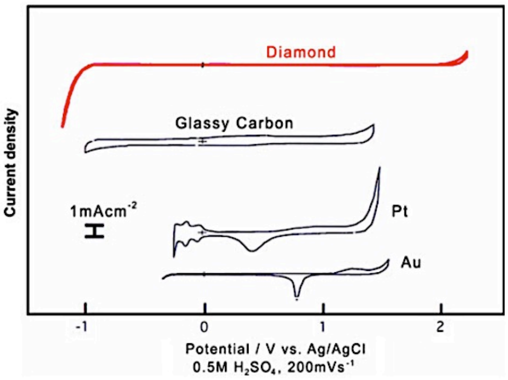

Figure 5. Potential window of Diamond electrode, compared to other electrodes. Reprinted with permission from reference [49]. Copyright (2010) Springer

Among those studies, only C_1 products have been successfully produced. However, none of the products were higher number of carbon atoms compounds. Moreover, high over potential still become a drawback. Thus, an attempt on metal deposition on BDD electrode has been proposed, whether to reduce the over potential or to produce compound with higher number of carbon atoms. Cu particles were deposited on surface of BDD electrode, and applied as the working electrode. The result shows that ethanol could be produced as high as 42%, at relatively low potential at -1.0 V [50]. Other studies were also reported on metal deposition on BDD electrode, including CO_2 reduction on Ag-BDD produced CO [41], on RuO_2-BDD produced HCOOH and methanol [51], and on CuSn-BDD produced CO [52]. The reported studies also show relatively lower potential compared to the bare BDD electrodes.

3. Outline of this thesis

This thesis will describe the study of CO_2 electrochemical reduction on bare BDD and modified-BDD electrode, specifically on the production of compound with higher number of carbon atoms and on the objective of suppressing the overall CO_2 reduction potential on BDD electrode.

The first part (chapter 2) is using bare BDD electrode, and utilizing aqueous ammonia solution as an electrolyte that has been known to have a strong CO_2 absorption. This topic is related and has direction to reduce stored-CO_2 in amine solution that is used in carbon capture and storage technology. However, as a start point, we use a simpler solution that is aqueous ammonia solution in order to simplify the product analysis, as amine solution is very easy to degrade. As the result, methanol could be produce as the main value-added product. The important of the ammonia solution and the attempt to improve the product efficiency will be discussed in this chapter.

The second part (chapter 3-5) is about the CO_2 reduction on surface of metal modified BDD electrode. This part is separated into several chapters since several experiments using different metals were tried. The production of higher number of carbon atoms compound and the attempt to decrease the CO_2 reduction overpotential are discussed. Finally, it was found that each metal particle deposited on surface of BDD has its own behavior for CO_2 reduction, and that, not all metal gives a catalytic effect toward CO_2 reduction.

4. References

[1] R. a Berner, The long-term carbon cycle, fossil fuels and atmospheric composition, Nature. 426 (2003) 323–326.

[2] NOAA, ESRL Global Monitoring Division - Global Greenhouse Gas Reference Network, (n.d.). Acces April 2019

[3] F. Cherubini, G.P. Peters, T. Berntsen, A.H. Strømman, E. Hertwich, CO_2 emissions from biomass combustion for bioenergy: Atmospheric decay and contribution to global warming, GCB Bioenergy. 3 (2011) 413–426.

[4] D.M. Etheddge, L.P. Steele, R.L. Langenfelds, R.J. Francey, Natural and anthropogenic changes in atmospheric CO_2 over the last 1000 years from air in Antarctic ice and firn, J. Geophys. Res. 101 (1996) 4115–4128.

[5] T.R. Anderson, E. Hawkins, P.D. Jones, CO_2, the greenhouse effect and global warming: from the pioneering work of Arrhenius and Callendar to today's Earth System Models, Endeavour. 40 (2016) 178–187.

[6] D.W. Keith, D.S. Angelo, D.W. Keith, G. Holmes, D.S. Angelo, K. Heidel, A Process for Capturing CO_2 from the Atmosphere A Process for Capturing CO_2 from the Atmosphere, Joule. 2 (2018) 1573–1594.

[7] D.Y.C. Leung, G. Caramanna, M.M. Maroto-Valer, An overview of current status of carbon dioxide capture and storage technologies, Renew. Sustain. Energy Rev. 39 (2014) 426–443.

[8] G.T. Rochelle, Amine Scrubbing for CO_2 Capture, Science. 325 (2009) 1652–1654.

[9] B. Dawoud, E. Amer, D. Gross, Comparison of MEA and DGA performance for CO2 capture under different operational conditions, Int. J. Energy Res. 36 (2012) 259–268.

[10] M.H. Jenab, M. Vahidi, M. Mehrabi, Solubility of carbon dioxide in aqueous mixtures of DIPA + MDEA and DIPA + PZ solutions, J. Chinese Chem. Soc. 53 (2006) 283–286.

[11] S. Santos, J. Gomes, J. Bordado, Scale-Up Effects of CO_2 Capture by Methyldiethanolamine (MDEA) Solutions in Terms of Loading Capacity, Technologies. 4 (2016) 19.

[12] B. Xue, Y. Yu, J. Chen, X. Luo, M. Wang, A comparative study of MEA and DEA for post-combustion CO_2 capture with different process configurations, Int. J. Coal

Sci. Technol. 4 (2017) 15–24.

[13] A. Veawab, A. Aroonwilas, P. Tontiwachwuthikul, CO_2 absorption performance of aqueous alkanolamines in packed columns, ACS Div. Fuel Chem. Prepr. 47 (2002) 49–50.

[14] F. Mani, M. Peruzzini, P. Stoppioni, CO_2 absorption by aqueous NH_3 solutions: speciation of ammonium carbamate, bicarbonate and carbonate by a 13C NMR study, Green Chem. 8 (2006) 995.

[15] P.K. Jiwanti, K. Natsui, K. Nakata, Y. Einaga, Selective production of methanol by the electrochemical reduction of CO_2 on boron-doped diamond electrodes in aqueous ammonia solution, RSC Adv. 6 (2016) 102214–102217.

[16] S. Saeidi, N.A.S. Amin, M.R. Rahimpour, Hydrogenation of CO_2 to value-added products - A review and potential future developments, J. CO_2 Util. 5 (2014) 66–81.

[17] M. Pérez-Fortes, J.C. Schöneberger, A. Boulamanti, E. Tzimas, Methanol synthesis using captured CO_2 as raw material: Techno-economic and environmental assessment, Appl. Energy. 161 (2016) 718–732.

[18] É.S. Van-Dal, C. Bouallou, Design and simulation of a methanol production plant from CO_2 hydrogenation, J. Clean. Prod. 57 (2013) 38–45.

[19] J.N. Park, E.W. McFarland, A highly dispersed Pd-Mg/SiO_2 catalyst active for methanation of CO_2, J. Catal. 266 (2009) 92–97.

[20] W. Wang, S. Wang, X. Ma, J. Gong, Recent advances in catalytic hydrogenation of carbon dioxide, Chem. Soc. Rev. 40 (2011) 3703–3727.

[21] P. Tundo, M. Selva, The chemistry of dimethyl carbonate, Acc. Chem. Res. 35 (2002) 706–716.

[22] N. Von Der Assen, A. Sternberg, A. Kätelhön, A. Bardow, Environmental potential of carbon dioxide utilization in the polyurethane supply chain, Faraday Discuss. 183 (2015) 291–307.

[23] S. Sahebdelfar, M. Takht Ravanchi, Carbon dioxide utilization for methane production: A thermodynamic analysis, J. Pet. Sci. Eng. 134 (2015) 14–22.

[24] H. Li, J.C. Liao, Biological conversion of carbon dioxide to photosynthetic fuels and electrofuels, Energy Environ. Sci. 6 (2013) 2892–2899.

[25] P.M. McTernan, H. Lian, R.M. Kelly, M.W. Adams, A.S. Hawkins, Biological conversion of carbon dioxide and hydrogen into liquid fuels and industrial chemicals, Curr. Opin. Biotechnol. 24 (2013) 376–384.

[26] J. Dexter, P. Fu, Metabolic engineering of cyanobacteria for ethanol production, Energy Environ. Sci. 2 (2009) 857–864.

[27] P.K. Jiwanti, K. Natsui, Y. Einaga, The Utilization of Boron-doped Diamond Electrodes for the Electrochemical Reduction of CO_2: Toward the Production Compounds with a High Number of Carbon Atoms, Electrochemistry. 2 (2019) 109–113.

[28] J.E. Pander, D. Ren, Y. Huang, N.W.X. Loo, S.H.L. Hong, B.S. Yeo, Understanding the Heterogeneous Electrocatalytic Reduction of Carbon Dioxide on Oxide-Derived Catalysts, ChemElectroChem. 5 (2018) 219–237.

[29] M. Gattrell, N. Gupta, A. Co, A review of the aqueous electrochemical reduction of CO_2 to hydrocarbons at copper, J. Electroanal. Chem. 594 (2006) 1–19.

[30] W. Zhang, Y. Hu, L. Ma, G. Zhu, Y. Wang, X. Xue, R. Chen, S. Yang, Z. Jin, Progress and Perspective of Electrocatalytic CO_2 Reduction for Renewable Carbonaceous Fuels and Chemicals, Adv. Sci. 5 (2018) 1700275.

[31] Q. Lu, F. Jiao, Electrochemical CO_2 reduction: Electrocatalyst, reaction mechanism, and process engineering, Nano Energy. 29 (2016) 439–456.

[32] N. Yang, S.R. Waldvogel, X. Jiang, Electrochemistry of Carbon Dioxide on Carbon Electrodes, ACS Appl. Mater. Interfaces. 8 (2016) 28357–28371.

[33] K.P. Kuhl, E.R. Cave, D.N. Abram, T.F. Jaramillo, New Insights into the Electrochemical Reduction of Carbon Dioxide on Metallic Copper Surfaces, Energy Environ. Sci. 5 (2012) 7050–7059.

[34] Y. Hori, H. Wakebe, T. Tsukamoto, O. Koga, Electrocatalytic process of CO selectivity in electrochemical reduction of CO_2 at metal electrodes in aqueous media, Electrochem. Commun. 39 (1994) 1833–1839.

[35] D. Kim, C.S. Kley, Y. Li, P. Yang, Copper nanoparticle ensembles for selective electroreduction of CO_2 to C_2–C_3 products, Proc. Natl. Acad. Sci. 114 (2017) 10560–10565.

[36] R. Kas, R. Kortlever, A. Milbrat, M.T.M. Koper, G. Mul, J. Baltrusaitis, Electrochemical CO_2 reduction on Cu_2O-derived copper nanoparticles: Controlling the catalytic selectivity of hydrocarbons, Phys. Chem. Chem. Phys. 16 (2014) 12194–12201.

[37] E. V. Kondratenko, G. Mul, J. Baltrusaitis, G.O. Larrazábal, J. Pérez-Ramírez, Status and perspectives of CO_2 conversion into fuels and chemicals by catalytic,

photocatalytic and electrocatalytic processes, Energy Environ. Sci. 6 (2013) 3112–3135.

[38] B. Kumar, M. Llorente, J. Froehlich, T. Dang, A. Sathrum, C.P. Kubiak, Photochemical and Photoelectrochemical Reduction of CO_2, Annu. Rev. Phys. Chem. 63 (2012) 541–569.

[39] H. Flaisher, R. Tenne, M. Halmann, Photoelectrochemical reduction of carbon dioxide in aqueous solutions on p-GaP electrodes: an a.c. impedance study with phase-sensitive detection Harvey, J. Electroanal. Chem. 402 (1996) 97–105.

[40] S. Sato, K. Koike, H. Inoue, O. Ishitani, Highly efficient supramolecular photocatalysts for CO_2 reduction using visible light, Photochem. Photobiol. Sci. 6 (2007) 454–461.

[41] N. Roy, Y. Hirano, H. Kuriyama, P. Sudhagar, N. Suzuki, K. Katsumata, K. Nakata, T. Kondo, M. Yuasa, I. Serizawa, T. Takayama, A. Kudo, A. Fujishima, C. Terashima, Boron-doped diamond semiconductor electrodes: Efficient photoelectrochemical CO_2 reduction through surface modification, Sci. Rep. 6 (2016) 38010.

[42] J. V. Macpherson, A practical guide to using boron doped diamond in electrochemical research, Phys. Chem. Chem. Phys. 17 (2015) 2935–2949.

[43] N. Yang, S. Yu, J. V. Macpherson, Y. Einaga, H. Zhao, G. Zhao, G.M. Swain, X. Jiang, Conductive diamond: synthesis, properties, and electrochemical applications, Chem. Soc. Rev. 48 (2019) 157–204.

[44] T.A. Ivandini, Y. Einaga, Polycrystalline boron-doped diamond electrodes for electrocatalytic and electrosynthetic applications, Chem. Commun. 53 (2017) 1338–1347.

[45] K. Natsui, H. Iwakawa, N. Ikemiya, K. Nakata, Y. Einaga, Stable and Highly Efficient Electrochemical Production of Formic Acid from Carbon Dioxide Using Diamond Electrodes, Angew. Chemie - Int. Ed. 57 (2018) 2639–2643.

[46] J. Xu, K. Natsui, S. Naoi, K. Nakata, Y. Einaga, Effect of doping level on the electrochemical reduction of CO_2 on boron-doped diamond electrodes, Diam. Relat. Mater. 86 (2018) 167–172.

[47] M. Tomisaki, K. Natsui, N. Ikemiya, K. Nakata, Y. Einaga, Influence of Electrolyte on the Electrochemical Reduction of Carbon Dioxide Using Boron-Doped Diamond Electrodes, ChemistrySelect. 3 (2018) 10209–10213.

[48] M. Tomisaki, S. Kasahara, K. Natsui, N. Ikemiya, Y. Einaga, Switchable Product Selectivity in the Electrochemical Reduction of Carbon Dioxide Using Boron-Doped Diamond Electrodes, J. Am. Chem. Soc. 114 (2019) 7414-7420.

[49] Y. Einaga, Diamond electrodes for electrochemical analysis, J. Appl. Electrochem. 40 (2010) 1807–1816.

[50] P.K. Jiwanti, K. Natsui, K. Nakata, Y. Einaga, The electrochemical production of C_2/C_3 species from carbon dioxide on copper-modified boron-doped diamond electrodes, Electrochim. Acta. 266 (2018) 414–419.

[51] N. Spataru, K. Tokuhiro, C. Terashima, T.N. Rao, A. Fujishima, Electrochemical reduction of carbon dioxide at ruthenium dioxide deposited on boron-doped diamond, J. Appl. Electrochem. 33 (2003) 1205–1210.

[52] N. Roy, N. Suzuki, Y. Nakabayashi, Y. Hirano, K. Katsumata, K. Nakata, A. Fujishima, C. Terashima, H. Ikari, Facile Deposition of Cu-SnOx Hybrid Nanostructures on the Lightly Boron-Doped Diamond Electrodes for CO_2 Reduction, ChemElectroChem. 5 (2018) 2542–2550.

2
Chapter

Electrochemical reduction of CO_2 on boron-doped diamond electrodes in aqueous ammonia solution

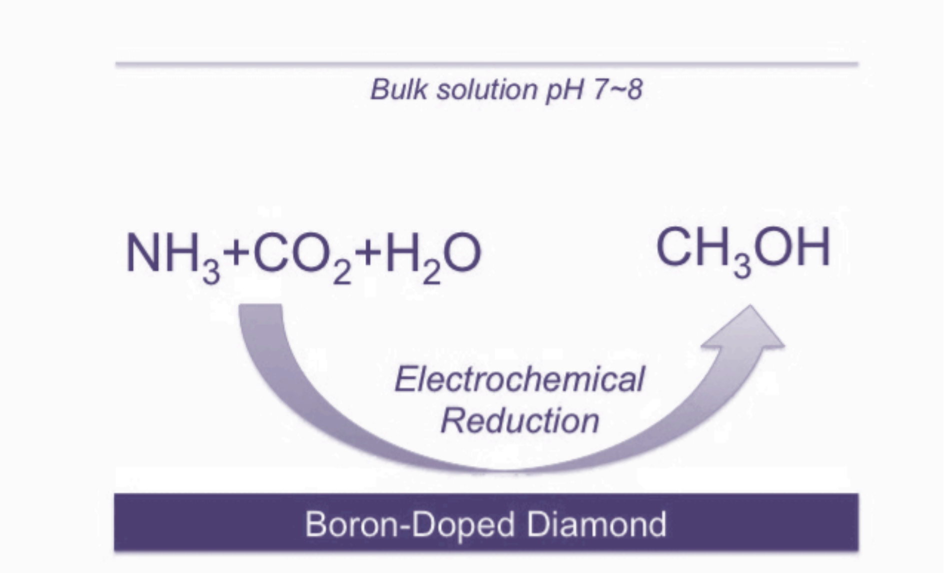

This chapter has been published as an article:
P. K. Jiwanti, K. Natsui, K. Nakata, and Y. Einaga, RSC. Adv. 18 (2016) 7075–7084

Abstract

In this work, the electrochemical reduction of CO_2 was investigated in an aqueous ammonia solution using boron-doped diamond electrodes. Methanol was mainly produced by the electrochemical reduction at a potential of −1.3 V (*vs.* Ag/AgCl) with a faradaic efficiency as high as 24.3%. Also, even in an aqueous ammonium bicarbonate solution (pH 7.9) without CO_2 bubbling, methanol was produced, meanwhile it was not observed at higher (10.6) and lower (3.38) pH. These observations suggest that the selectivity for methanol production in aqueous ammonia solution is due to the electrochemical reduction of bicarbonate ions, which are formed by the reaction between ammonia and CO_2. Moreover, this work presents the important role of ammonia as an electrolyte for the selective production of methanol by electrochemical reduction of CO_2.

1. Introduction

In this few decades, CO_2 electrochemical reduction has been known to attract high attention for many researchers. Many attempts have been made to possibly convert the CO_2 to fuels. Useful strategies, such as by using catalyst, has been reported in numerous publications [1-5]. Meanwhile, as it has been widely known, carbon dioxide capture and storage (CCS) technology is one of the promising technologies for reducing carbon emissions. Amine solutions, such as monoethanolamine (MEA) and diethanolamine (DEA), are used for CCS technology, since they are chemically strong CO_2 absorbers [6-8]. The absorbed CO_2, and thus, become attractive, due to its large quantity, that will be much beneficial to be converted into useful chemicals than to be forever stored. Among those absorbers, ammonia (NH_3) solution is also known as a strong absorber and has high loading capacity for CO_2 scrubbing systems, as high as 1.76 kg CO_2/kg NH_3 (3 times higher than MEA solutions, in which, has loading capacity 0.55-0.58 kg CO_2/kg MEA) [9]. Along these lines, the electrochemical reduction of CO_2 in amine or ammonia solution as a CO_2 absorber is attractive and worth to be explored.

BDD electrode, as has been described in chapter 1, is a material of great interest due to its superior electrochemical properties, such as wide potential window, low background current, chemical inertness, and mechanical durability, and it has been used for many electrochemical applications [10-13]. This wide potential window is very helpful to suppress the production of hydrogen gas, namely hydrogen evolution, that used to be a competitor for CO_2 reduction reaction [14]. Previously, the study of CO_2 reduction on bare BDD electrode has been studied in methanol, seawater, and aqueous NaCl solution. Several products have been detected, such as formaldehyde and formic acid [15]. As it shows excellent result, the study of this CO_2 reduction using bare BDD electrode was continued and expanded, developing the system for industrial application, especially the study using amine solution.

2. Experimental

2.1 Chemical

NH_4HCO_3 was purchased from Sigma Aldrich, and other reagents were purchased from Wako Pure Chemical Industries. All reagents were used without any further purification. Ultra- pure water was obtained from a Symply-Lab water system (Direct-Q UV3, Millipore).

2.2 Preparation of the BDD electrodes

BDD (1% B/C) films were deposited onto Si (111) wafers using a microwave plasma-assisted chemical vapor deposition system (MPA-CVD, Model AX 5400, CORNES Technology Corp.). Details of the preparation are described elsewhere [16]. A mixture of trimethoxyborane and acetone was used as the carbon and boron sources. (Figure 1)

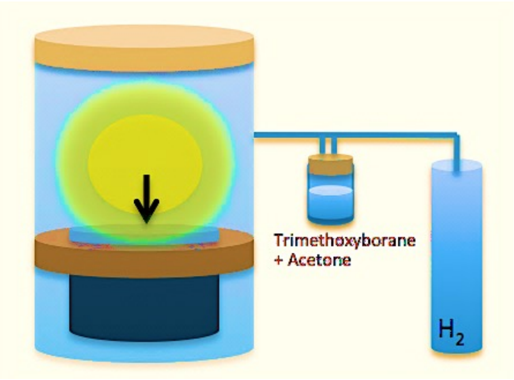

Figure 1. Illustration of BDD preparation

2.3 Electrochemical measurement

The electrochemical measurements were conducted in two compartment cells separated by a Nafion membrane with 100 mL of solution in each cell (Figure 2). BDD, Pt mesh, and Ag/ AgCl were used as a working electrode, a counter electrode, and a reference electrode, respectively. BDD with an area of 4.9 cm^2 and the Ag/AgCl electrode were immersed on the catholyte side (1 M NH_3), and the Pt mesh electrode was on the anolyte side (0.1 M NaCl). The BDD and Pt electrodes were pretreated by ultrasonication in ultrapure water. Ultrasonication in acetone and ultrapure water was also performed after each reduction process to clean the electrodes. Before reduction started, N_2 gas was purged for 30 minutes to remove oxygen gas in the solution, followed by CO_2 gas bubbling for 2 hours with a flow rate of 200 sccm. Cyclic voltammograms were taken before and after gas bubbling with a scan rate of 100 mV/s. Electrochemical reduction of CO_2 was performed by chronoamperometry for 2 hours at potentials ranging from −1.2 V to −1.5 V (*vs.* Ag/AgCl) at the room temperature and the atmospheric pressure. To study the mechanism, the reduction of an aqueous ammonium bicarbonate (NH_4HCO_3) solution was performed without CO_2 bubbling. In addition, the pH of the solution was measured before and after CO_2 bubbling using pH meter (LAQUA, HORIBA), and the concentration of CO_2 in the solution was measured using CO_2 measure CGP-31 (DKK-TOA Corp., Japan). All electrochemical measurements were recorded using a potentiostat under stirring condition (Autolab PGSTAT204, Metrohm Autolab B.V.).

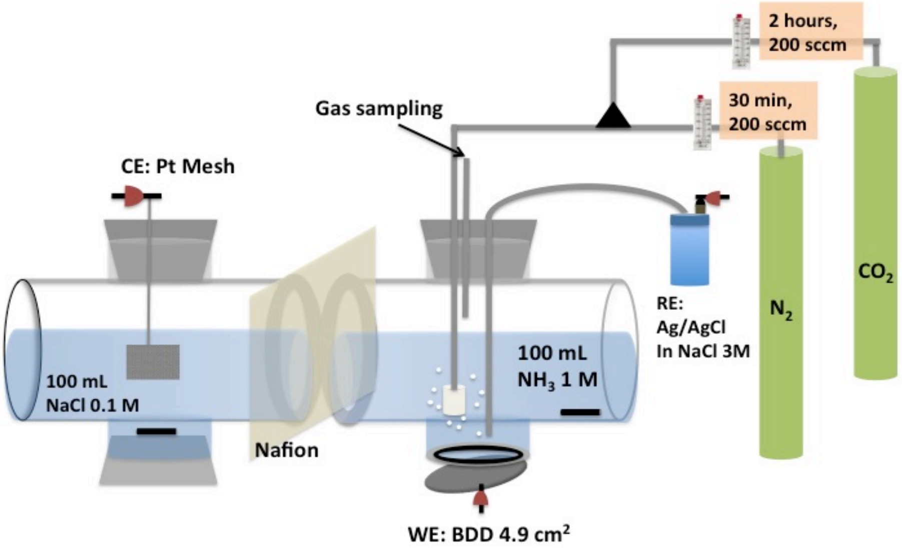

Figure 2. The apparatus for electrochemical reduction of CO_2.

2.4 Sample Analysis

2.4.1 Gas sample analysis

The gas was collected in 1 L gas back after completed the electrolysis. CO and CH_4 gas products were analyzed using gas chromatography (GC) with FID detector (Table 1). 5 mL of gas was taken from the gas bag and analyzed in GC-FID. Meanwhile, H_2 gas was analyzed using TCD detector, by taking 1 mL gas sampling.

Table 1. Details of gas sample analysis using GC instrumentation.

Gas Product	
Instrument	Gas Chromatography
Column	Molecular Sieve 13X, 3.00 mm I.D., 2m
Detector	
a. FID	
Injection temperature	100°C
Carrier Gas	He, 20 mL/min
Oven	60°C
Detector temperature	120°C
Injection volume	5 mL of gas sample
b. TCD	
Injection temperature	70°C
Carrier Gas	Ar, 10 mL/min
Oven	70°C
Detector temperature	100°C
Injection Volume	1 mL of gas sample

2.4.2 Liquid sample analysis

The liquid sample was analyzed separately from the gas sample, by using gas chromatography-mass spectrometry (GC-MS). The injection method, using headspace method (Figure 3). 5 mL of sample in a 20-mL vial was heated for 30 minutes or more at 80°C to achieve a balanced condition in the vial. A 1-mL gas sample was taken from the headspace area of the vial, and then directly injected manually into the GC-MS instrument using a gas tight syringe.

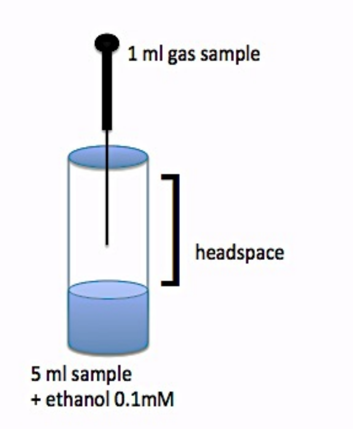

Figure 3. Illustration of headspace method

The GC-MS instrument was operated in specific condition, using SIM mode to specifically analyze the target sample by using ethanol as an internal standard. The certain ion fragment will be entered into the instrument and detected by the mass spectrometer. This method aims to improve the sensitivity of the analysis, and thus, the analysis with a very low limit detection and low of matrix interferences could be achieved. This may possibly a low concentration of the sample to be detected. The selected mass fragments for methanol analysis were m/z 15, 31, 32, and 29. This chosen fragment is based on the most significant MS signal detected by methanol and ethanol. The details are in Table 2.

Table 2. Details of liquid sample analysis using GC-MS instrumentation.

Liquid Product	
Instrument	Gas Chromatography-Mass Spectrometry (GC-MS)
Condition	
a. GC	
Column	Stabilwax 60m, 0.32mm I.D., 1µm df
Carrier Gas	He
Oven	40°C (3 min), adjusted to 150°C (10°C/min) continued to 240°C (25°C)
Method	Splitless
b. MS	
Ion Source	200°C
Interface	250°C
Mode	SIM

3. Results and Discussions

First of all, the prepared BDD electrode was examined to make sure that the BDD electrode in a proper condition for used. The characterization was conducted using Raman spectroscopy (excited wavelength: 532 nm) and scanning electron microscope (SEM) using SIRION (FEI). SEM images of the BDD films showed the polycrystalline with the grain sizes of about 4~7 µm (Figure 4a). Raman spectra were recorded with Acton SP2500 (Prinston Instruments), which showed the typical peak at 1332 cm^{-1} related to the center zone phonon of diamond. The two peaks were also observed at around 500 cm^{-1} and 1230 cm^{-1}, which can be interpreted as due to a carbon disorder arising from the boron doping (Figure 4b). In addition, there was no peak observed at around 1500 cm^{-1} that related to sp^2 carbon. Therefore, the BDD was successfully deposited on Si (111) wafer with a proper condition to be applied for CO_2 electrochemical reduction.

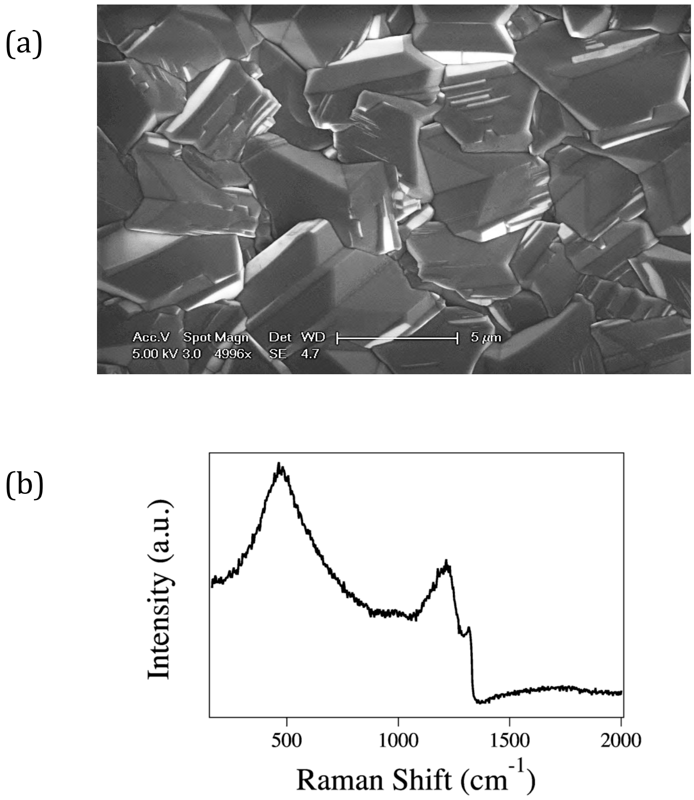

Figure 4. Characterization of obtained BDD electrode using SEM (a) and Raman spectroscopy (b)

After obtaining the proper BDD electrode, the first study for CO_2 reduction was begun with the cyclic voltammetry measurement, to know the behavior of the system after N_2 and CO_2 gas bubbling. Therefore, the CV was carried out right after 30 minutes N_2 gas bubbling and 2 hours CO_2 gas bubbling at a flow rate of 200 sccm. Figure 5 shows the CVs on a BDD electrode in 1M NH_3 aqueous solutions that was run at a scan rate of 100 mV/s. As we can see from the figure, after nitrogen gas purging, there was no reduction peak was observed for potentials ranging from 0 V to −1.8 V (*vs.* Ag/AgCl) (Figure 5a). This is the same as after CO_2 gas was bubbled into the solution there was no special reduction peak was observed. However, a cathodic current was increased from around −1.0 V (*vs*. Ag/AgCl) (Figure 5b). This shows that CO_2 has been dissolved into the solution, and thus, the pH was decreased and the potential window becomes narrower.

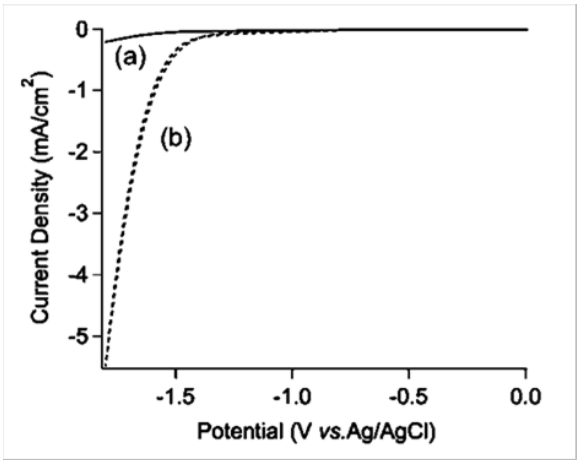

Figure 5. Cyclic voltammetry on a BDD electrode in 1 M NH_3 aqueous solution after nitrogen gas purging (a: solid line) and after CO_2 bubbling for 2 hours (b: dashed line) with a scan rate of 100 mV/s.

After CO_2 saturation (2 hours bubbling) in 1M NH_3 aqueous solution, the electrochemical reduction was performed for 2 hours at various potentials at room temperature and atmospheric pressure. The products after electrolysis at −1.3 V (*vs.* Ag/AgCl) were methanol (0.25 mg L^{-1}, faradaic efficiency: 24.3%), carbon monoxide (0.002 mg L^{-1}, faradaic efficiency: 0.05%), methane (0.0006 mg L^{-1}, faradaic efficiency: 0.13%), and hydrogen (0.04 mg L^{-1}, faradaic efficiency: 19.7%). Here, the dependence of the faradaic efficiency on the applied potential is summarized in Figure 6. The production of methanol after 5 hours reduction was about 0.5 mg/L with the faradaic efficiency about 22%. Beside, the chromatograms of the products detected by GC and GC-MS are shown in Figure 7.

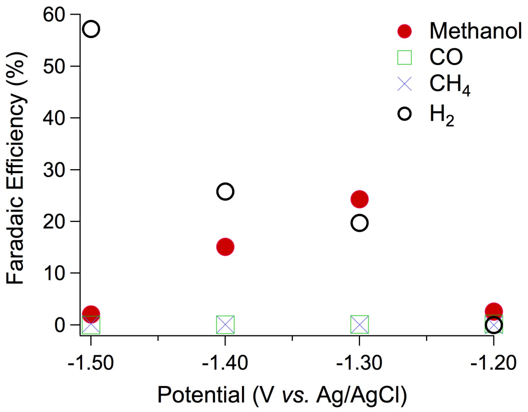

Figure 6. The faradaic efficiencies of the products for 2 hours reduction of CO_2 on a BDD electrode in 1 M NH_3 aqueous solution at the potentials from −1.2 V to −1.5 V (*vs.* Ag/AgCl).

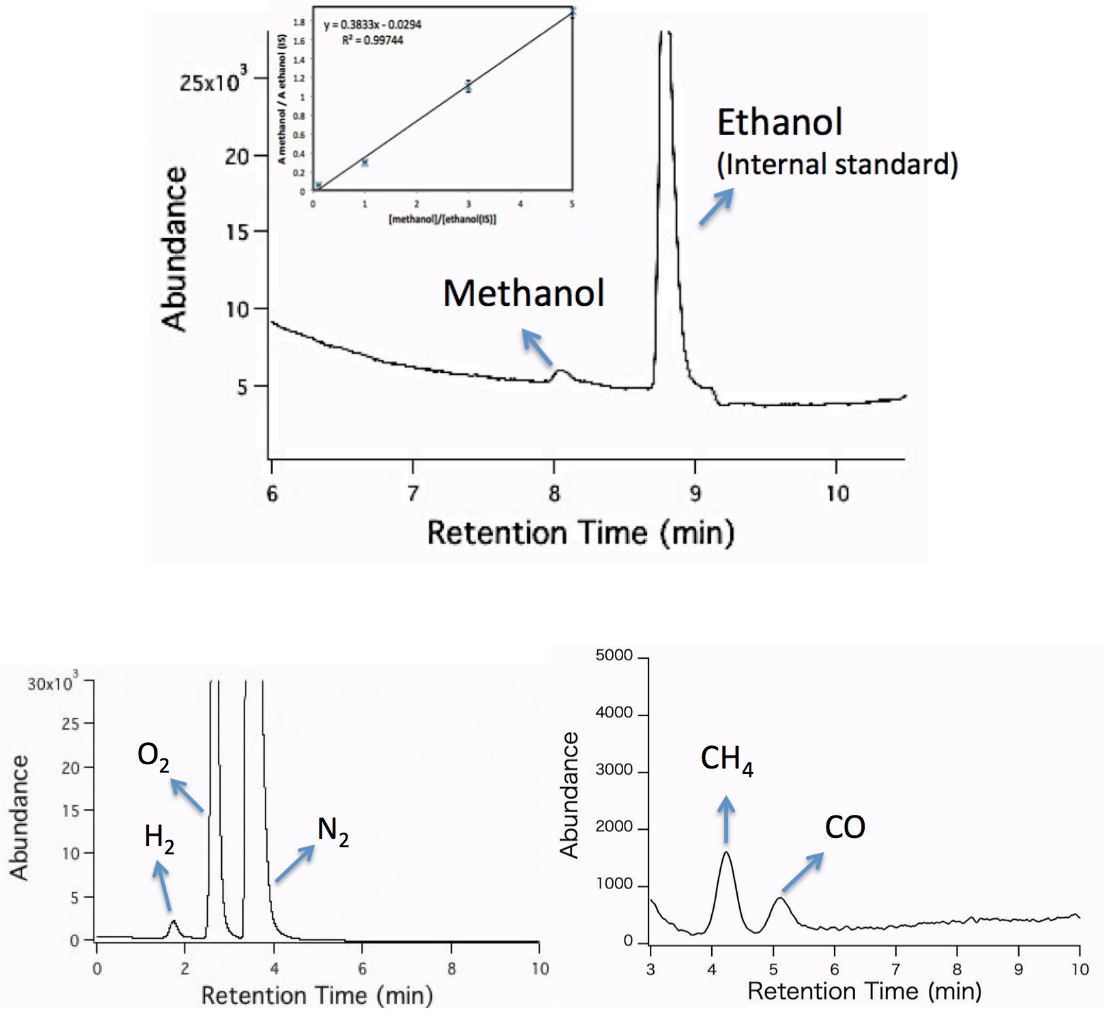

Figure 7. Chromatograms of each product, analyzed by GC-MS and GC with TCD and FID detectors.

When the applied potential was −1.3 V (*vs.* Ag/AgCl), the efficiency of the methanol production was the highest. At the same time, the efficiencies for the production of CO and CH_4 were quite low. Thus, methanol can be selectively produced by CO_2 reduction on a BDD electrode in an aqueous NH_3 solution. On the other hand, when the applied potential was more negative, the faradaic efficiency of the hydrogen evolution increased and that of the methanol production diminished. No other products were analyzed in a quantifiable amount in this range of potential. The repeatability of the CO_2 electrochemical reduction at potential -1.3 V *vs.* Ag/AgCl during 2 hour was also carried out for four times experiment (Figure 8). The standard deviation was calculated as low as 1.97%.

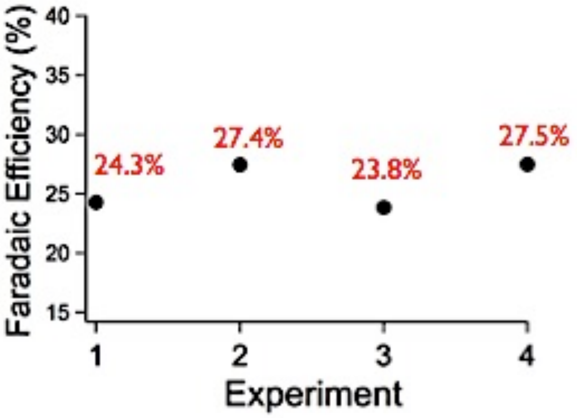

Figure 8. Four times CO_2 electrochemical reduction in aqueous ammonia solution at potential -1.3 V *vs.* Ag/AgCl during 2 hours

The CO_2 electrochemical reductions were carried out using chronoamperometry technique, thus the current during the electrolysis was monitored (Figure 8). The current was increased, as the potential reduction was more negative. At potential reduction -1.5 V, the spectra shows a lot of signal noise that might be due to the interference of H_2 evolution.

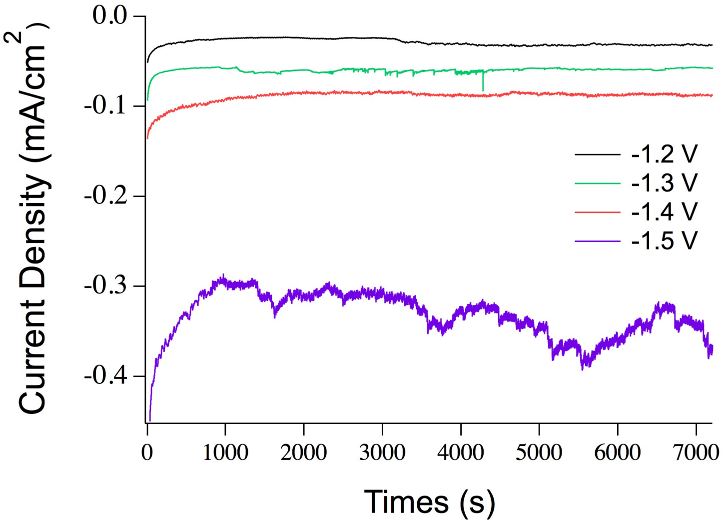

Figure 8. Chronoamperometry of CO_2 reduction in various potential during 2 hours electrolysis on bare BDD electrode in 1 M NH_3 solution.

Meanwhile, to understand the saturation of CO_2 gas in the solution, we measure the pH that was monitored during CO_2 bubbling in the 1 M NH_3 aqueous solution. The initial pH was 11.7. During CO_2 bubbling for 2 hours, the pH decreased to 7.7 (Figure 9). In aqueous solutions, NH_3 and CO_2 react as follows (eqn (2)–(4)):[9]

$$NH_3 + CO_2 + H_2O \rightleftarrows NH_4^+ + HCO_3^- \quad K_{eq}(293) = 1.02 \times 10^3 \qquad (2)$$

$$NH_3 + HCO_3^- \rightleftarrows NH_2CO_2^- + H_2O \quad K_{eq}(293) = 3.61 \qquad (3)$$

$$NH_3 + HCO_3^- \rightleftarrows CO_3^{2-} + NH_4^+ \quad K_{eq}(293) = 1.04 \times 10^{-1} \qquad (4)$$

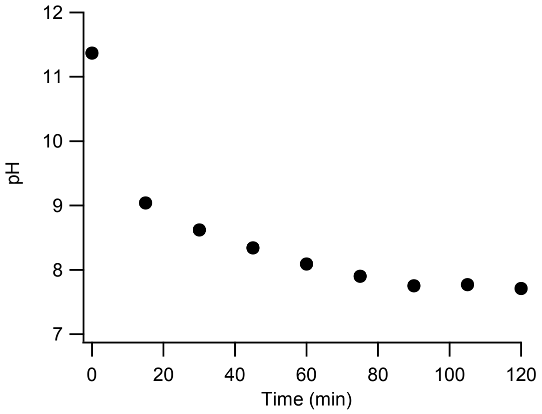

Figure 9. pH of the aqueous ammonia solution during CO_2 gas bubbling. The measurement was conducted while stirring the solution at ~25°C. After 2 hours bubbling, pH decreased to 7.7

On the other hand, according to the distribution of carbonaceous species in the aqueous solution, the pH determines which species are dominant in the solution. It is known that dissolved $CO_{2(aq)}$ is the dominant species at $pH < 5$, while at pH levels from 7.5 to 9, HCO_3^- (bicarbonate ion) is dominant, and CO_3^{2-} (carbonate ion) is dominant above pH 12 (Figure 10). The reaction is generally denoted as follows (eqn. (5) and (6)):[17]

$$CO_2\,(aq) + H_2O\,(l) \rightleftarrows H^+(aq) + HCO_3^-\,(aq) \quad pK_1 = 6.35 \qquad (5)$$

$$H^+(aq) + HCO_3^-\,(aq) \rightleftarrows 2H^+(aq) + CO_3^{2-}\,(aq) \quad pK_2 = 10.33 \qquad (6)$$

Since the reaction of aqueous NH_3 with CO_2 rapidly produces bicarbonate (pH 7.6–8.0) after CO_2 saturation, it is assumed that bicarbonate ions are reduced to methanol in our system.

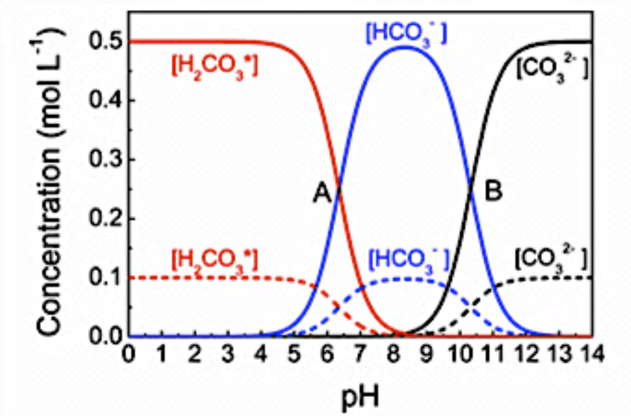

Figure 10. Distribution of carbonaceous species in aqueous solution with the dependence of pH, at temperature 25°C. Reprinted with permission from reference [17]. Copyright (2015) American Chemical Society.

In order to confirm that bicarbonate ions are reducible species, the electrochemical reduction of a 0.1 M NH_4HCO_3 aqueous solution (pH 7.9) was performed without CO_2 bubbling. As the result, methanol was mainly produced in common with the reduction in an aqueous NH_3 solution saturated with CO_2 (Figure 11). In addition, we investigated into the influence of pH by adding HCl for low pH (<4) and NaOH for high pH (>10) to the NH_4HCO_3 solution. As the results, methanol was not detected in either condition at the same reduction potential of −1.3 V (*vs.* Ag/AgCl). These results suggest that bicarbonate ions are reducible species, not CO_2 and CO_3^{2-}. That is, we propose the mechanism of methanol production in our system as follows (eqn (7)):

$$HCO_3^- + 5H_2O + 6e^- \rightarrow CH_3OH + 7OH^- \tag{7}$$

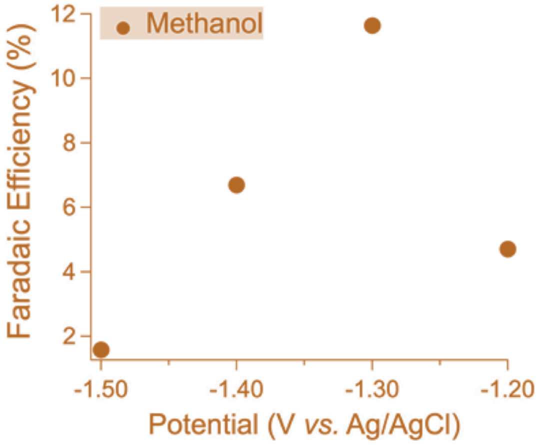

Figure 11. Faradaic efficiencies of methanol production by the 2 hours reduction of 0.1 M NH_4HCO_3 aqueous solution (pH 7.9) on a BDD electrode at the potentials from −1.2 V to −1.5 V (*vs*. Ag/AgCl). The faradaic efficiencies of the products for 2 hours reduction of CO_2 on a BDD electrode in 1 M NH_3 aqueous solution at the potentials from −1.2 V to −1.5 V (*vs*. Ag/AgCl)

On the hand, we considered the effect of NH_3 on methanol production by the electrochemical reduction of bicarbonate ions. There are several studies that show the dependence of product selectivity and product distribution by changing the electrolyte. [3,18,19]. Figure 12 shows one of the example of electrolyte dependence, in which, the production of $HCOO^-$ could be improve by changing the electrolyte from $KHCO_3$ to Na_2SO_4 solution.

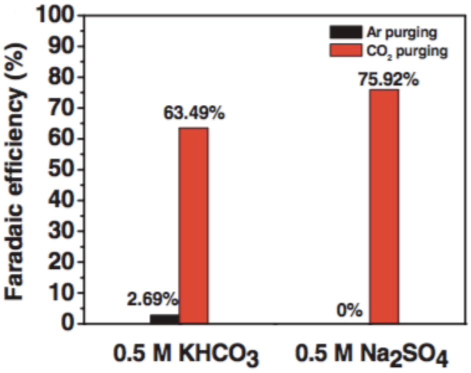

Figure 12. $HCOO^-$ production improvement by changing the electrolyte. Reprinted with permission from reference [18]. Copyright (2012) Electrochemical Society

Thus, the electrochemical reduction was performed in 0.1 M KOH solution saturated with CO_2 (pH 7.0) and in 0.1 M NaOH solution saturated with CO_2 (pH 7.2) at a potential of −1.3 V (*vs*. Ag/AgCl) for 2 hours on a BDD electrode, resulting in no methanol production. It can be explained by the buffering effect of the solution.

During the electrochemical reduction, the hydroxide ions (OH^{-}) were produced by the reduction of bicarbonate ions and also by the hydrogen evolution (eqn. (8-9)):

$$HCO_3^- + 5H_2O + 6e^- \rightarrow CH_3OH + 7OH^- \qquad (8)$$

$$2H_2O + 2e^- \rightarrow H_2 + 2OH^- \qquad (9)$$

Therefore, the local pH will become slightly higher. However, in the aqueous NH_3 solution, OH^{-} reacts with ammonium ions to form ammonia and water by the reaction (eqn. (10)):

$$NH_4^+ + OH^- \rightleftarrows NH_3 + H_2O \qquad (10)$$

On the other hand, in the KOH and NaOH solution, the bicarbonate ions will react with OH^{-} to form carbonate ions by the following reaction (eqn. (11)):

$$HCO_3^- + OH^- \rightleftarrows CO_3^{2-} + H_2O \qquad (11)$$

As mentioned previously, the reducible species are bicarbonate ions, and carbonate ions could not be reduced to methanol. Therefore, the presence of NH_3 is important for methanol production. In addition, ammonia has the advantage of the higher loading capacity of CO_2 than other aqueous solutions (Tables 2 and 3). However, a clear and complete mechanism will need further study.

Table 3. CO_2 concentration in the solution depending on the aqueous ammonia concentration (5 minutes CO_2 bubbling in 50-mL solutions).

Concentration	
$NH_{3(aq)}$ (M)	CO_2 (mg/L)
0.001	1520
0.01	2580
0.1	10380
1	67000

Table 4. CO_2 absorption in 0.1 M NH_3, 0.1 M KOH, and 0.1 M NaOH aqueous solutions (15 minutes CO_2 bubbling in 100-mL solutions).

Electrolyte	Concentration of CO_2 (mg/L)
0.1 M NH_3	18400
0.1 M KOH	9960
0.1 M NaOH	7100

Furthermore, for comparison, the electrochemical reduction of CO_2 on glassy carbon electrode was conducted at a potential of −1.3 V (*vs.* Ag/AgCl) for 2 hours. However, no methanol was detected, and most of the product was H_2 reaching an amount of 0.26 mg/L (on the BDD electrode, it was 0.04 mg/L). Therefore, methanol can be selectively produced by CO_2 reduction on a BDD electrode, as long as the hydrogen evolution can be suppressed. This kind of continuous electrochemical reduction at quite high potential may cause surface corrosion of the glassy carbon electrode (emphasizing roughness, changing pores volume, etc.) [20]. On the other hand, BDD has high durability. In order to show evidence for the durability of BDD, the surface morphology of a BDD electrode was examined by SEM after using the BDD electrode for more than 30 hours in a reduction process. The SEM images revealed no difference as compared to the as-grown BDD (Fig. 5). This is consistent with the results in our previous report [15].

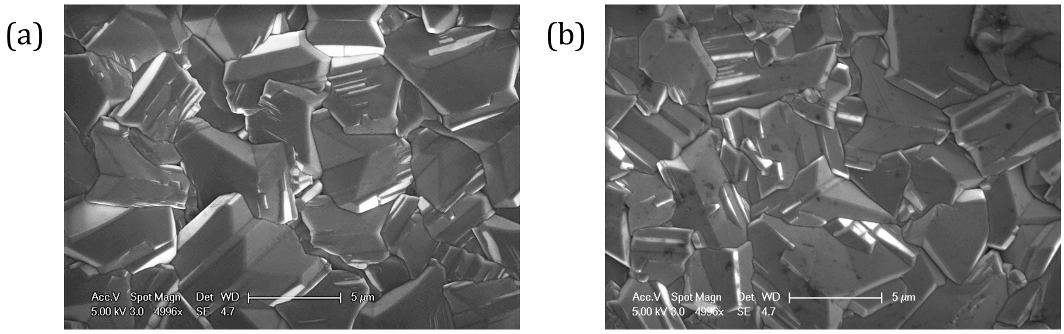

Figure 13. SEM images of BDD electrode before (a) and after (b) more than 30 hours CO_2 electrochemical reduction

4. Conclusion

CO_2 electrochemical reduction on surface of bare BDD electrode in aqueous ammonia solution has been successfully carried out. The main product was methanol with maximum faradaic efficiency of 24.3% at potential -1.3 V *vs.* Ag/AgCl. Other products including CO and CH_4 were produced in a low efficiency. A mechanism for methanol production was revealed to be the reduction of bicarbonate ion by performing the reduction of ammonium bicarbonate solution without CO_2 bubbling at final pH lies about 7.7. Finally, as long as the hydrogen production can be suppressed, the selectivity of methanol production in weakly alkaline aqueous ammonia solution can be achieved, since no other products produced in high amount except methanol itself. Thus, it will be a good opportunity for practical application especially in reducing industrial stored-CO_2(HCO_3^-) reduction, that usually use amine based solution for CO_2 scrubbing system.

5. References

[1] F. Sastre, A. V. Puga, L. Liu, A. Corma, H. García, Complete Photocatalytic Reduction of CO_2 to Methane by H $_2$ under Solar Light Irradiation, J. Am. Chem. Soc. 136 (2014) 6798–6801.

[2] C. Song, CO2 Conversion and Utilization : An Overview, ACS Symp. Ser. Am. Chem. Soc. Washingt. DC. 809 (2002) 1–30.

[3] J. Wu, F.G. Risalvato, F.-S. Ke, P.J. Pellechia, X.-D. Zhou, Electrochemical Reduction of Carbon Dioxide I. Effects of the Electrolyte on the Selectivity and Activity with Sn Electrode, J. Electrochem. Soc. 159 (2012) F353–F359.

[4] Q. Lu, J. Rosen, Y. Zhou, G.S. Hutchings, Y.C. Kimmel, J.G. Chen, F. Jiao, A selective and efficient electrocatalyst for carbon dioxide reduction, Nat. Commun. 5 (2014) 1–6.

[5] J.N. Park, E.W. McFarland, A highly dispersed Pd-Mg/SiO_2 catalyst active for methanation of CO_2, J. Catal. 266 (2009) 92–97.

[6] J.C.M. Pires, F.G. Martins, M.C.M. Alvim-Ferraz, M. Simões, Recent developments on carbon capture and storage: An overview, Chem. Eng. Res. Des. 89 (2011) 1446–1460.

[7] D.Y.C. Leung, G. Caramanna, M.M. Maroto-Valer, An overview of current status of carbon dioxide capture and storage technologies, Renew. Sustain. Energy Rev. 39 (2014) 426–443.

[8] A. Veawab, A. Aroonwilas, P. Tontiwachwuthikul, CO_2 absorption performance of aqueous alkanolamines in packed columns, ACS Div. Fuel Chem. Prepr. 47 (2002) 49–50.

[9] F. Mani, M. Peruzzini, P. Stoppioni, CO_2 absorption by aqueous NH_3 solutions: speciation of ammonium carbamate, bicarbonate and carbonate by a 13C NMR study, Green Chem. 8 (2006) 995.

[10] T.A. Ivandini, Y. Einaga, Polycrystalline boron-doped diamond electrodes for electrocatalytic and electrosynthetic applications, Chem. Commun. 53 (2017) 1338–1347.

[11] N. Yang, S. Yu, J. V. Macpherson, Y. Einaga, H. Zhao, G. Zhao, G.M. Swain, X. Jiang, Conductive diamond: synthesis, properties, and electrochemical

applications, Chem. Soc. Rev. 48 (2019) 157–204.

[12] S.R. Waldvogel, S. Lips, Use of Boron-doped Diamond Electrodes in Electro-organic Synthesis, ChemElectroChem. 6 (2019) 1649–1660.

[13] Y. Einaga, Diamond electrodes for electrochemical analysis, J. Appl. Electrochem. 40 (2010) 1807–1816.

[14] Y.J. Zhang, V. Sethuraman, R. Michalsky, A.A. Peterson, Competition between CO_2 reduction and H_2 evolution on transition-metal electrocatalysts, ACS Catal. 4 (2014) 3742–3748.

[15] K. Nakata, T. Ozaki, C. Terashima, A. Fujishima, Y. Einaga, High-yield electrochemical production of formaldehyde from CO_2 and seawater, Angew. Chemie - Int. Ed. 53 (2014) 871–874.

[16] T. Yano, D.A. Tryk, K. Hashimoto, A. Fujishima, Electrochemical Behavior of Highly Conductive Boron-Doped Diamond Electrodes for Oxygen Reduction in Alkaline Solution, J. Electrochem. Soc. 145 (1998) 1870–1876.

[17] H. Zhong, K. Fujii, Y. Nakano, F. Jin, Effect of CO_2 bubbling into aqueous solutions used for electrochemical reduction of CO_2 for energy conversion and storage, J. Phys. Chem. C. 119 (2015) 55–61.

[18] S. Verma, X. Lu, S. Ma, R.I. Masel, P.J.A. Kenis, The effect of electrolyte composition on the electroreduction of CO_2 to CO on Ag based gas diffusion electrodes, Phys. Chem. Chem. Phys. 18 (2016) 7075–7084.

[19] Y. Huang, C.W. Ong, B.S. Yeo, Effects of Electrolyte Anions on the Reduction of Carbon Dioxide to Ethylene and Ethanol on Copper (100) and (111) Surfaces, ChemSusChem. 11 (2018) 1–9.

[20] G.M. Swain, The Susceptibility to Surface Corrosion in Acidic Fluoride Media: A Comparison of Diamond, HOPG, and Glassy Carbon Electrodes, J. Electrochem. Soc. 141 (2006) 3382.

3

Chapter

Electrochemical reduction of CO_2 on copper-modified boron-doped diamond electrodes

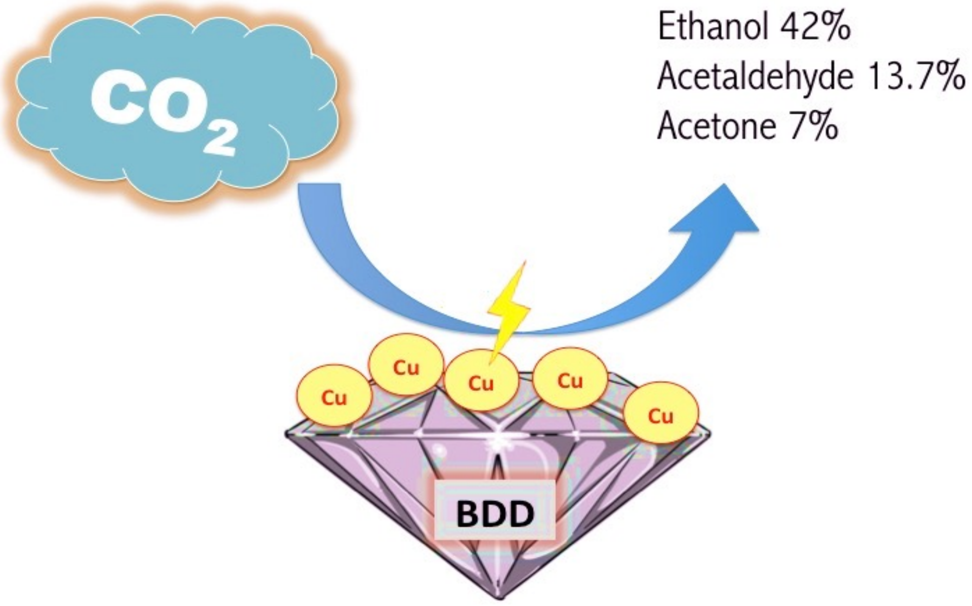

This work has been published in:
P. K. Jiwanti, K. Natsui, K. Nakata, and Y. Einaga, Electrochim. Acta. 266 (2018) 414-419

Abstract

The electrochemical reduction of CO_2 to C_2/C_3 species on the surface of copper modified boron doped diamond (Cu-BDD) electrode for the first time in aqueous solution at room temperature and pressure. Ethanol (42.4%), acetaldehyde (13.7%), and acetone (7%) were observed at potential -1.0 V *vs.* Ag/AgCl. The product distribution is dependent on the amount of deposited Cu particles and also the applied potential. The Cu particles were remained stable at particular condition, showing the insignificant differences after CO_2 reduction. Moreover, the comparison of CO_2 reduction using glassy carbon electrode as a support electrode for Cu deposition is also presented.

1. Introduction

CO_2 electrochemical reduction on the surface of bare BDD electrode has been studied and reported in several publications [1-4]. The quantifiable products that could be achieved are C_1 products, such as formaldehyde, formic acid, methanol, and CO. Meanwhile, the compound with higher number of carbon atoms is desired, in which the production of ready-to-use fuel can be developed. [5] Therefore, to improve the catalytic effect to produce compound with higher number of carbon atom, and also to decrease the over potential that used to be found on bare BDD electrode for CO_2 reduction, metal particle was suggested to be deposited on surface of BDD electrode.

Determining the suitable metal to deposit on surface of BDD is an important point to be considered. There have been numerous studies on CO_2 reduction using metal electrode. [6-8]. Figure 1 shows the product distribution of CO_2 reduction on many metal electrodes. All those metal are categorized based on ability to adsorb CO. First, low binding strength of CO such as Au, Zn, and Ag. Those metals usually produce CO as the main product. Second, high binding strength of CO such as Ni, Pt, Fe, and Co. These metals do not active for CO_2 reduction since it produces H_2 in high rate. Generally, this second type of metals is not preferable for CO_2 reduction. Meanwhile, the third type has moderate binding strength of CO. Cu metal is the only metal in this type. It has a special behavior toward CO_2 reduction, that is, possibly produces hydrocarbon and oxygenated species in quantifiable amount. [9-12] Up to this moment, Cu is the best-known metal catalyst for the electrochemical reduction of CO_2.

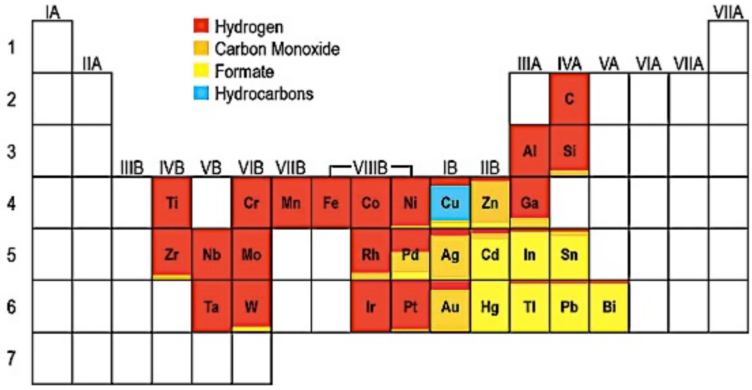

Figure 1. Distribution of CO_2 reduction products on many metal electrodes. Reprinted with permission from reference [8]. Copyright (2015) American Chemical Society

The modification of bare BDD surface with metal particles has been known to improve electrocatalytic and also selectivity. It has been used for many applications, such as for sensor and also synthesis application [13,14]. Therefore, the modification of BDD electrode with copper particles was carried out, aiming to produce compound with higher number of carbon atoms and it is expected that the applied potential could be suppressed. In this work, the deposition of metal was carried out by a sample electrochemical deposition. Despite of its stability issue, this method was used as it easy to prepare and recover. The amount of deposited Cu particle and also potential dependence were studied and presented in this chapter.

2. Experimental

2.1 Chemicals

All the reagents were purchased from Wako Pure Chemical Industries and were used without further purification. Ultra-pure water was obtained from a Symply-Lab water system (Direct-Q UV3, Millipore).

2.2 Electrode preparation

BDD electrode was prepared by depositing the films onto Si (111) wafers using microwave plasma-assisted chemical vapor deposition system. (Model 5400, CORNES Technology Corp.) [15]. The deposition was carried out electrochemically in 10 ml of 0.1 M H_2SO_4 containing a 1 mM $CuSO_4$ solution. cyclic voltammetry (CV) electrodeposition of Cu nanoparticles was carried out (Figure 2).

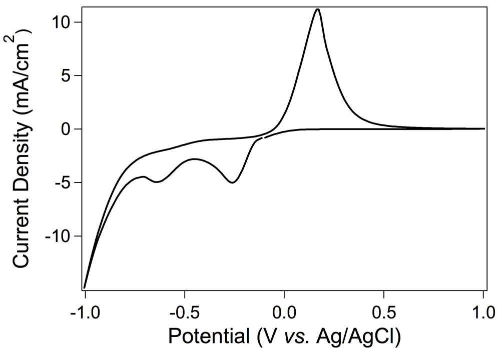

Figure 2. CV of BDD electrode in 10 ml of 0.1 M H_2SO_4 containing a 1 mM $CuSO_4$ solution.

The reduction peak of Cu^{2+} is at -0.6 V (*vs.* Ag/AgCl). The Cu particle was deposited in different deposition time, 50 s (Cu-BDD-50), 100 s (Cu-BDD-100), and 300 s (Cu-BDD-300). N_2 gas purging was performed for 5 minutes prior to electrodeposition to remove the dissolved oxygen [16]. The Cu-BDD electrodes were then rinsed with water and dried at room temperature and pressure for 1 hour, followed by ultrasonication in water for about 5 minutes and dried under N_2 gas. Moreover, the modified electrodes were recovered by immersion in an aqua regia solution for 10 minutes followed by ultrasonication in ultrapure water for 15 minutes. This recovery method was confirmed to not broke the BDD, and can be use again for many times. Electrode characterization was performed using X-ray photoelectron spectroscopy (XPS), scanning electron microscopy (SEM) (JCM-6000, JEOL) before and after electrolysis.

2.3 Electrochemical CO_2 reduction

The electrochemical measurements were conducted in a cell with two compartments, separated by a Nafion membrane (Figure 3).

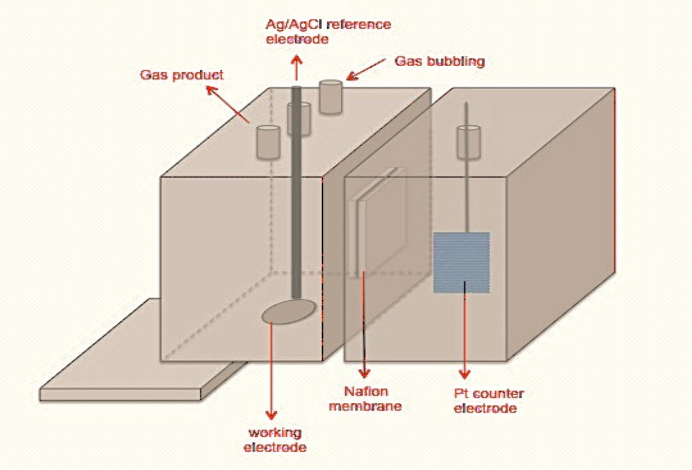

Figure 3. Compartment cell for CO_2 electrochemical reduction of CO_2

A 0.5 M KCl solution was used as the catholyte, and a 0.5 M KOH solution as the anolyte (15 mL in each cell).[17] Cu-BDD, a Pt Mesh, and Ag/AgCl were used as the working, counter, and reference electrodes, respectively. Prior to electrochemical reduction, the catholyte side was purged with N_2 gas for 5 minutes, followed by CO_2 bubbling for 15 minutes. Linear sweep voltammetry (LSV) was performed with a scan rate of 20 mV/s in the potential range from 0 V to -1.8 V (*vs.* Ag/AgCl). The electrochemical reduction of CO_2 was conducted for 2 hours at potentials ranging from -0.8 V to -1.2 V (*vs.* Ag/AgCl) at room temperature and pressure.

2.4 Product analysis

The liquid products were analyzed using gas chromatography-mass spectrometry (GCMS-QP2010 Ultra, Shimadzu Corp.) by the autoinjection headspace method (5 mL sample in 20 mL volume vial) with the selected ion monitoring (SIM) mode for the target products. The selected mass fragments for analysis were m/z 15, 29, 31, 32, 46, 45, 42, 26, 19, 14, 43, 44, and 58. Meanwhile, the GC-MS condition was summarized in Table 1. Beside that, high performance liquid chromatography (HPLC) with electroconductivity and UV/Vis detectors (Prominence, Shimadzu Corp.) were also used for HCOOH and aldehyde analysis. The gas products were analyzed by gas chromatography with a flame ionization detector and a thermal conductivity detector (GC-2014, Shimadzu Corp.).

Table 1. Details of GC-MS condition for sample analysis

Liquid Product	
Instrument	Gas Chromatography-Mass Spectrometry (GC-MS)
Condition	
a. GC	
Column	Stabilwax 60m, 0.32mm I.D., 1µm df
Carrier Gas	He
Oven	40°C (3 min), adjusted to 150°C (10°C/min) continued to 240°C (25°C)
Method	Splitless
b. MS	
Ion Source	200°C
Interface	250°C
Mode	SIM

3. Results and Discussions

First of all, Cu modified BDD electrode was examined by performing the linear sweep voltammetry (LSV) using Cu-BDD-100 in 0.5 M KCl solution. The LSV was performed at potential ranging from 0V to -1.8 V *vs*. Ag/AgCl (Figure 4).

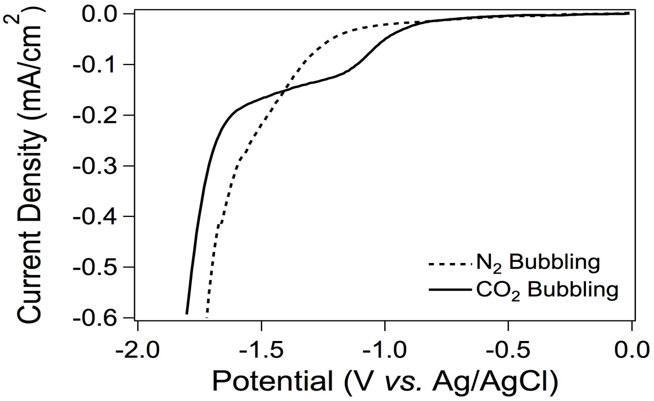

Figure 4. The LSV of Cu-BDD-100 in 0.5 M KCl solution saturated with N_2 gas (dashed line) and CO_2 gas (solid line). The scan rate was 20 mV/s, swept from potential 0 V to -1.8 V *vs*. Ag/AgCl

The LSVs were carried out after saturated with N_2 gas and CO_2 gas. We can see that at potential around -1.0 V, there is an increase in absolute value of the current. This peak is increased up to potential -1.7 V and sharply increased as the hydrogen evolution begins. This peak is believed to be a CO_2 reduction peak, since it could not be observed in the N_2 saturation solution. The shift of the onset peak of the hydrogen evolution is assuming that the hydrogen evolution can be suppressed.

The Cu modified on surface of BDD electrode and then used for CO_2 electrochemical reduction. Three kind of modified electrodes, that is, Cu-BDD-50, Cu-BDD-100, and Cu-BDD-300 were prepared. These electrodes were characterized using SEM and XPS. Figure 5a shows the change of XPS spectra after Cu deposition on BDD surface. The peak at binding energy of 932.05 and 952 eV correspond to Cu $2p_{3/2}$ and Cu $2p_{1/2}$ respectively (Figure 5b). A Cu/C ratio of 0.08 was calculated. Furthermore, an increase of O/C ratio from 0.006 to 0.09 was observed after Cu deposition, indicating that not only Cu but also there may be some species of CuO or Cu_2O are formed on the surface of BDD electrode. However, the detail requires further study.

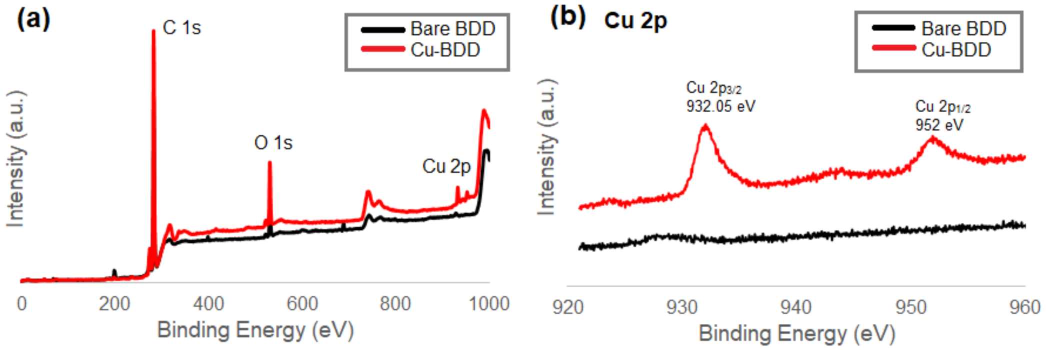

Figure 5. XPS spectra of bare and Cu modified BDD electrodes (a) wide scan (b) narrow scan

Figure 6 shows the SEM images before and after CO_2 electroreduction for 2 hours at -1.0 V (*vs.* Ag/AgCl). However, on the Cu-BDD-300 electrode surface, accumulation of the Cu particles made it easy for them to become detached. On the other hand, the SEM images of the Cu-BDD-100 surface before and after electroreduction show insignificant differences, indicating the Cu-BDD had remained stable. The average sizes of the Cu particles on the Cu-BDD electrode surfaces were around 50-85 nm, as has been calculated manually by ImageJ software application. The detailed calculation can be seen at Figure 7.

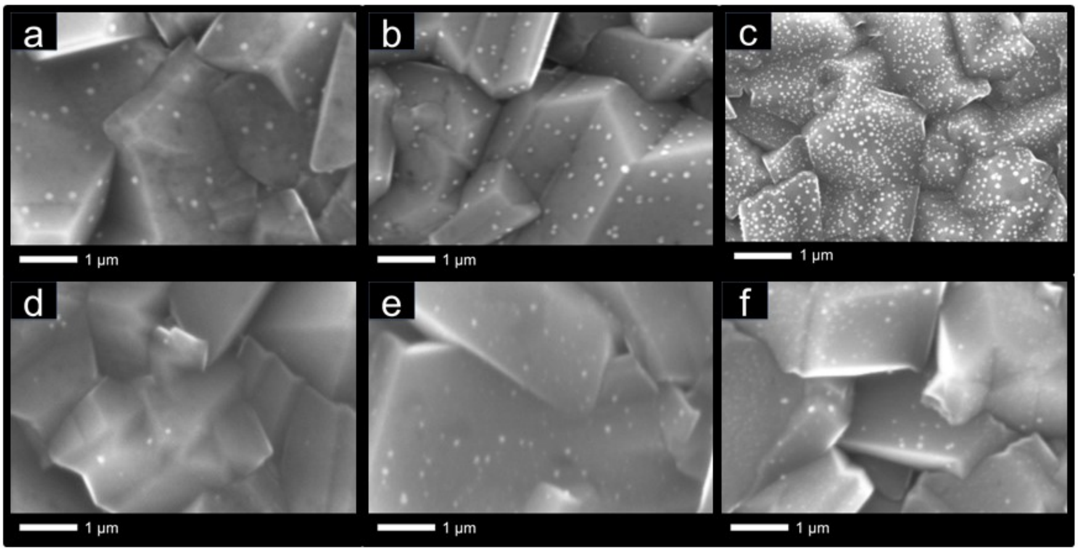

Figure 6. SEM images of Cu-BDD electrodes formed by electrodeposition at -0.6 V (*vs.* Ag/AgCl) in 0.1 M H_2SO_4 solution containing 1 mM $CuSO_4$. (a), (b), (c) show images of the Cu-BDD-50, Cu-BDD-100, Cu-BDD-300 electrodes before electrochemical reduction, and (d), (e), (f) show images of the same electrodes after electrochemical reduction of CO_2 at -1.0 V (*vs.* Ag/AgCl) for 2 hours at room temperature and pressure

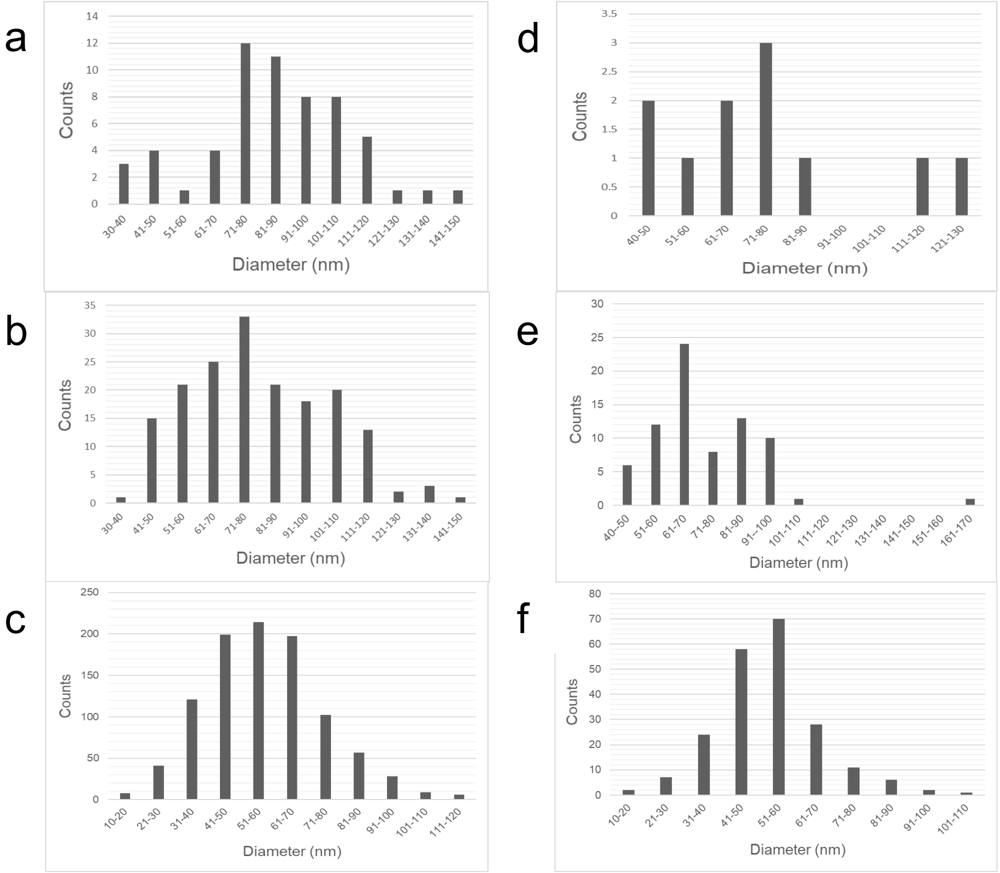

Figure 7. The average particle size as measured by ImageJ software. (a), (b), (c) are Cu-BDD-50, Cu-BDD-100, Cu-BDD-300 electrodes before electrochemical reduction, and (d), (e), (f) are the same electrodes after electrochemical reduction of CO_2 at -1.0 V (*vs.* Ag/AgCl) for 2 hours at room temperature and pressure.

Those three electrodes and thus to be applied for CO_2 electrochemical reduction at potential -1.0 V *vs*. Ag/AgCl during 2 hours reduction. The C_2/C_3 products that could be achieved were ethanol, acetaldehyde, and acetone. The product efficiencies were calculated based on this equation (1):

$$\text{Faradaic Efficiency} = \frac{n\ x\ F\ x\ M}{\sqrt{It}} \text{ x } 100\ \% \qquad (1)$$

Where, *n* is electron involved in reduction, *F* is faraday constant, *M* is concentration of sample, *I* is current and *t* is reduction time.

The highest faradaic efficiencies for those compounds were ethanol 42.4 %, acetaldehyde 13.7%, and acetone 7% (Figure 8), which were obtained on Cu-BDD-100. With the Cu-BDD-50 electrode, the amount of Cu nanoparticles was insufficient to catalyze the production of ethanol. However, for Cu deposition times of more than 100 s, the efficiency dropped due to the instability of the Cu nanoparticles deposited on the BDD surface (Figure 6). Manthiram et al. [18] has reported that isolated nanoparticles expose the catalytic sites for the methanation of CO_2, but that, as the nanoparticles begin to aggregate, these catalytic sites are lost. To the best of our knowledge, this is the first time that C_2/C_3 species have been produced with reasonable efficiency by the electrochemical reduction of CO_2 using a modified BDD electrode. Moreover, ethanol is well known to be widely used as solvent, feedstock, and even as a fuel.

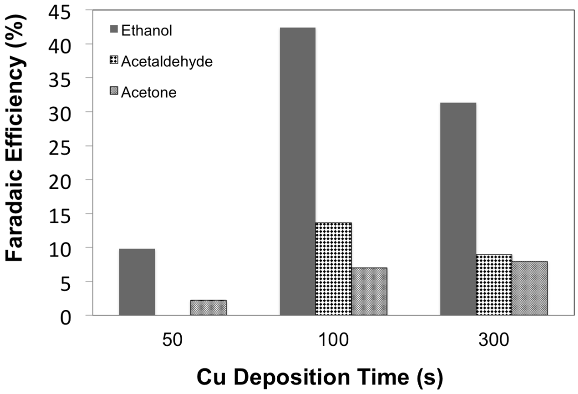

Figure 8. Liquids produced CO_2 electrochemical reduction for two hours on surface of Cu-BDD-50, Cu-BDD-100, and Cu-BDD-300.

Since the best performance was achieved with the Cu-BDD-100 electrode, we used this electrode to examine the dependence of the faradaic efficiencies for the production of ethanol, acetone, and acetaldehyde over the range from 0.8 V to -1.2 V (*vs*. Ag/AgCl) (Figure 9). The chemical equations for the production of ethanol, acetone, and acetaldehyde are given below by (2), (3), and (4), where *E* is the equilibrium potential [7]:

$$2CO_2 + 12e^- + 12H^+ \rightarrow CH_3CH_2OH + 3H_2O \qquad E = 0.09\text{ V } (vs.\text{ RHE}) \qquad (2)$$

$$2CO_2 + 10e^- + 10H^+ \rightarrow C_2H_4O + H_2O \qquad E = 0.05\text{ V } (vs.\text{ RHE}) \qquad (3)$$

$$2CO_2 + 16e^- + 16H^+ \rightarrow C_3H_6O + H_2O \qquad E = -0.14\text{ V } (vs.\text{ RHE}) \qquad (4)$$

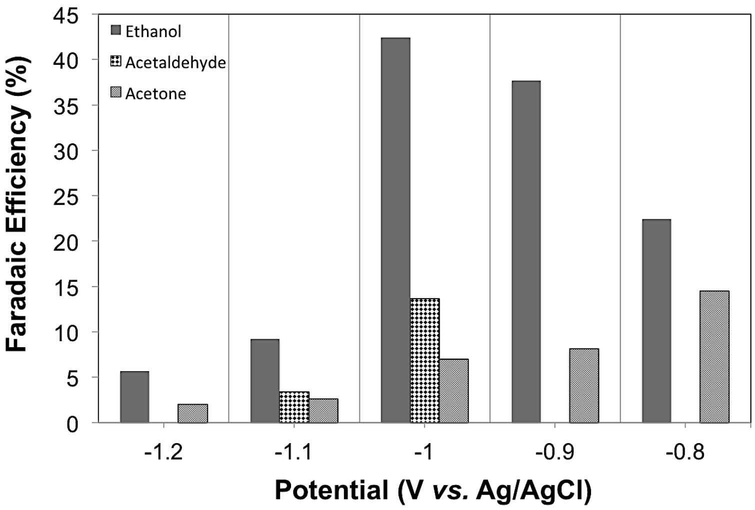

Figure 9. The faradaic efficiencies of the products from CO_2 electrochemical reduction on Cu-BDD-100 at various potential reductions ranging from -1.2 V to -0.8 V *vs*. Ag/AgCl in room temperature and pressure.

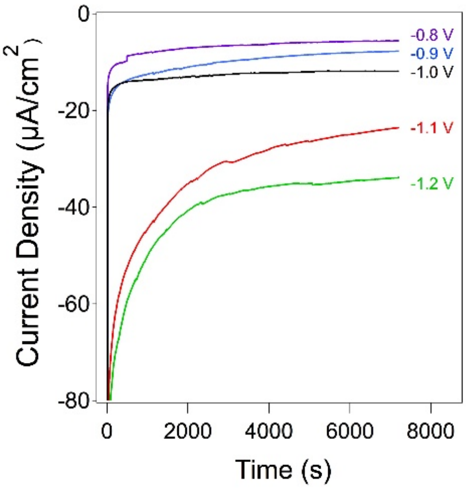

Figure 10. The Chromatogram of CO_2 electrochemical reduction on Cu-BDD-100 during 2 hours reduction at various potentials.

The highest faradaic efficiency for the production of ethanol was achieved at -1.0 V (*vs*. Ag/AgCl). From Figure 9, we can see the production efficiency of acetone increased as the reduction potential was reduced, signifying that the coupling mechanism is more preferable compared to electron and proton transfer. Moreover, a significant decline in the faradaic efficiency for the production of ethanol at more than -1.0 V (*vs*. Ag/AgCl), which might be due to the high production of hydrogen gas detaching Cu nanoparticles from the surface of the electrode. This can also be explained by referring to Figure 10, in which the current density *vs*. time profiles for the reduction of CO_2 at different potentials are plotted, and which shows that, at more than -1.0 V (*vs.* Ag/AgCl), there are large changes in current density with time. The repeatability of the amount produced is indicated by the standard deviation obtained from three different experiments at this potential for 2 hours (Figure 11). The standard deviation of ethanol, acetaldehyde, and acetone are 9.31%, 3.73%, and 1.92% respectively.

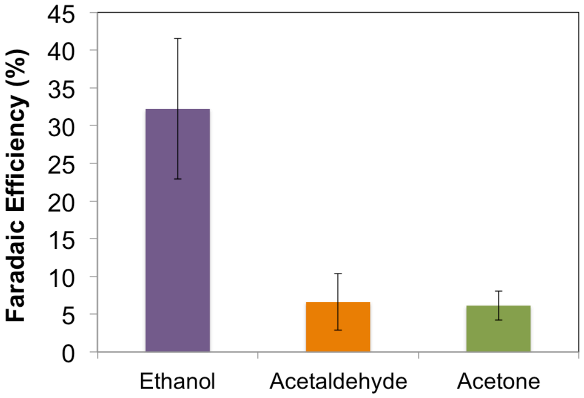

Figure 11. The repeatability of ethanol, acetaldehyde, and acetone production at reduction potnetial -1.0 V *vs.* Ag/AgCl during 2 hours.

In addition, the differences on the BDD surfaces can be seen from the SEM images after 2 hours reduction at various potentials (Figure 12). After reduction at -1.2 V (*vs.* Ag/AgCl), the Cu nanoparticles had become detached, and the Cu nanoparticles remaining on the surface became smaller on average by about 50 nm. On the other hand, at less than -1.0 V *vs.* Ag/AgCl, the Cu nanoparticles seemed to have been stable.

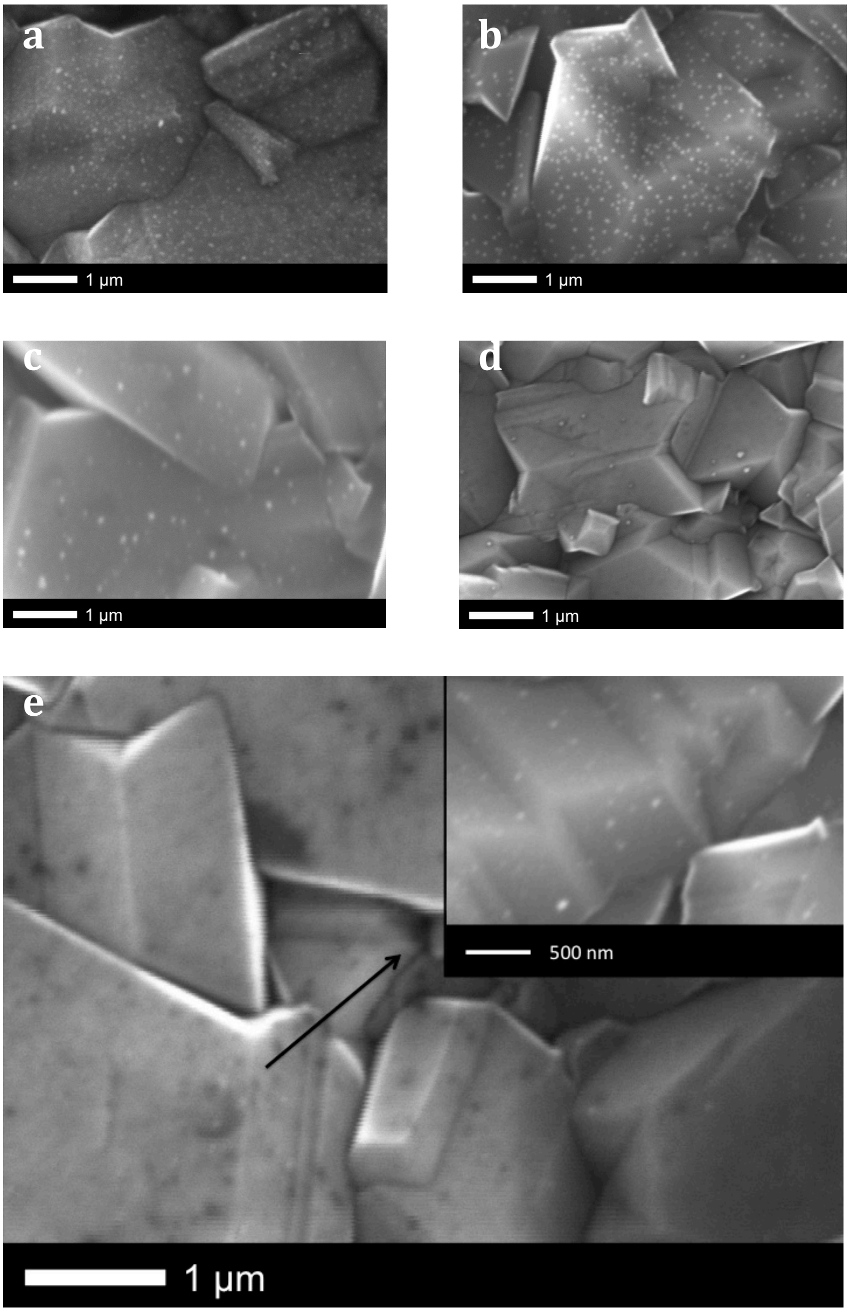

Figure 12. SEM images of Cu-BDD after 2 hours reduction at potential (a) -0.8 V (b) -0.9 V (c) -1.0 V (d) -1.1 V (e) -1.2 V *vs.* Ag/AgCl

Other liquid products, such as formic acid and formaldehyde, and gas products were not detected in quantifiable amounts, since they were beneath the detection limits of our instrument (Table 2). This Limit of Detection (LOD) were determined by calculating the standard deviation of the response (S_y) of the curve and the slope of the standard calibration curve (S) according to this equation (5)

$$\mathrm{LOD} = 3\,(S_y/S) \qquad (5)$$

The standard deviation of the response was determined from the standard deviation of y-intercept of the regression line. In addition, the values of both standard deviation of the response and the slope were calculated by using LINEST function from 4 to 9 different concentration values of standard solutions.

Table 2. Limit detection of the instrument for each product

Liquid products	
Name	LOD (ppm)
Acetone	0.006
Ethanol	0.022
Acetaldehyde	0.003
Formaldehyde	0.014
Formic acid	0.056
Gas products	
Name	LOD (μmol)
H_2	0.002
CO	1.5×10^{-4}
CH_4	1.8×10^{-4}

For comparison, the electrochemical reduction of CO_2 on a bare Cu electrode was also carried out at -1.0 V (*vs.* Ag/AgCl) for 2 hours in the same experimental system. However, in the same applied potential, ethanol, acetone, or acetaldehyde were not observed as on the Cu-BDD electrodes. Considering the potential dependence, we carried out experiments with the Cu electrode at -1.6 V (*vs.* Ag/AgCl), resulting in the production of ethanol, acetone, acetaldehyde, and formic acid with faradaic efficiencies of less than 1%. On the other hand, the production was dominated by the evolution of hydrogen gas and a small amount of CO gas. This is in line with previous reports [19][5] showing that, with a bare Cu electrode, a high overpotential was required to produce hydrocarbons or multi-carbon oxygenated species. However, this behavior was not found with the Cu-BDD electrodes, where ethanol, acetaldehyde, and acetone were produced at low potentials of -1.0 V (*vs.* Ag/AgCl). This suggests that the nano-sized Cu particles deposited on the surface of the BDD electrodes have high affinity, and tend, therefore, to interact more efficiently with the CO_2 molecules and their intermediates.

Studies of the production of C_2 species at the surfaces of Cu electrodes have, so far, only been observed on rough surfaces, such as those produced by electrodeposition or after a thermal pretreatment [20-22]. Beside that, producing compound with high number of carbon atoms, such as C_2/C_3 species, C-C coupling reactions are necessary during the reduction process. [23] C-C coupling reactions are strongly influenced by the amount of CO bonded to the surface of the electrode, which influences the CO-CO coupling or the coupling with other hydrogenated intermediates. Vollmer et al. [24] reported that CO binds more strongly with stepped edges and kinks rather than Cu electrodes with terraced surfaces. The binding energy has also been measured for defect sites on sputtered and polycrystalline Cu electrodes. These studies clearly show that rough surfaces are needed to increase the adsorption of CO, and thus promotes C-C coupling reactions. To give a clear suggested mechanism, the summary of the general mechanism that include the formation of adsorbed species on the surface of electrode, written by Kuhl, et al., [7] and Calle-Vallejo, et al [23], can be combined as follow:

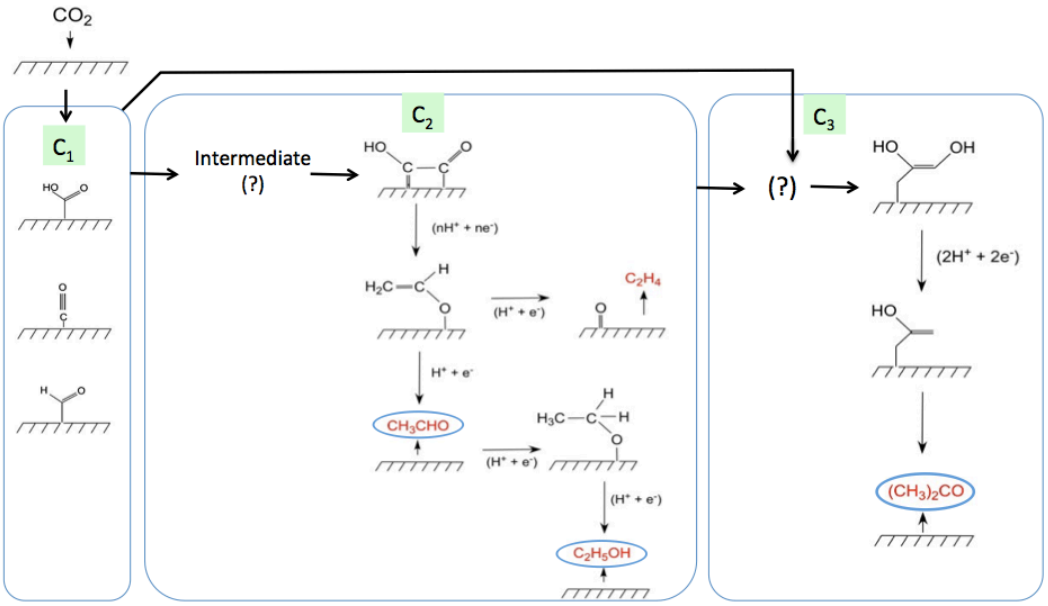

CO_2 is adsorbed on surface of electrode to form C_1 intermediates. This C_1 intermediate could release from the surface of electrode and detected as a product. On the other hand, C-C coupling from C_1 species can also forms C_2 species. Continues coupling reaction of C_1 species and/or with C_2 species could be occurred and producing thus producing C_3 species.

Back to Cu-BDD electrodes, the formation of C_2/C_3 products on this modified electrode is at a low potential (-1.0 V). This can be explained by the fact that at more negative potentials, electron and proton transfer are more favorable, thus the intermediate C_1 species on the surface of the electrode are likely to desorb as C_1 products (i.e. CO, CH_4, HCOOH, etc.) rather than remain and couple with other intermediates to form higher carbon-containing compounds. It is also in line with previously reported results for the electrochemical reduction of CO_2 to HCOOH on a bare BDD electrode, which took place by reduction at high potential [25][2]. Indeed, a more detailed understanding of the mechanism is worth further study.

For comparison with other carbon-based electrodes, the electroreduction of CO_2 with traditional carbon electrode, that is, glassy carbon (GC) and Cu-modified GC (Cu-GC) electrodes was also conducted at -1.0 V (*vs.* Ag/AgCl) for 2 hours (Figure 14). As a result, on both electrodes, hydrogen evolution dominated. At the same time, the efficiency for the production of C_2/C_3 species was less than 1% with the Cu-GC electrode. This suggests that the larger Cu particles and narrower potential window increase the rate of hydrogen production (Figure 13).

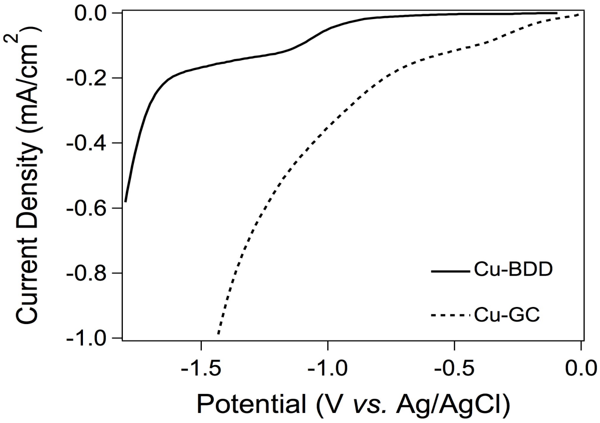

Figure 13. LSV of Cu-BDD and Cu-GC electrodes in 0.5 M KCl after CO_2 gas bubbling

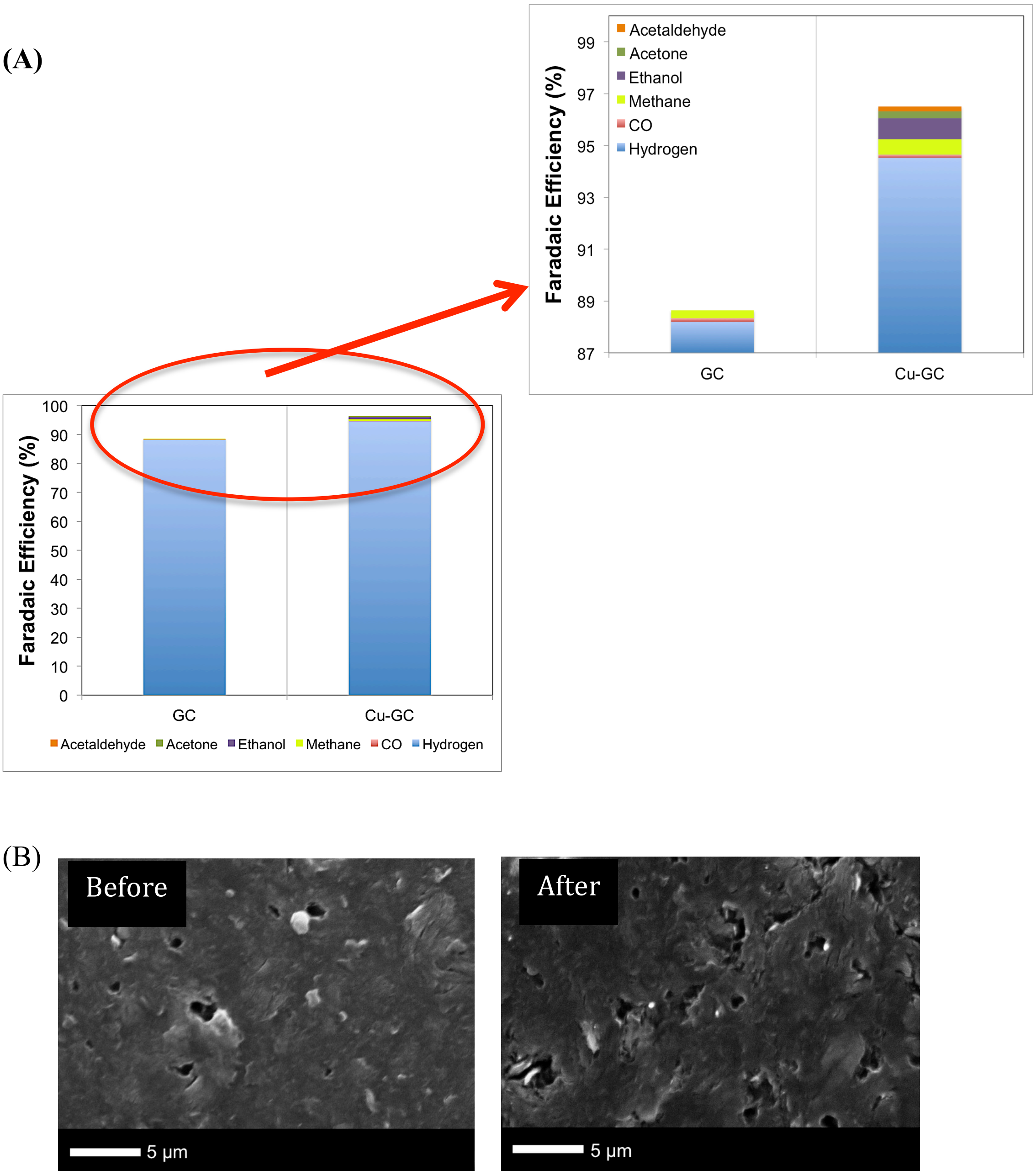

Figure 13. (A) Faradaic efficiency of CO_2 electrochemical reduction on GC and Cu-GC electrode (B) SEM images of Cu-BDD electrode before and after reduction at potential reduction -1.0 V (*vs*. Ag/AgCl) during 2 hours.

In conclusion, the production of C_2/C_3 species is feasible on a relatively inert BDD electrode by modifying it with Cu. Previously, Roy et al. [26] reported a study on a copper-modified BDD electrode in aqueous ionic liquid. Nonetheless, products higher than C_1 species were not reported and they were dominated by hydrogen gas. Despite using similarly modified electrodes, the higher potentials applied and the bigger sizes and greater amounts of Cu particles, which promote faster electron and proton transfer, may be the reasons for this. Recently, Song et al. [27] reported ethanol production on a Cu nanoparticle/N-doped graphene electrode. The reaction pathway, however, remains in question, and although similar behavior was shown using a doped material, the other benefit of using BDD electrodes is that they are highly durable and promising for real applications. Moreover, using BDD electrodes, C_3 species, which were not observed by Song et al., were observed for the first time. The future challenge is to develop an optimum procedure for the reduction of CO_2 to high carbon-containing compounds.

4. Conclusion

The electrochemical reduction of CO_2 on Cu-BDD electrodes was successfully carried out, producing C_2/C_3 species with high efficiency at low reduction potentials. The Cu deposited on the electrodes remained stable, showing insignificant differences after 2 hours reduction at -1.0 V *vs*. Ag/AgCl or less. The wide potential window of BDD seems to be responsible for suppressing the production of hydrogen compared to a glassy carbon electrode. Moreover, nano-sized Cu particles increase the affinity with which CO_2 becomes attached to the surface of the electrode, thus increasing the feasibility of C-C coupling, leading to the production of higher carbon-containing compounds. The production of C_2/C_3 species will give impetus to further studies using BDD electrodes to possibly produce high carbon-containing compounds with certain types of catalyst.

5. References

[1] K. Nakata, T. Ozaki, C. Terashima, A. Fujishima, Y. Einaga, High-yield electrochemical production of formaldehyde from CO_2 and seawater, Angew. Chemie - Int. Ed. 53 (2014) 871–874.

[2] N. Ikemiya, K. Natsui, K. Nakata, Y. Einaga, Effect of alkali-metal cations on the electrochemical reduction of carbon dioxide to formic acid using boron-doped diamond electrodes, RSC Adv. 7 (2017) 22510–22514.

[3] P.K. Jiwanti, K. Natsui, K. Nakata, Y. Einaga, Selective production of methanol by the electrochemical reduction of CO_2 on boron-doped diamond electrodes in aqueous ammonia solution, RSC Adv. 6 (2016) 102214–102217.

[4] N.S. Romero Cuellar, K. Wiesner-Fleischer, O. Hinrichsen, M. Fleischer, Electrochemical Reduction of CO_2 in Water-Based Electrolytes $KHCO_3$ and K_2SO_4 Using Boron Doped Diamond Electrodes, ChemistrySelect. 3 (2018) 3591–3595.

[5] C.W. Li, J. Ciston, M.W. Kanan, Electroreduction of carbon monoxide to liquid fuel on oxide-derived nanocrystalline copper, Nature. 508 (2014) 504–507.

[6] Y. Hori, H. Wakebe, T. Tsukamoto, O. Koga, Electrocatalytic process of CO selectivity in electrochemical reduction of CO_2 at metal electrodes in aqueous media, Electrochem. Commun. 39 (1994) 1833–1839.

[7] K.P. Kuhl, E.R. Cave, D.N. Abram, T.F. Jaramillo, New insights into the electrochemical reduction of carbon dioxide on metallic copper surfaces, Energy Environ. Sci. 5 (2012) 7050–7059.

[8] J.L. White, M.F. Baruch, J.E. Pander, Y. Hu, I.C. Fortmeyer, J.E. Park, T. Zhang, K. Liao, J. Gu, Y. Yan, T.W. Shaw, E. Abelev, A.B. Bocarsly, Light-Driven Heterogeneous Reduction of Carbon Dioxide: Photocatalysts and Photoelectrodes, Chem. Rev. 115 (2015) 12888–12935.

[9] M. Gattrell, N. Gupta, A. Co, A review of the aqueous electrochemical reduction of CO_2 to hydrocarbons at copper, J. Electroanal. Chem. 594 (2006) 1–19.

[10] A.A. Peterson, F. Abild-Pedersen, F. Studt, J. Rossmeisl, J.K. Nørskov, How copper catalyzes the electroreduction of carbon dioxide into hydrocarbon fuels,

Energy Environ. Sci. 3 (2010) 1311–1315.

[11] D. Kim, C.S. Kley, Y. Li, P. Yang, Copper nanoparticle ensembles for selective electroreduction of CO_2 to C_2–C_3 products, Proc. Natl. Acad. Sci. 114 (2017) 10560–10565.

[12] O.A. Baturina, Q. Lu, M.A. Padilla, L. Xin, W. Li, A. Serov, K. Artyushkova, P. Atanassov, F. Xu, A. Epshteyn, T. Brintlinger, M. Schuette, G.E. Collins, CO_2 electroreduction to hydrocarbons on carbon-supported Cu nanoparticles, ACS Catal. 4 (2014) 3682–3695.

[13] T.W. Wahyuni, T.A. Ivandini, P.K. Jiwanti, S. Endang, J. Gunlazuardi, Y. Einaga, Electrochemical Behavior of Zanamivir at Gold-Modified Boron-Doped Diamond Electrodes for an Application in Neuraminidase Sensing, Electrochemistry. 83 (2015) 357–362.

[14] T.A. Ivandini, Y. Einaga, Polycrystalline boron-doped diamond electrodes for electrocatalytic and electrosynthetic applications, Chem. Commun. 53 (2017) 1338–1347.

[15] T. Yano, D.A. Tryk, K. Hashimoto, A. Fujishima, Electrochemical Behavior of Highly Conductive Boron-Doped Diamond Electrodes for Oxygen Reduction in Alkaline Solution, J. Electrochem. Soc. 145 (1998) 1870–1876.

[16] T. Yano, E. Popa, D.A. Tryk, K. Hashimoto, A. Fujishima, Electrochemical Behavior of Highly Conductive Boron-Doped Diamond Electrodes for Oxygen Reduction in Acid Solution, J. Electrochem. Soc. 146 (1999) 1081–1087.

[17] H.Y. Kim, I. Choi, S.H. Ahn, S.J. Hwang, S.J. Yoo, J. Han, J. Kim, H. Park, J.H. Jang, S.K. Kim, Analysis on the effect of operating conditions on electrochemical conversion of carbon dioxide to formic acid, Int. J. Hydrogen Energy. 39 (2014) 16506–16512.

[18] K. Manthiram, B.J. Beberwyck, A.P. Alivisatos, Enhanced electrochemical methanation of carbon dioxide with a dispersible nanoscale copper catalyst, J. Am. Chem. Soc. 136 (2014) 13319–13325.

[19] Y. Hori, A. Murata, R. Takahashi, Formation of Hydrocarbons in the Electrochemical Reduction of Carbon Dioxide at a Copper Electrode in Aqueous Solution, J. Chem. Soc. Faraday Trans Actions 1. 85 (1989) 2309–2326.

[20] M.R. Gonçalves, A. Gomes, J. Condeço, T.R.C. Fernandes, T. Pardal, C.A.C.

Sequeira, J.B. Branco, Electrochemical conversion of CO_2 to C_2 hydrocarbons using different ex situ copper electrodeposits, Electrochim. Acta. 102 (2013) 388–392.

[21] R. Kas, R. Kortlever, A. Milbrat, M.T.M. Koper, G. Mul, J. Baltrusaitis, Electrochemical CO_2 reduction on Cu_2O-derived copper nanoparticles: Controlling the catalytic selectivity of hydrocarbons, Phys. Chem. Chem. Phys. 16 (2014) 12194–12201.

[22] J.H. Montoya, A.A. Peterson, J.K. Nørskov, Insights into C-C Coupling in CO_2 Electroreduction on Copper Electrodes, ChemCatChem. 5 (2013) 737–742.

[23] F. Calle-Vallejo, M.T.M. Koper, Theoretical Considerations on the Electroreduction of CO to C_2 Species on Cu(100) Electrodes, Angew. Chemie Int. Ed. 52 (2013) 7282–7285.

[24] S. Vollmer, G. Witte, C. Wöll, Determination of site specific adsorption energies of CO on copper, Catal. Letters. 77 (2001) 97–101.

[25] N. Ikemiya, K. Natsui, K. Nakata, Y. Einaga, Long-Term Continuous Conversion of CO_2 to Formic Acid Using Boron-Doped Diamond Electrodes, ACS Sustain. Chem. Eng. 6 (2018) 8108–8112.

[26] N. Roy, Y. Shibano, C. Terashima, K.I. Katsumata, K. Nakata, T. Kondo, M. Yuasa, A. Fujishima, Ionic-Liquid-Assisted Selective and Controlled Electrochemical CO_2 Reduction at Cu-Modified Boron-Doped Diamond Electrode, ChemElectroChem. 3 (2016) 1044–1047.

[27] Y. Song, R. Peng, D.K. Hensley, P. V. Bonnesen, L. Liang, Z. Wu, H.M. Meyer, M. Chi, C. Ma, B.G. Sumpter, A.J. Rondinone, High-Selectivity Electrochemical Conversion of CO_2 to Ethanol using a Copper Nanoparticle/N-Doped Graphene Electrode, ChemistrySelect. 1 (2016) 6055–6061.

4

Chapter

Electrochemical reduction of CO_2 on palladium modified boron-doped diamond electrodes

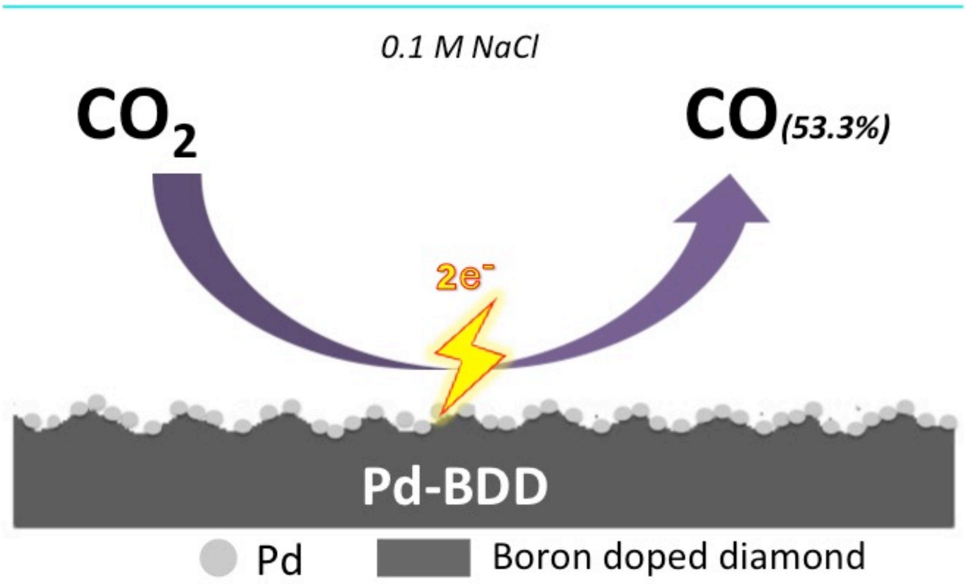

This chapter has been published as an article:
P. K. Jiwanti, Y. Einaga, Phys. Chem. Chem. Phys (2016) DOI:10.1039/C9CP01409H

Abstract

In recent years, the utilization of boron doped diamond (BDD) as an excellent electrode for CO_2 electrochemical reduction is attractive and has been published in several reports. Its wide potential window may decrease the hydrogen evolution that is known as a CO_2 reduction reaction competitor. On the other hand, a high overpotential still become an obstacle. We report a surface modification with deposited metal as an effort to overcome the issue. Pd metal was chosen to be modified onto surface of BDD electrode (PdBDD), resulting in enhancement of CO production (53.3% faradaic efficiency) as a used-to-be side product on CO_2 reduction using BDD electrode, by applying lower potential of -1.6 V *vs.* Ag/AgCl. Various attempts are presented to improve the production of CO.

1. Introduction

Carbon dioxide (CO_2) has been known as a notorious greenhouse gas, which is abundantly available in atmosphere. It is produced naturally or artificially through fuel combustion in transportations and many industrial processes. Ideally, as what we hope, the produced CO_2 will be equal or even less than what is consumed. However, with the high industrial activity, the concentration of CO_2 gas increases every year and unfortunately, go beyond the balance of environmental stability [1,2]. Therefore, increasing the value of this cheap and high available gas in atmosphere by CO_2 conversion method is enormously attractive and also necessary to support the environmental protection issue. Meanwhile the conversion of CO_2 gas to useful chemical stocks [3-5], or more further to convert it back to fuel [6], have been studied by many researchers around the world, as one of the attempt to obtain a value added chemicals [7] . Among many techniques that have been attempted, electrochemical reduction is one of a widely used method. However, this method suffers for a drawback. CO_2 gas is thermodynamically stable and chemically inert molecule [8], which requires a very high potential as high as -1.9 V *vs.* NHE to transfer 1 electron to CO_2 molecule. Therefore, this causes the hydrogen evolution to take place, and interferes the CO_2 reduction.

These few years, an excellent electrode, namely BDD electrode, that has been known to have excellent results on numerous application such as sensor and synthesis applications [9-12], has been utilized for CO_2 electrochemical reduction in a form of unmodified/modified electrode. BDD has a wide potential window that may suppress the production of H_2 gas, in addition of this superior mechanically and chemically stable electrode behavior that is promising for practical applications. Einaga group has successfully utilized bare BDD electrode for CO_2 reduction and producing HCOOH with highest faradaic efficiency of 94.7% and the selectivity that reach more than 99% using a circulation flow cell [13,14]. Since then, many parameters have been carried out to improve the system and scientifically studied in detail about the phenomenon [15-17]. However, high overpotential is still being observed to reduce CO_2 gas, and moreover only C_1 product is successfully produced with bare BDD.

Therefore, an attempt has been carried out by modifying the surface of BDD electrode with the nanoparticle size of metal, in order to decrease the overpotential or to find the new products, which has higher number of carbon atoms. In a first result in copper modified on BDD electrode (Cu-BDD) could improve the production of C_2/C_3 species, in which ethanol, acetaldehyde, and acetone were produced with faradaic efficiency of 42.4%, 13.7%, and 7% respectively [18]. Hereafter, modification of other promising metal on surface of BDD electrode has been explored, to study and find new system with BDD electrode. There were not many studies on metal modified BDD electrode for CO_2 reduction, however several reports [19-23] show that metal modified on BDD electrode could improve the efficiency, producing new products, and lowering the overpotential for CO_2 reduction. Among those studies, palladium (Pd) metal modified on BDD electrode was not investigated yet so far, regardless of its well-known and widely used metal catalyst. Moreover, addressing of its behavior toward CO_2 reduction, Pd is a “special” metal in group VIIIB elements (i.e. Pt, Ir, Ni, etc), in which it has been observed about its ability to not only producing H_2 gas as it is generally being shown in this group [24,25]. Therefore, in this report, we present a Pd modification on surface of BDD electrode for CO_2 electrochemical reduction to CO, which has been known widely as an important starting material for chemicals in industry, such as manufacture of alcohol, aldehyde, and liquid hydrocarbons.

2. Experimental

2.1 Chemicals

NaCl (99.5%), Na_2SO_4 (99%), H_2SO_4 (98%), HCl (35%), and HNO_3 (60%) were purchased from Wako Pure Chemical Industries. $PdCl_2$ (99%) was purchased from Sigma Aldrich. All those reagents are used without any further purification. Ultra-pure water was obtained from Symply-Lab water system (Direct-Q UV3, Millipore).

2.2 Working electrodes preparation

BDD (1% B/C) electrodes were prepared by depositing on the surface of Si(111) wafers using a micro-wave plasma-assisted chemical vapor deposition system (Model AX-5400, CORNES Technology Corp.). The details are described elsewhere [26]. Meanwhile, the electrodeposition of Pd particles on BDD surface was carried out using chronoamperometry technique in one compartment cell containing 10 mL of 1mM $PdCl_2$/0.1 M HCl. The applied potential for deposition was -0.15 V during 30 s

(PdBDD30), 100 s (PdBDD100), 300 s (PdBDD300), 500 s (PdBDD500), and 1000 s (PdBDD1000). The palladium modified on BDD (PdBDD) electrodes were rinsed with ultra-pure water and dried under N_2 gas afterward. All PdBDD electrodes were recovered by immersing in aqua regia solution for 10 minutes, and then ultrasonicated in ultra-pure water during 5 minutes (2 times), and followed by pretreatment in 0.1 M H_2SO_4 by applying cyclic voltammetry (CV) performance from -3.5 V to 3.5 V (20 cycles), continued from 0 V to 3.5 V (10 cycles) with scan rate 1 V/s. The electrodes were characterized using scanning electron microscopy (SEM) (JCM-6000, JEOL), and X-Ray photoelectron spectroscopy (XPS) (JPS-9010TR, JEOL).

2.3 CO_2 reduction method

The electrolysis of CO_2 was conducted in two cells (15 mL in each cell) separated by Nafion membrane. 0.1 M Na_2SO_4 was used as an anolyte, and 0.1 M NaCl as a catholyte. Pt mesh and PdBDD electrodes were used as counter electrode and working electrodes respectively. All potentials were measured against Ag/AgCl (3M NaCl) unless otherwise stated. Prior to the electrochemical reduction, N_2 gas was bubbled into the catholyte to remove remained oxygen gas during 15 minutes in 100 sccm, followed by CO_2 gas purging in the same time and gas rate. CV performance at potential -0.5 V to 1.2 V was performed for each gas bubbling. The electrochemical reduction of CO_2 was then performed during 1 hour under stirring condition at various applied potentials (-1.4 V to -1.9 V). A low flow rate of CO_2 gas was purged into the cell to maintain CO_2 concentration during reduction. All electrochemical measurements were recorded using a potentiostat (Autolab PGSTAT204, Metrohm Autolab B.V.).

2.4 Products analysis method

The gas products were collected in a 1 L gas and 1 mL of liquid sample was taken from the cell and both of them were analyzed subsequently after reduction process. The gas products were analyzed by gas chromatography with a flame ionization detector and a thermal conductivity detector (GC-2014, Shimadzu Corp.). Liquid product was analyzed using high performance liquid chromatography (HPLC) with electroconductivity detector (Prominence, Shimadzu Corp.).

3. Results and Discussions

Figure 1 shows CV performances of PdBDD electrodes with different time depositions, in comparison with bare BDD electrode. The CVs were performed after CO_2 bubbling in 0.1 M NaCl solution, from potential -0.5 V to 1.2 V, before the CO_2 reduction was taken place. On bare BDD electrode, there are not any peaks can be observed around this potential range, showing one of excellent BDD behavior, that is a low background current of BDD electrode. As the Pd particles deposited on BDD surface, it shows typical Pd CV performance. On negative-going potential, H_2 adsorption happened at around potential -0.3 V, and continued by hydrogen evolution at >-0.4 V. On positive-going potential, we can see the H_2 desorption peak at around potential -0.3 V, followed by the oxidation peak of Pd^0 to Pd^{2+} at around potential 0.7 V and back as a reduction of Pd^{2+} to Pd^0 at around potential 0.2 V. The CV performance also shows that as the deposition time longer, the amount of deposited Pd particles increases, and thus the Pd oxidation peak at potential 0.7 V increases.

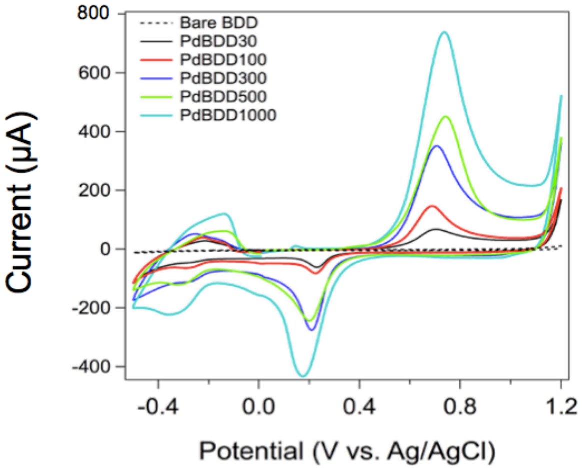

Figure 1. The CV performances of PdBDD electrodes with different Pd time deposition. The scan rate was 100 mV/s, from potential -0.5 V to 1.2 V *vs.* Ag/AgCl.

Meanwhile, SEM images were performed for all PdBDD electrodes after the electrodeposition at potential -0.15 V in different time depositions (Figure 2(1)-(5)). The particles are deposited quite homogeneously on all active deposition surface, with the particles size are around ~50 nm in average, except on PdBDD500 and

PdBDD1000 electrodes where the particles agglomerate, forms larger size of particles (~160 nm). In addition, the mass of Pd particles is calculated based on the total charge consumed during the electrodeposition, by considering of no contribution of hydrogen evolution. On PdBDD30, the mass of particles is 2.75 μg/cm^2, and increases as the deposition time becomes longer (Figure 2(6)). Moreover, the presence of Pd particles on surface of BDD electrode was also characterized using XPS, showing the peak of Pd$^{5/2}$ at 335.3 eV and Pd$^{3/2}$ at 340.5 eV, that represent the metallic form of Pd (Pd^0). Deconvolution method shows that the amount of PdOx on the surface is less than 10%, and thus the catalytic effect of Pd is considered coming from the Pd^0 species (Figure 3).

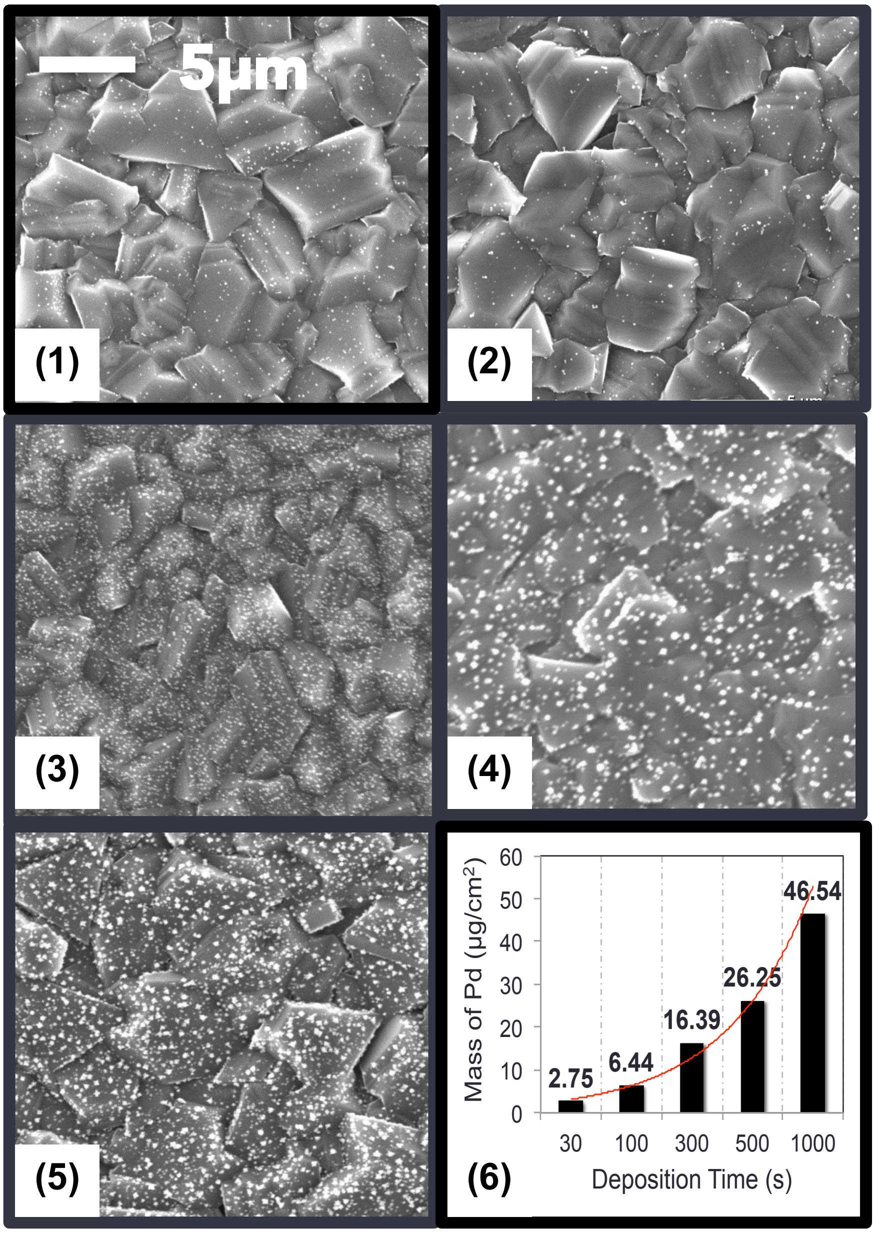

Figure 2. The SEM images of PdBDD electrodes prepared at potential -0.15 V with deposition time 30 s (1), 100 s (2), 300 s (3), 500 s (4), 1000 s (5), and the mass of Pd particles *vs*. deposition time dependence (6).

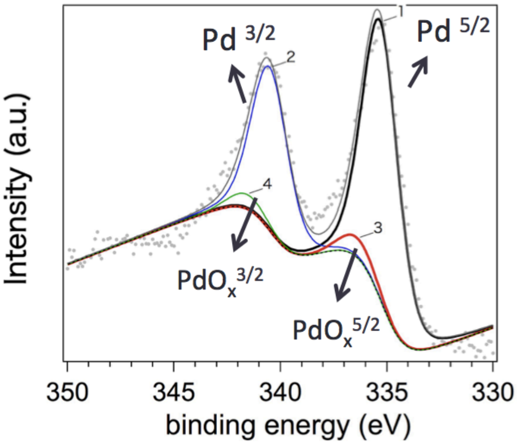

Figure 3. XPS spectra (narrow scan) with deconvolution method of Pd-BDD electrode

The electrochemical reduction of CO_2 was evaluated from the CVs after N_2 and CO_2 bubbling by scanning from potential -1.8 V to 1.2 V (Figure 4). The scan was carried out from 0 V to the anodic potential 1.2 V and go through the cathodic potential, and back to 0 V. At this potential range, CO_2 reduction was considered to be taken place, as it can be observed from the reduction peak at potential around -1.0 V, which contributed to the reduction of CO_2 to reduced-CO_2 species as it cannot be seen at the CV after N_2 bubbling. This result is consistent with the results mentioned in Ref.[27,28], where the adsorbed-CO (CO_{ad}) is formed on the surface of electrode during the CV in bicarbonate solution containing CO_2 gas, and this CO_{ad} is oxidized again back to CO_2 at anodic potential. In addition, in the presence of CO_2, the hydrogen evolution is shifted in more negative potential, explaining that the CO_2 reduction is catalyzed, producing reduced-CO_2 species and covering the surface of BDD, and thus decreasing the H_2 evolution itself. Beside that, all CVs of PdBDD electrodes in different Pd deposition time show that as the deposition time of Pd increases, the oxidation peak of Pd (at 0.7 V) is increased, as well as the intensity of peak at -1.0 V that indicates the increasing of the reduced-CO_2 species amount attached to the surface of BDD electrode.

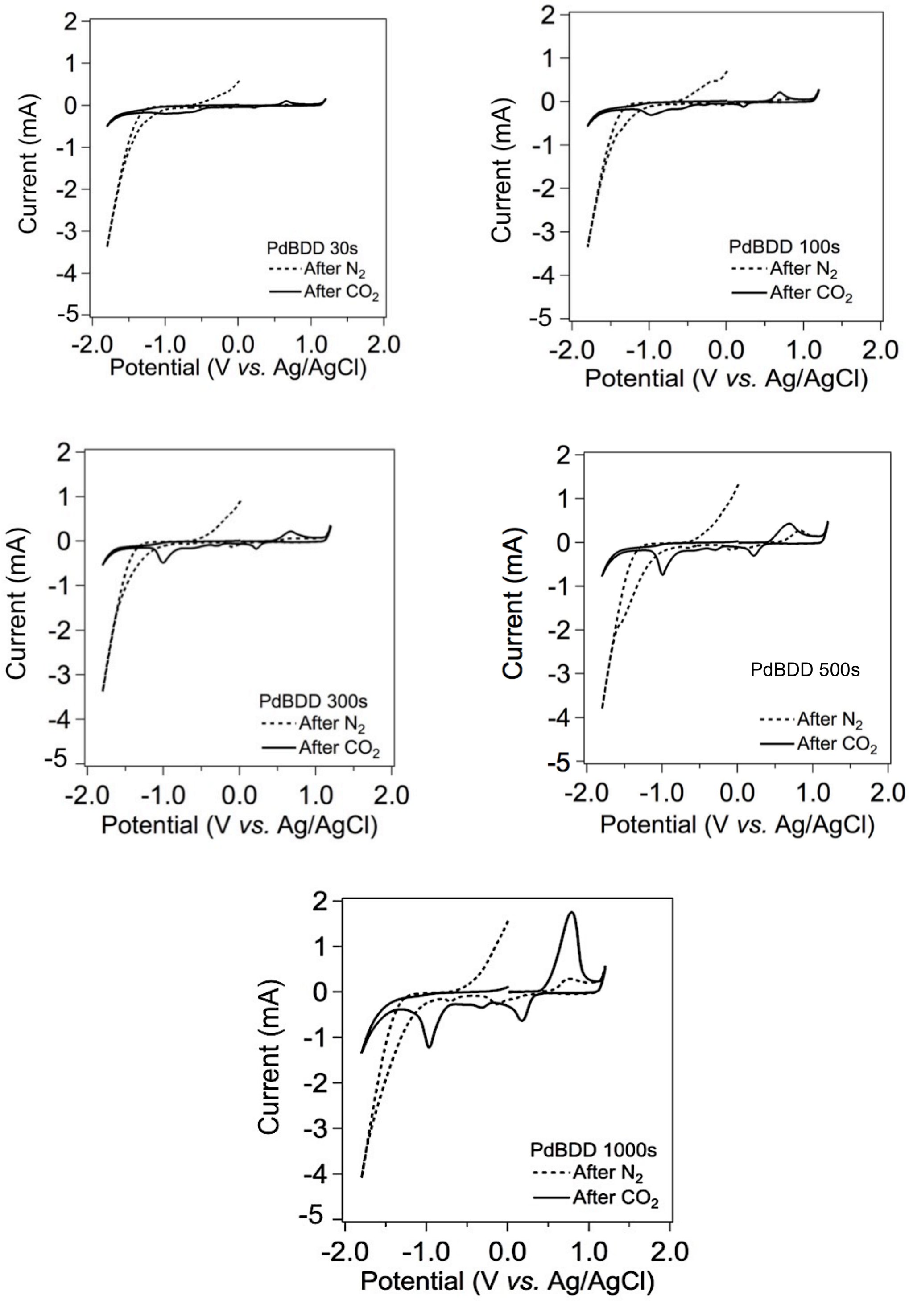

Figure 4. CV of PdBDD after N_2 and CO_2 gas bubbling performed at potential -1.8 V to 1.2 V with scan rate of 100 mV/s.

Although we perform the CV performance before the electrochemical reduction, we found that it did not affect the Pd modified electrode significantly. To be sure about the surface of the modified electrode, SEM images before and after one-time

CV performance was carried out (Figure 5). The results show that there were insignificant differences.

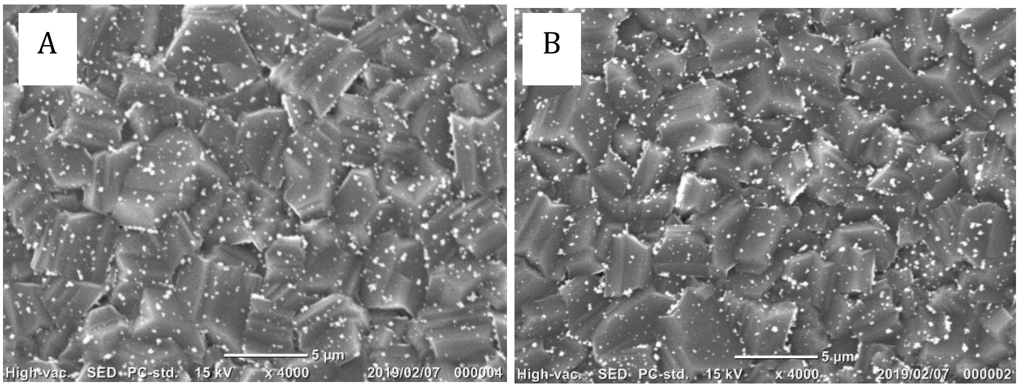

Figure 5. SEM images of PdBDD electrode (A) before and (B) after CV performance (-0.5 V to 1.2 V *vs.* Ag/AgCl)

The electrochemical reduction of CO_2 was then carried out on all PdBDD electrodes. The products detected were CO, HCOOH, and H_2 gas. The chromatograms of each product are shown in Figure 6.

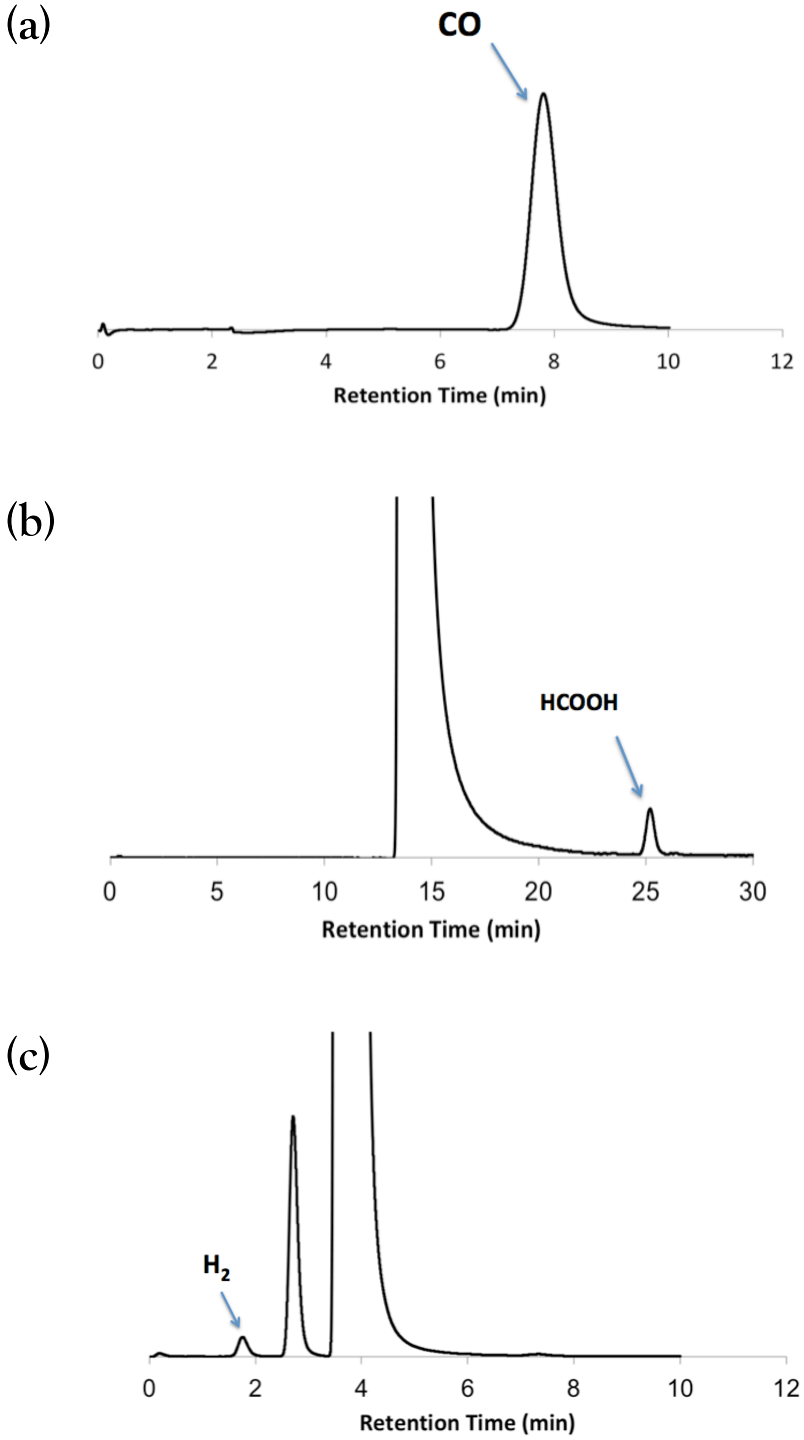

Figure 6. The product's chromatogram of (a) CO (b) HCOOH and (c) H_2 from the CO_2 electrochemical reduction on PdBDD300 at potential -1.6 V during 1 hour.

Meanwhile, the electrochemical reduction of CO_2 at potential -1.5 V during 1 hour shown in Figure 7. CO is the main product of CO_2 reduction, with HCOOH as the side products. There are no other products detected, and that the total faradaic efficiencies are more or less ~100%. Faradaic efficiency of CO is calculated based on $2e^-$ consumed in reduction, according to this reaction:

$$CO_2 + H^+_{(aq)} + 2e^- \rightarrow CO_{(g)} + OH^-_{(aq)} \qquad (1)$$

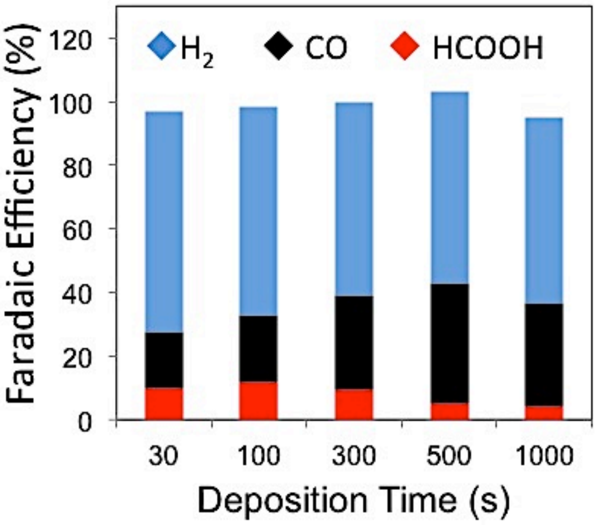

Figure 7. Faradaic efficiency of CO_2 electrochemical reduction products performed at potential -1.5 V during 1 hour reduction on PdBDD electrodes with different Pd deposition time.

The faradaic efficiency of CO is increased as the amount of Pd particles increased, and it slightly decreases after 500 s deposition. It can be explained by the instability of deposited Pd particles, where the Pd particles are agglomerated on longer deposition time, and thus easier to be detached from surface of electrode, that also causes the decreasing of current density value for CO_2 reduction (Figure 8).

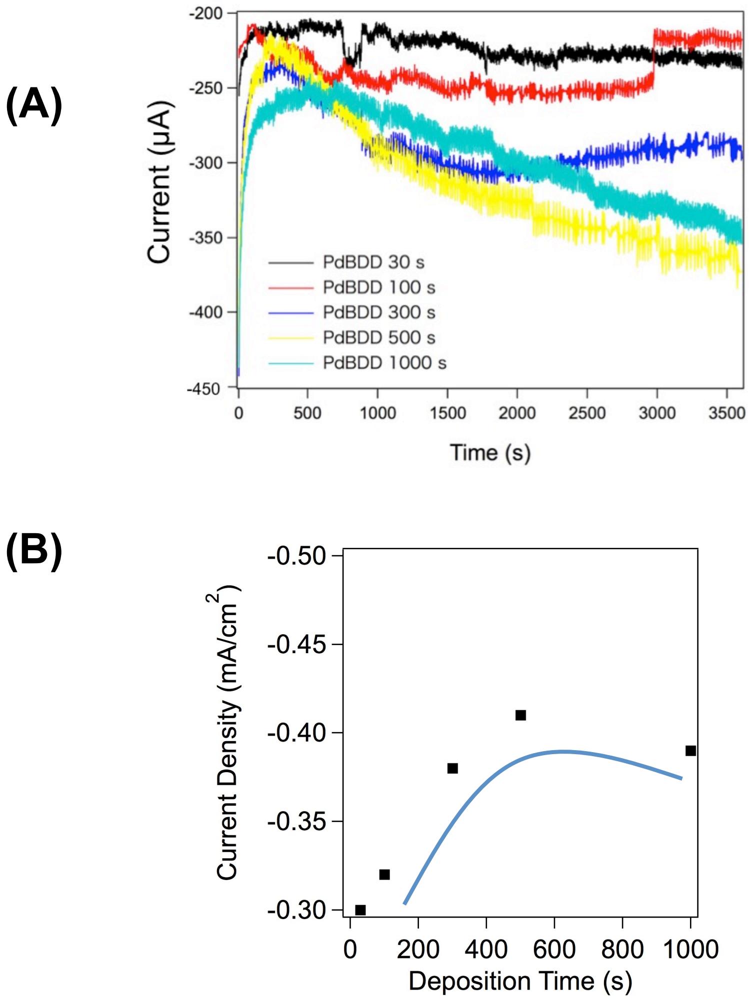

Figure 8. Chronoamperometry for the electrochemical reduction of CO_2 (A) and the current density at a potential of -1.5 V (B) during 1 hour reduction using PdBDD electrodes with different Pd deposition time.

In order to study in detailed, the potential dependence, ranging from -1.4 V to -1.9 V was performed on each PdBDD electrodes (Figure 9). The maximum production of CO is 53.3% (HCOOH 9.29%, H_2 39.86%) on PdBDD300 at potential -1.6 V. This production of CO is approximately five times higher than that on bare BDD and even on Pd metal electrode in the same system and conditions, where the production of CO is around ~9% (Table 1). Thus, deposited Pd particles on surface of BDD may catalyze the production of CO at relatively lower potential than that used-to-be in CO_2 reduction on bare BDD (>-2.0 V), to produce higher CO_2 reduction products [13].

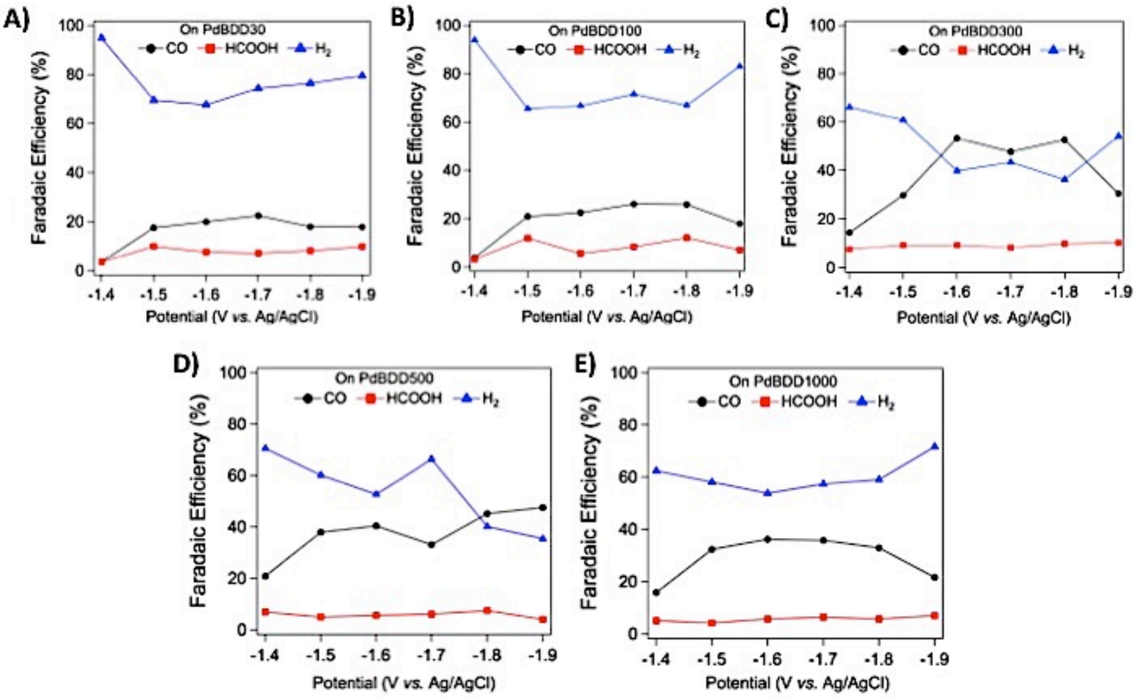

Figure 9. Faradaic efficiency *vs.* potential dependence of CO_2 electrochemical reduction products on A) PdBDD30, B) PdBDD100, C) PdBDD300, D) PdBDD500, E) PdBDD1000, performed during 1hour reduction.

Table 1. Faradaic efficiencies for the products produced using bare BDD and Pd metal electrodes

Electrode	Potential/V	Faradaic Efficiency/%		
		HCOOH	CO	H_2
Bare BDD	-1.6	5.76	9.95	84.92
Pd metal*	-1.6	0.70	9.34	8.53

*The total faradaic efficiency of the products with the Pd metal electrode is far from 100%. This might be due to dissolution of H_2 into the electrode [29].

Meanwhile, the CO production on PdBDD30 and PdBDD100 are maximum at the value of ~20% faradaic efficiency in all potential variations, which is two times higher than that on bare BDD. Whereas on PdBDD300, PdBDD500, and PdBDD1000, it can be improved to about 30-50% faradaic efficiencies, which is three to five times higher than that on bare BDD, by applying potential of -1.5 V or more. It shows that sufficient amount of Pd particles are necessary to obtain best result for CO production. Small amount of Pd particles are improving the faradaic efficiency up to two times higher only, on the other hand high amount of Pd particles have a shortage in case of its stability during electrochemical reduction. The SEM images (Figure 10) and particle size of Pd particles measurements (Figure 11-12) on the surface of BDD electrode shows the difference before and after electrochemical reduction on PdBDD electrodes at potential -1.5 V during 1 hour reduction, where the size of Pd particles on PdBDD500 and PdBDD1000 are decreasing, that might be due to the particles that detached from the surface of BDD. Unlike the particle size dependence study in literatures [30,31], however, it is suggested that the particle size dependence in this range is not visibly affecting the CO production since the faradaic efficiency of CO could be achieved up to ~40% on PdBDD500 which has larger particle size than that on PdBDD300. In addition, since the production of HCOOH is relatively same (more or less 5~10%) in all variations, it may explain that the catalytic effect of Pd particles might only influence the CO productions. Regardless of the recent study on metal modified BDD electrode produces CO on Cu-SnO_x/BDD electrode [22], this study is giving new point of view of the Pd utilization on BDD electrode for CO_2 reduction, which has high catalytic activity yet has stability from corrosion, unlike Cu. And thus, it is assumed that using Pd as a noble metal to be modified onto BDD surface may increase the durability of electrocatalytic effect on electrode.

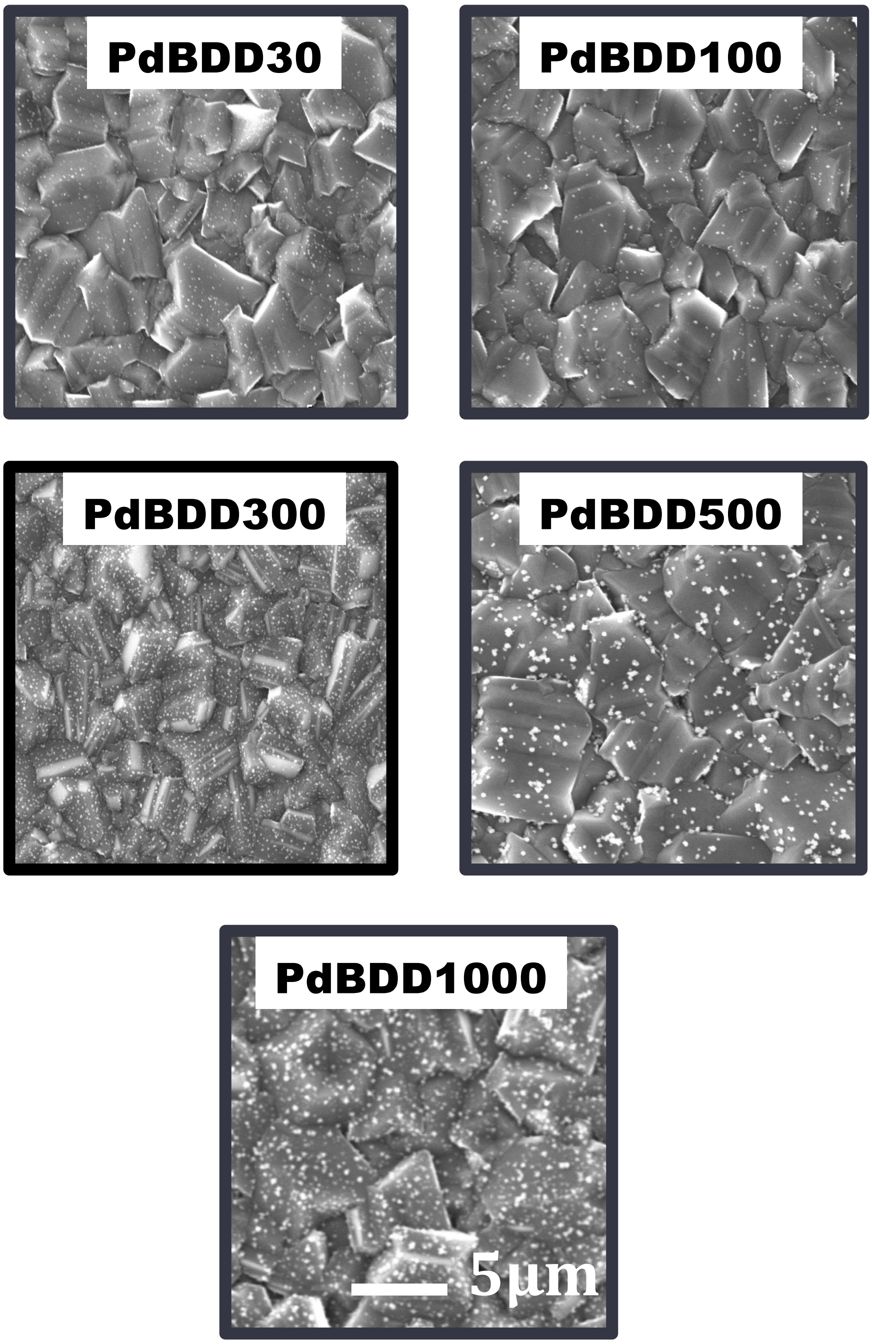

Figure 10. SEM images of PdBDD electrodes after the electrochemical reduction of CO_2 at a potential of -1.5 V for 1 hour.

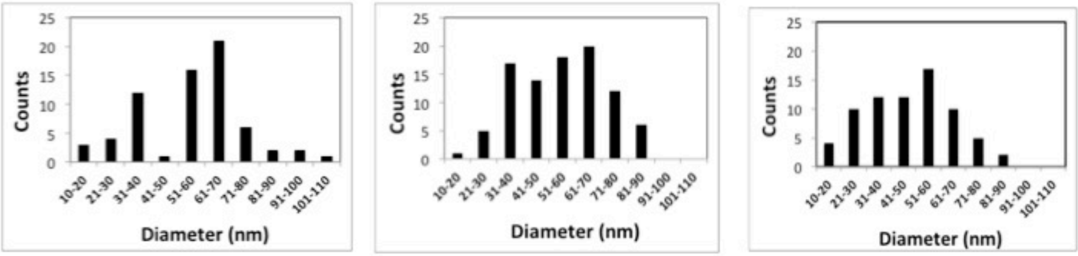

PdBDD30
Mean: 55.02 nm

PdBDD100
Mean: 55.21 nm

PdBDD300
Mean: 47.13 nm

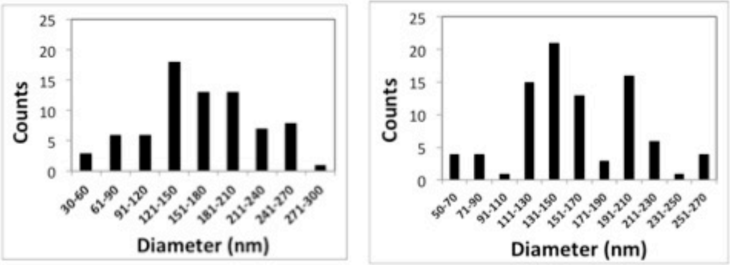

PdBDD500
Mean: 160.36 nm

PdBDD1000
Mean: 156.65 nm

Figure 11. Pd particle size distribution after electrochemical deposition at a potential of -0.15 V using electrodes with different deposition times

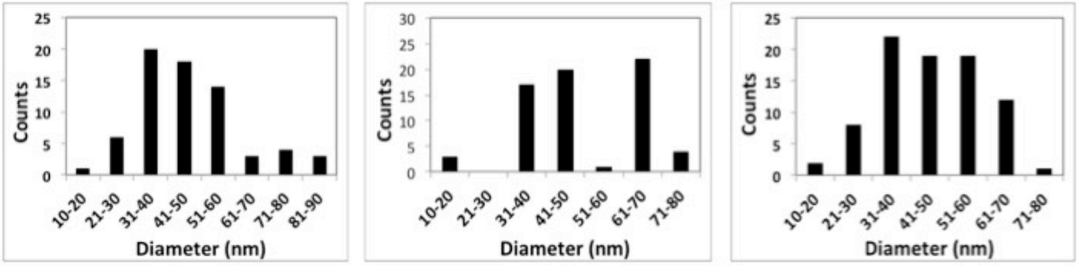

PdBDD30
Mean: 46.64 nm

PdBDD100
Mean: 48.85 nm

PdBDD100
Mean: 45.25 nm

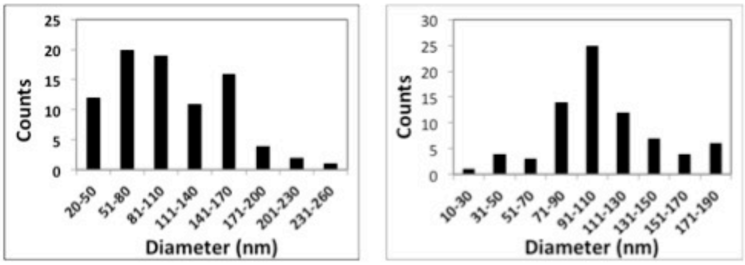

PdBDD500
Mean: 104.19 nm

PdBDD1000
Mean: 107.74 nm

Figure 12. Pd particle size distribution on the different PdBDD electrodes, after electrochemical reduction of CO_2 at a potential of -1.5 V for 1 hour.

In addition, the stability of the PdBDD500 for the CO_2 electrochemical reduction to CO at potential -1.6 V *vs*. Ag/AgCl was carried out. Each experiment was conducted for 1 hour. The result showed the faradaic efficiency for CO was not changed significantly for up to four times electrolysis with the same condition, without any electrode recovery (Figure 13)

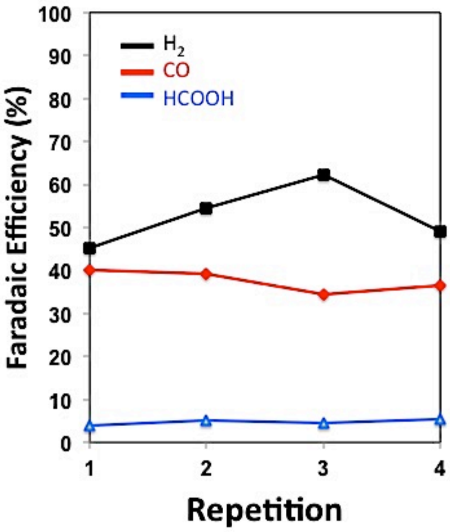

Figure 13. Products faradaic efficiency of CO_2 electrochemical reduction on PdBDD500 electrode for four times reduction at potential -1.6 V *vs*. Ag/AgCl.

Moreover, since the system was carried out under stirring condition, the effect of stirring speed was studied. It has been known that the mass transfer to surface of electrode has also a big meaning for CO_2 reduction activity and selectivity [32]. A stirring will improve the transfer of dissolved CO_2 in a bulk to come closer to the electrode [33], and further affecting the CO_2 products efficiency. The stirring speeds were applied as a low (~120 rpm), middle (~240 rpm), and fast (~480 rpm) speed, performed at potential -1.6 V on PdBDD300 (Figure 14).

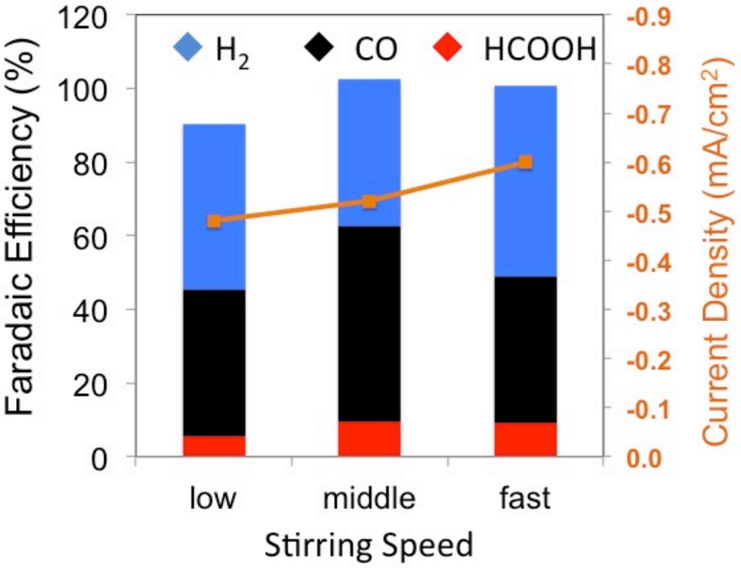

Figure 14. Stirring speed dependence of the faradaic efficiencies of the products and the current density during the electrochemical reduction of CO_2 carried out using PdBDD300 at a potential of -1.6 V for 1 hour.

At low stirring speed, 39.92% faradaic efficiency of CO was produced, and it was increased to 53.29% at middle stirring speed. However, the faradaic efficiency of CO was dropped to 39.79% at fast stirring speed, as a contrary to higher hydrogen production. This can be explained by paying attention to the current consumed during the electroreduction. As we can see, the current density was increased gradually as the stirring speed went faster. Taking a concern to the trend of exchange current of various metals *vs.* calculated free energy of H adsorption, known as “the volcano plot”[34,35], metals stand in the left side of volcano plot has a large H coverage, in contrary to metals stand in right side of volcano plot which has small H coverage. Meanwhile, Pd is in the left side of volcano plot, where the high current density may result in the higher faradaic efficiency of hydrogen production. Therefore, it limits the CO_2 reduction itself. Finally, the appropriate stirring speed is necessary to control the mass transfer, while taking into account the catalytic activity of metal toward hydrogen production.

4. Conclusion

In summary, we successfully modified the Pd particles onto the surface of BDD electrode to be applied for CO_2 electrochemical reduction for the first time. CO is the main CO_2 reduction product at potential -1.6 V with the existence of Pd particles 16.39 μg/cm^2 modified on surface of BDD electrode. The deposited Pd particles remained stable after electrochemical reduction at potential -1.5 V on the surface of PdBDD30, PdBDD100, and PdBDD300. As the particles grow bigger on PdBDD500 and PdBDD1000, the size of Pd particles decreases subsequently after reduction. At last, Pd is an alternative metal to be deposited on the surface of BDD electrode that has high activity for CO_2 reduction, and thus it possibly decreases the overpotential for CO_2 reduction on BDD electrode, especially for increasing the CO production that used to be known as a side product in CO_2 reduction using BDD electrode.

5. References

[1] J.S. Sawyer, Man-made Carbon Dioxide and the “Greenhouse” Effect, Nat. N. 239 (1972) 23–26.

[2] S. Willie, L.B. Sallie, B.R. Arthur, W.R. Zachary, Environmental effects of increased atmospheric carbon dioxide, Clim. Res. 13 (1999) 149–164.

[3] M. Gattrell, N. Gupta, A. Co, A review of the aqueous electrochemical reduction of CO_2 to hydrocarbons at copper, J. Electroanal. Chem. 594 (2006) 1–19..

[4] J. Qiao, Y. Liu, F. Hong, J. Zhang, A review of catalysts for the electroreduction of carbon dioxide to produce low-carbon fuels, 2014.

[5] W. Zhang, Y. Hu, L. Ma, G. Zhu, Y. Wang, X. Xue, R. Chen, S. Yang, Z. Jin, Progress and Perspective of Electrocatalytic CO_2 Reduction for Renewable Carbonaceous Fuels and Chemicals, Adv. Sci. 5 (2018) 1700275.

[6] J. Wei, Q. Ge, R. Yao, Z. Wen, C. Fang, L. Guo, H. Xu, J. Sun, Directly converting CO_2 into a gasoline fuel, Nat. Commun. 8 (2017) 1–8.

[7] S. Möhle, M. Zirbes, E. Rodrigo, T. Gieshoff, A. Wiebe, S.R. Waldvogel, Modern Electrochemical Aspects for the Synthesis of Value-Added Organic Products, Angew. Chemie - Int. Ed. 57 (2018) 6018–6041.

[8] Y. Einaga, Diamond electrodes for electrochemical analysis, J. Appl. Electrochem. 40 (2010) 1807–1816.

[9] T.A. Ivandini, Y. Einaga, Polycrystalline boron-doped diamond electrodes for electrocatalytic and electrosynthetic applications, Chem. Commun. 53 (2017) 1338–1347.

[10] S.R. Waldvogel, S. Lips, Use of Boron□doped Diamond Electrodes in Electro□organic Synthesis, ChemElectroChem. 6 (2019) 1649–1660.

[11] N. Yang, S. Yu, J. V. Macpherson, Y. Einaga, H. Zhao, G. Zhao, G.M. Swain, X. Jiang, Conductive diamond: synthesis, properties, and electrochemical applications, Chem. Soc. Rev. 48 (2019) 157–204.

[12] N. Yang, S.R. Waldvogel, X. Jiang, Electrochemistry of Carbon Dioxide on Carbon Electrodes, ACS Appl. Mater. Interfaces. 8 (2016) 28357–28371.

[13] K. Natsui, H. Iwakawa, N. Ikemiya, K. Nakata, Y. Einaga, Stable and Highly Efficient Electrochemical Production of Formic Acid from Carbon Dioxide

Using Diamond Electrodes, Angew. Chemie - Int. Ed. 57 (2018) 2639–2643.

[14] N. Ikemiya, K. Natsui, K. Nakata, Y. Einaga, Long-Term Continuous Conversion of CO_2 to Formic Acid Using Boron-Doped Diamond Electrodes, ACS Sustain. Chem. Eng. 6 (2018) 8108–8112.

[15] M. Tomisaki, K. Natsui, N. Ikemiya, K. Nakata, Y. Einaga, Influence of Electrolyte on the Electrochemical Reduction of Carbon Dioxide Using Boron-Doped Diamond Electrodes, ChemistrySelect. 3 (2018) 10209–10213.

[16] N. Ikemiya, K. Natsui, K. Nakata, Y. Einaga, Effect of alkali-metal cations on the electrochemical reduction of carbon dioxide to formic acid using boron-doped diamond electrodes, RSC Adv. 7 (2017) 22510–22514.

[17] M. Tomisaki, S. Kasahara, K. Natsui, N. Ikemiya, Y. Einaga, Switchable Product Selectivity in the Electrochemical Reduction of Carbon Dioxide Using Boron-Doped Diamond Electrodes, J. Am. Chem. Soc. 114 (2019) 7414-7420

[18] P.K. Jiwanti, K. Natsui, K. Nakata, Y. Einaga, The electrochemical production of C_2/C_3 species from carbon dioxide on copper-modified boron-doped diamond electrodes, Electrochim. Acta. 266 (2018) 414–419.

[19] N. Roy, Y. Shibano, C. Terashima, K.I. Katsumata, K. Nakata, T. Kondo, M. Yuasa, A. Fujishima, Ionic-Liquid-Assisted Selective and Controlled Electrochemical CO_2 Reduction at Cu-Modified Boron-Doped Diamond Electrode, ChemElectroChem. 3 (2016) 1044–1047.

[20] N. Roy, Y. Hirano, H. Kuriyama, P. Sudhagar, N. Suzuki, K. Katsumata, K. Nakata, T. Kondo, M. Yuasa, I. Serizawa, T. Takayama, A. Kudo, A. Fujishima, C. Terashima, Boron-doped diamond semiconductor electrodes: Efficient photoelectrochemical CO_2 reduction through surface modification, Sci. Rep. 6 (2016) 38010.

[21] N. Spataru, K. Tokuhiro, C. Terashima, T.N. Rao, A. Fujishima, Electrochemical reduction of carbon dioxide at ruthenium dioxide deposited on boron-doped diamond, J. Appl. Electrochem. 33 (2003) 1205–1210.

[22] N. Roy, N. Suzuki, Y. Nakabayashi, Y. Hirano, K. Katsumata, K. Nakata, A. Fujishima, C. Terashima, H. Ikari, Facile Deposition of Cu-SnOx Hybrid Nanostructures on the Lightly Boron-Doped Diamond Electrodes for CO_2 Reduction, ChemElectroChem. 5 (2018) 2542–2550.

[23] N.S. Romero Cuellar, K. Wiesner-Fleischer, O. Hinrichsen, M. Fleischer,

Electrochemical Reduction of CO_2 in Water-Based Electrolytes $KHCO_3$ and K_2SO_4 Using Boron Doped Diamond Electrodes, ChemistrySelect. 3 (2018) 3591–3595.

[24] W. Zheng, H.W. Man, L. Ye, S.C.E. Tsang, Electroreduction of Carbon Dioxide to Formic Acid and Methanol over a Palladium/Polyaniline Catalyst in Acidic Solution: A Study of the Palladium Size Effect, Energy Technol. 5 (2017) 937–944.

[25] R. Kortlever, I. Peters, C. Balemans, R. Kas, Y. Kwon, G. Mul, M.T.M. Koper, Palladium–gold catalyst for the electrochemical reduction of CO $_2$ to C $_1$ –C $_5$ hydrocarbons, Chem. Commun. 52 (2016) 10229–10232.

[26] T. Yano, D.A. Tryk, K. Hashimoto, A. Fujishima, Electrochemical Behavior of Highly Conductive Boron-Doped Diamond Electrodes for Oxygen Reduction in Alkaline Solution, J. Electrochem. Soc. 145 (1998) 1870–1876.

[27] D. Kolbe, W. Vielstich, Adsorbate formation during the electrochemical reduction of carbon dioxide at palladium-A DEMS study, 41 (1996) 2457–2460.

[28] S. Pérez-Rodríguez, N. Rillo, M.J. Lázaro, E. Pastor, Pd catalysts supported onto nanostructured carbon materials for CO2valorization by electrochemical reduction, Appl. Catal. B Environ. 163 (2015) 83–95.

[29] Y. Hori, A. Murata, Electrochemical evidence of intermediate formation of adsorbed CO in cathodic reduction of CO_2 at a nickel electrode, Electrochim. Acta. 35 (1990) 1777–1780.

[30] R. Reske, H. Mistry, F. Behafarid, B.R. Cuenya, P. Strasser, Particle Size Effects in the Catalytic Electroreduction of CO_2 on Cu Nanoparticles, J. Am. Chem. Soc. 136 (2014) 6978–6986.

[31] D. Gao, H. Zhou, J. Wang, S. Miao, F. Yang, G. Wang, J. Wang, X. Bao, Size-Dependent Electrocatalytic Reduction of CO_2 over Pd Nanoparticles, J. Am. Chem. Soc. 137 (2015) 4288–4291.

[32] D. Raciti, M. Mao, J.H. Park, C. Wang, Mass transfer effects in CO_2 reduction on Cu nanowire electrocatalysts, Catal. Sci. Technol. 8 (2018) 2364–2369.

[33] C.F.C. Lim, D.A. Harrington, A.T. Marshall, Effects of mass transfer on the electrocatalytic CO_2 reduction on Cu, Electrochim. Acta. 238 (2017) 56–63.

[34] S. Trasatti, WORK FUNCTION, ELECTRONEGATIVITY, AND

ELECTROCHEMICAL BEHAVIOUR OF METALS, J. Electroanal. Chem. Interfacial Electrochem. 39 (1972) 163–184.

[35] Y.J. Zhang, V. Sethuraman, R. Michalsky, A.A. Peterson, Competition between CO_2 reduction and H_2 evolution on transition-metal electrocatalysts, ACS Catal. 4 (2014) 3742–3748.

5

Chapter

CO_2 electrochemical reduction on metal-oxide modified BDD electrode: Study on Ni and Ir based metal

1. Introduction

The global monitoring for CO_2 concentration in atmosphere reports increasing of its well-known gas, called greenhouse gas. The high concentration of CO_2 gas in atmosphere could lead to the dangerous environmental effect. Accordingly, converting this cheap and abundant gas in atmosphere to be useful chemicals, not only will add the value of this gas, but broadly, will give a positive contribution for environment [1]. CO_2 electrochemical reduction has attracted researchers all over the world, as one of the method of CO_2 conversion [2-4].

Meanwhile, in electrochemical method, electrode material is very important point to be noticed as an important part to create the suitable system, which has high performance and efficiency for CO_2 electrochemical reduction. Recently, boron doped diamond (BDD), that has been widely used for sensor or synthesis application [5,6], has also been utilized for CO_2 reduction [7-9]. Its low background current may suppress the production of H_2 gas that has been known as a CO_2 reduction competitor. Moreover, BDD has high mechanical and chemical stability that may lead for practical application. However, a drawback is still existed due to its high over potential required for the process. Many attempts have been reported, especially by metal modification on BDD surface [10,11]. This method may decrease the over potential, and even more, producing higher chain of carbon compound, that is hardly produced only on bare BDD electrode.

Moreover, the study of CO_2 electrochemical reduction on metal-oxide electrode is attractive, since it has been found that possibly giving other activity and selectivity on products distribution [12]. A mixed metal transition oxide electrode has been reported to have an activity for methanol production in a low current density [13]. Therefore, in this thesis, metal oxide form of Ir and Ni metal deposited on BDD electrode were tried for its activity toward CO_2 reduction. Meanwhile, recently, Iridium-based catalyst were reported for CO_2 reduction [14,15]. The reported results were succeed to convert CO_2 to formate. Following this, the modification of Iridium on surface of BDD electrode is desired to give catalytic effect and active for CO_2 reduction. Meanwhile, several applications using iridium modified on surface of BDD electrode has been reported, especially for sensor application [16-18]. However, there was no report related for CO_2 electrochemical reduction application. In addition, Ni metal has been known to have low activity for CO_2 reduction, since it mainly produces H_2 gas. Therefore, by modify it to its oxide form, an activity for CO_2 reduction was desired, as well as for Ir. Therefore, for the first time, the oxide/hydroxide form of iridium and nickel metal were modified on surface of BDD (IrO_2-BDD) electrode, and applied for CO_2 reduction, desired to decrease the over potential, or else, for a new finding of other useful chemicals.

2. Experimental

2.1 Chemicals

All reagents were purchased from Wako Pure Chemical Industries, and were used without any further purification. Ultra-pure water was obtained from a Symply-Lab water system (Direct-Q UV3, Millipore).

2.2 Preparation of $Ni(OH)_2$ electrode

BDD electrode was prepared by depositing the films onto Si (111) wafers using microwave plasma-assisted chemical vapor deposition system. (Model 5400, CORNES Technology Corp.) [19]. The deposition was carried out electrochemically in 10 ml of 0.1 M acetate buffer pH 5 containing 1 mM $Ni(NO_3)_2$. The electrodeposition was carried out using pulse chronoamperometry at potential -1.2 V for 5 seconds followed by applying potential -0.2 V for 0.2 secons (for 50 times repetition). The modified BDD electrodes were then rinsed with water and dried under N_2 gas and used for application as a fresh nickel modified BDD electrode (Ni-BDD). To prepare the oxide/hydroxide form of nickel modified BDD electrode, the step was followed by annealing at high temperature (300, 500, 800^{o}C) for 30 minutes ($Ni(OH)_2$-BDD). Moreover, the modified electrodes were recovered by immersion in an aqua regia solution for 10 minutes followed by ultrasonication in ultrapure water for 15 minutes. Electrode characterization was performed using X-ray photoelectron spectroscopy (XPS), scanning electron microscopy (SEM) (JCM-6000, JEOL).

2.3 Preparation of the IrO_2 electrode

The iridium-contained solution was prepared before the electrochemical deposition on surface of BDD (B/C 1%) electrode that has been prepared as described in previous report [19]. 0.5 mM Na_2IrCl_6 was dissolved in 0.1 M KNO_3 solution (ratio v/v 1:1) (deep reddish-black color). The solution was heated at 80°C for 1 hour, while adding the ethanol (approx. 100 µl) several times in it until no color changed was observed (light brown color). The heating was continued for another 15 minutes to evaporate the excess ethanol. The solution was cooled down at room temperature afterward. This solution can be stored for a long time. Prior the using, the solution was purge with N_2 gas for 15 minutes under stirring condition and added by 0.5 M KOH until pH 10.5 (pale yellow color). This solution thus ready to use for electrochemical deposition [18,20].

A pretreatment of BDD electrode was carried out prior the deposition by cyclic voltammetry (CV) scans from -3.5 V to 3.5 V for 20 cycles with scan rate of 1 V/s. The electrochemical deposition was then carried out to prepare several IrO_2 modified on BDD electrodes (IrO_2-BDD) using the prepared pale yellow solution, by applying CV from 0.2 V to 1.2 V for several cycles, 10 (IrO_2-BDD-A), 20 (IrO_2-BDD-B), 30 (IrO_2-BDD-C), 40 (IrO_2-BDD-D), 50 (IrO_2-BDD-E), 200 (IrO_2-BDD-F) cycles at scan rate of 0.1 V/s. The reaction is stated as follow (eqn. (1)):

$$Ir_2O_3.xH_2O_{(aq)} + 2OH^- \rightarrow 2IrO_2.xH_2O_{(s)} + H_2O + 2e^- \qquad (1)$$

The modified electrodes were then characterized using scanning electron microscopy (SEM) (JCM-6000, JEOL), and x-ray photoelectron spectroscopy (XPS) (JPS-9010TR, JEOL).

2.4 Electrochemical CO_2 reduction and products analysis

The electrochemical reductions of CO_2 were carried out in 2 compartment cells separated by Nafion membrane. For CO_2 electrochemical reduction on IrO_2-BDD electrode, each cell contained 15 mL of solution, in which, 0.1 M Na_2SO_4 as anolyte and 0.1 M NaCl as catholyte. Whereas for nickel modified BDD electrode, each cell contained 15 mL of solution, in which, 0.5 M KCl as catholyte, and 0.5 M KOH as anolyte. BDD, IrO_2-BDD, Ni-BDD, or $Ni(OH)_2$-BDD were used as a working electrode, Pt mesh for counter electrode and Ag/AgCl for reference electrode. All potentials were measured against Ag/AgCl (3M NaCl) unless otherwise stated. The N_2 gas was purged for 15 minutes in 100 sccm, followed by CO_2 gas for the same time and flow rate before each potentiostatic electrochemical reduction of $CO_{2,}$ which are carried out for 1 hour under stirring condition. CO_2 gas was flow into the cell with low flow rate to maintain the CO_2 concentration during reduction process. All the electrochemical measurements were conducted by using potentiostat (Autolab PGSTAT204, Metrohm Autolab B.V).

The gas products were collected in one liter gas bag connected to the compartment cell, whereas liquid product was sampled from the catholyte by taking 1 mL sample from the catholyte. Both of the samples were analyzed after the reduction. The gas products were analyzed by gas chromatography with a flame ionization detector and a thermal conductivity detector (GC-2014, Shimadzu Corp.). The liquid was analyzed using high performance liquid chromatography (HPLC) with an electroconductivity detector (Prominence, Shimadzu Corp.).

3. Results and Discussion

3.1 CO_2 electrochemical reduction on nickel modified BDD electrode

3.1.1 Characterization of nickel modified BDD electrode

SEM image of each nickel modified BDD electrode are shown in Figure 1. The increasing of particles size after annealing treatment could be observed. In addition, the surface of BDD electrode was found to have holes. However, it did not show any damages on sp^3 structure of the diamond. However, it is suggested that the high annealing temperature is not preferable.

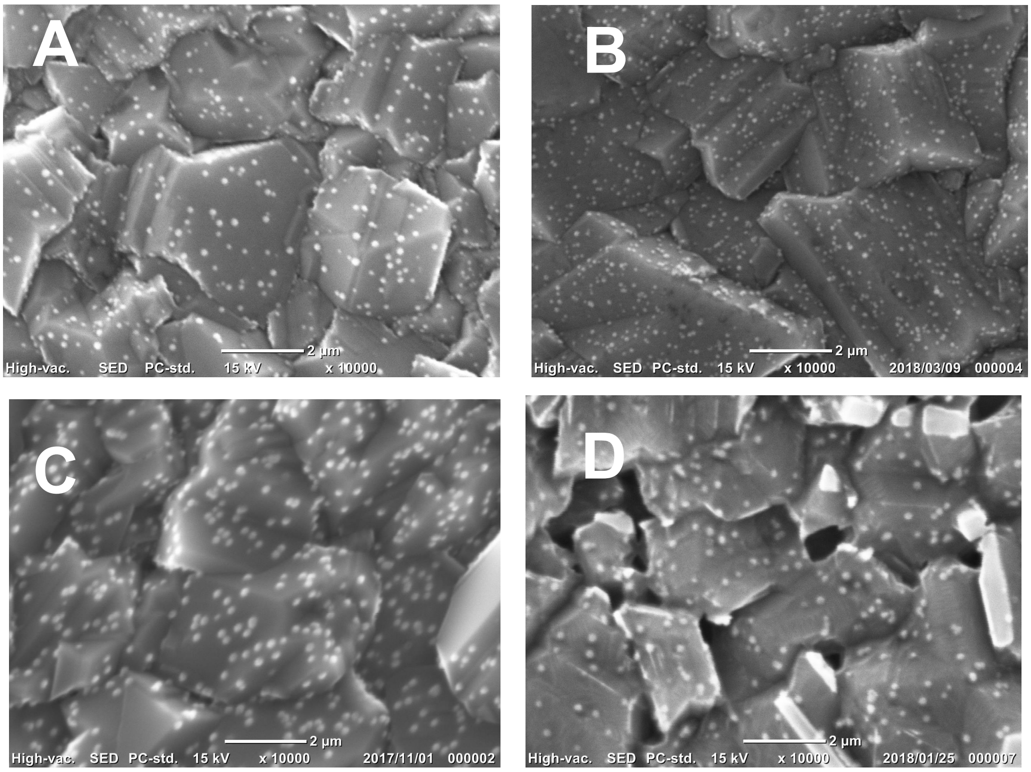

Figure 1. SEM images of Ni-BDD (A) and $Ni(OH_2)_2$ annealed at 300°C (B) 500°C (C) and 800°C (D)

Beside the SEM image, the XPS analysis (narrow scan) was carried out to understand whether the deposited nickel was metallic form or in its oxide form. In Figure 2 we can see that the as deposited Ni-BDD shows 2 peaks that belong to the nickel metallic at binding energy 852.7 eV, and the peak at binding energy of 855 eV that belong to $Ni(OH)_2$. Since the peak was relatively broadening, the NiO species might also exist. The $Ni(OH)_2$-BDD electrode annealed in all various temperatures show the diminish of Ni metallic peak. Therefore, it is concluded that by annealing treatment, the deposited metallic nickel particles were oxidized whether in its oxide/hydroxide form.

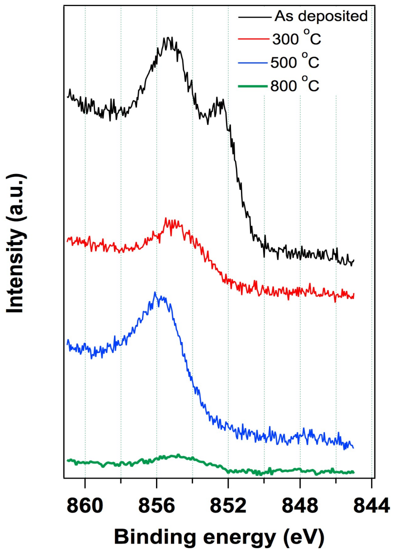

Figure 2. XPS spectra (narrow scan) of as deposited and annealed nickel modified BDD electrode

Cyclic voltammetry was also performed in 0.5 M KCl solution for all electrodes. Unfortunately, it is difficult to understand completely the behavior of each electrode from the voltammogram. However, the starting point for hydrogen evolution on annealed electrode seems to be more negative compare to the as deposited nickel modified BDD electrode (Figure 3). Thus, to know the activity of the electrodes, we carried out directly the CO_2 electrochemical reduction using all those modified electrodes.

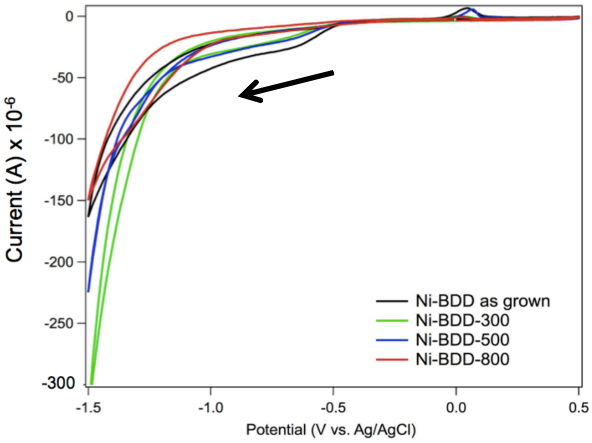

Figure 3. CV performance of as deposited and annealed nickel modified BDD electrode in 0.5 M KCl solution, scanned from potential 0.5 V to -1.5 V *vs.* Ag/AgCl after N_2 and CO_2 bubbling. The scan rate was 100 mV/s.

3.1.2 CO_2 electrochemical reduction performance

The products efficiency for CO_2 electrochemical reduction on each annealed electrode are summarized in Table 1-3. The product for HCOOH, CO, CH_4, and H_2 was calculated. The reductions were carried out for several potential reductions from potential -0.8 V to -1.3 V. The potential was kept at lower potential, as the purpose of this metal modification is lowering the overpotential of using only bare BDD electrode. Therefore, we expect the useful products produced at lower potential.

Table 1. Faradaic efficiency of products from CO_2 electrochemical reduction on $Ni(OH)_2$-BDD electrode annealed at temperature 300°C

Potential V vs. Ag/AgCl	C	Faradaic Efficiency (%)					
		HCOOH	CO	CH_4	H_2	TOTAL	Total CO_2 Reduction
-0.8	0.10	0	0	0	102.3	102.3	0
-1.0	0.34	2.6	0	2	54.5	59.1	4.6
-1.1	0.57	0	0	0	58.3	59	0.7
-1.2	0.12	4.1	1.8	9.5	103	118.4	15.4
-1.3	0.33	1.5	0.9	2.9	44.9	50.2	5.3

Table 2. Faradaic efficiency of products from CO_2 electrochemical reduction on $Ni(OH)_2$-BDD electrode annealed at temperature 500°C

Potential V vs. Ag/AgCl	C	Faradaic Efficiency (%)					
		HCOOH	CO	CH_4	H_2	TOTAL	Total CO_2 reduction
-0.8	0.08	0	0	0	100	100	0
-1.0	0.20	0	0	4.5	67.5	72	4.5
-1.1	0.18	0	0	0	63.3	63.3	0
-1.2	0.52	0	0	0	36.7	36.7	0
-1.3	0.54	0	0	0	55.9	55.9	0

Table 3. Faradaic efficiency of products from CO_2 electrochemical reduction on $Ni(OH)_2$-BDD electrode annealed at temperature 800°C

Potential V vs. Ag/AgCl	C	Faradaic Efficiency (%)					
		HCOOH	CO	CH_4	H_2	TOTAL	Total CO_2 reduction
-0.8	0.10	3.2	0	12.7	94.9	110.8	15.9
-1.0	0.39	0.98	0	2.5	25.85	29.33	3.48
-1.1	0.108	8.3	2.1	7.8	100	118.2	18.2
-1.2	0.15	0	1.4	7.1	75.1	83.6	8.5
-1.3	0.23	3.4	1.7	5.2	64.6	74.9	10.3

However, the trend was far difficult to explain. The CO_2 reduction efficiency was far so low compared to the hydrogen production. It is suggested that the surface of the electrode was passivized after annealing treatment, the epitaxial lattice structure was assumed to be formed as has been studied by Gao, et al [21]. Therefore, activation to the electrode using cyclic voltammetry/chronoamperometry after annealing treatment is suggested. Moreover, we observed the reduction of $Ni(OH)_2$ species during the electrochemical reduction of CO_2, as the XPS peak shows the shifting of $Ni(OH)_2$ peak after reduction at potential -1.1 V and -1.3 V on $Ni(OH)_2$-BDD electrode with 500^{o}C annealing treatment (Figure 4), that may cause the less overall total faradaic efficiency.

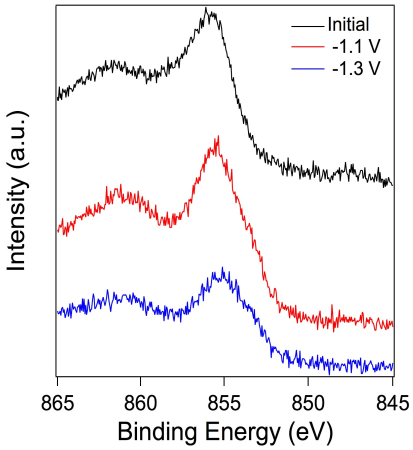

Figure 4. XPS spectra of $Ni(OH)_2$-BDD electrode annealed at 500^{o}C, before and after CO_2 electrochemical reduction at potential -1.1 V and -1.3 V *vs.* Ag/AgCl during 2 hours

In addition, since we could not find any satisfying result on the oxide/hydroxide form of nickel modified on BDD electrode, we performed the CO_2 electrochemical reduction on as deposited BDD electrode. The reduction was started at low potential -1.3 V. However, the activity was poor. Thus, we increased the potential reduction up to -2 V. However, again the product was dominated by hydrogen evolution (Table 4). Therefore, the final conclusion was determined, that nickel modified BDD electrode was not suitable enough for CO_2 electrochemical reduction performance. It is suggested that the combination of other metal, such as Cu will improve the overall performance for future experiment.

Table 4. Faradaic efficiency of products from CO_2 electrochemical reduction on as deposited Ni-BDD electrode

Potential V vs. Ag/AgCl	C	Faradaic Efficiency (%)					
		HCOOH	CO	CH_4	H_2	Total	Total CO_2 reduction
-1.3	0.81	4.31	0.6	1.29	46.9	53.14	6.20
-1.4	0.54	0	0.99	1.66	91.44	94.09	2.65
-1.5	0.96	4.9	3.21	1.54	90.22	99.91	9.65
-1.6	11.10	0.35	0.05	0.06	106.63	107.09	0.46
-1.7	16.94	0.24	0.12	0.08	96.62	97.06	0.44
-1.8	19.52	0.53	0.23	0.09	95.63	96.47	0.85
-2.0	40.31	0.83	0.31	0.06	97.4	98.6	1.20

3.2 CO_2 electrochemical reduction on IrO_2-BDD electrode

3.2.1 Characterization of IrO_2-BDD electrode

A simple CV performance was applied for modified BDD electrodes, in order to ensure the deposition of IrO_2 on surface of BDD electrodes (Figure 5). The CV was performed from potential -1.5 V to 1.2 V in 0.1 M NaCl solution. As we can see, in this potential range, the bare BDD electrode does not shows any peaks. However, IrO_2-BDD electrodes show the oxidation peak at around potential 0.7 V, increases as the amount of deposition CV cycles was increased. It shows that the amount of deposited IrO_2 is increased. This result is also linear to the previous works [18,20].

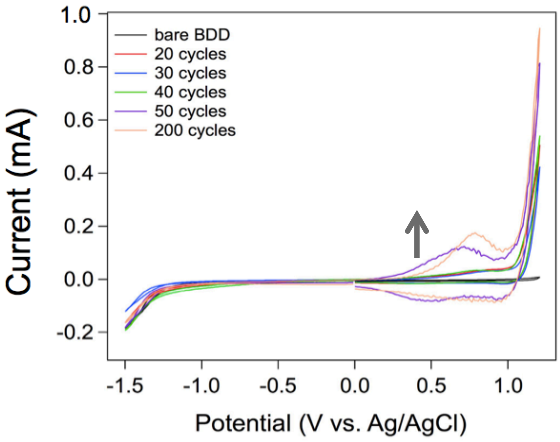

Figure 5. CVs of IrO_2-BDDE electrodes with different amount of deposition CV cycles. The CVs were performed from potential -1.5 V to 1.2 V in 0.1 M NaCl solution with scan rate 100 mV/s.

Beside the CV performance, the elemental characterization of IrO_2-BDD electrode was carried out using XPS. Figure 6 shows the wide scan of XPS spectra. The IrO_2 peak was observed after electrochemical deposition. The narrow scan shows a detailed peak of IrO_2 $4f_{7/2}$ at binding energy 62 eV, and IrO_2 $4f_{5/2}$ at binding energy 65 eV. The peak was not shifted even after reduction, explaining that the oxide form of iridium was not significantly reduced and remained stable after electrochemical reduction.

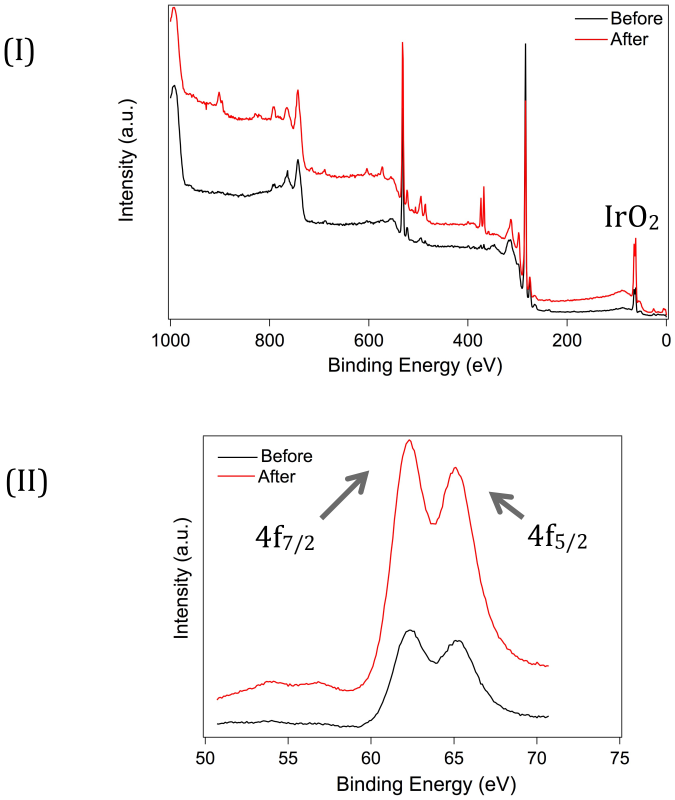

Figure 6. (I) Wide scan and (II) narrow scan of XPS spectra of IrO_2-BDDE, before and after CO_2 electrochemical reduction at potential -1.7 V

The morphology of IrO_2-BDD electrodes was examined by SEM analysis. The deposited IrO_2 particles was confirmed and noted as a spherical white dote. The amount of the particles is increased as the deposition CV cycles are increased (Figure 7 (I-VI).

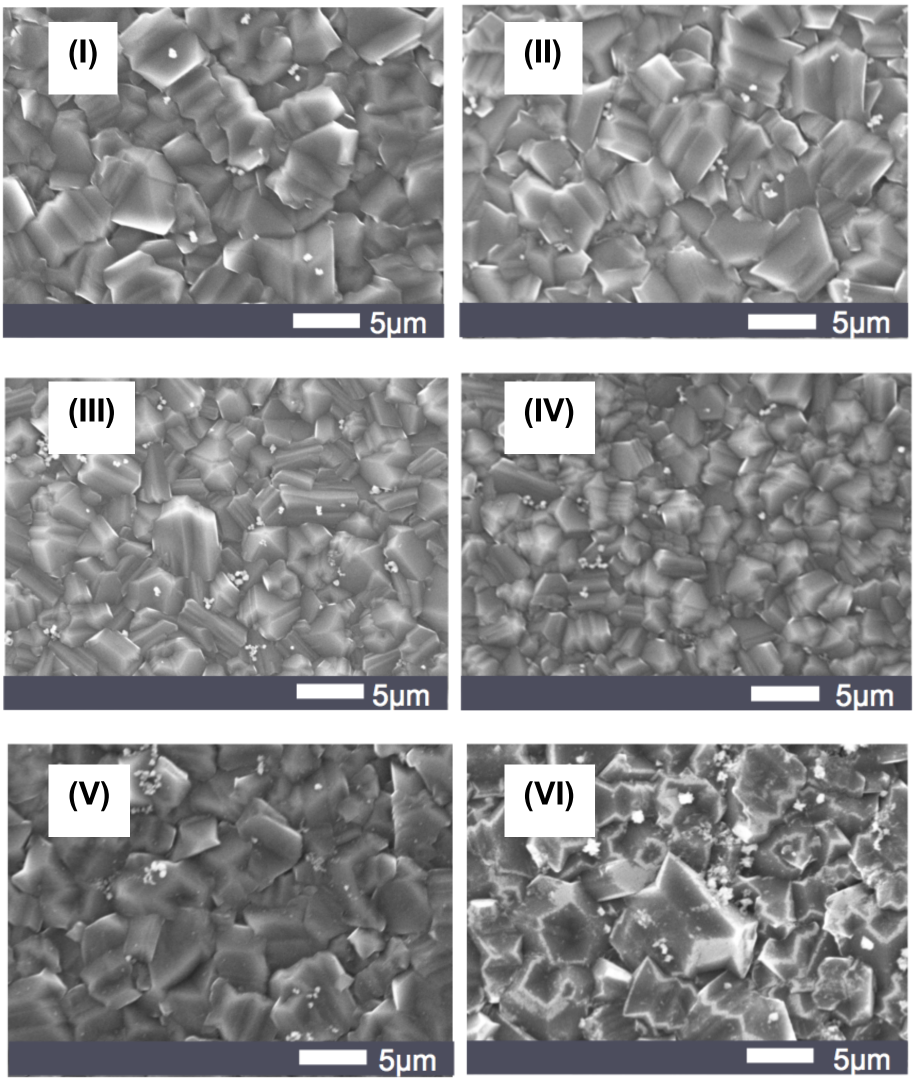

Figure 7. SEM images of IrO_2-BDD electrodes. (I) IrO_2-BDD-A (II) IrO_2-BDD-B (III) IrO_2-BDD-C (IV) IrO_2-BDD-D (V) IrO_2-BDD-E (VI) IrO_2-BDD-F

3.2.2 CO_2 electrochemical reduction

Firstly, CV performance was conducted on IrO_2-BDD after N_2 and CO_2 bubbling from potential -1.5 V to 1.0 V. As we can see from Figure 8, after CO_2 bubbling, the reduction peak was shifted to more positive potential, explaining that the hydrogen evolution is occurred earlier. It could be explained, due to the lower pH measured after CO_2 bubbling (around pH 4), based on this reactions (Eq. (1)(2)):

$$CO_{2(aq)} + H_2O_{(l)} \rightleftarrows H_2CO_{3(aq)} \quad (1)$$

$$H_2CO_{3(aq)} \rightleftarrows H^+_{(aq)}\ HCO_3^-{}_{(aq)} \quad (2)$$

The bubbling of CO_2 leads to the H^+ production, thus the amount of H^+ increases and increasing the rate of hydrogen evolution.

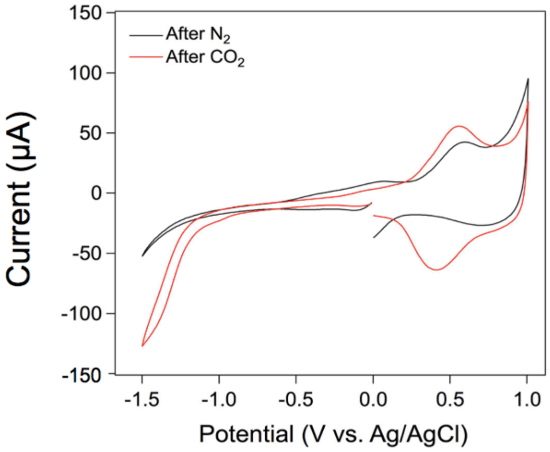

Figure 8. CV performance of IrO_2-BDD-E in 0.1 M NaCl solution, after N_2 and CO_2 bubbling, conducted at the potential -1.5 V to 1.0 V with scan rate 100 mV/s.

The modified BDD electrodes were then applied for CO_2 electrochemical reduction on each modified electrode at potential -1.7 V during 1 hour (Figure 9A). HCOOH and CO were produced as the main products. The faradaic efficiency of HCOOH is increased, as the deposition CV cycles are longer and remained stable after 50 cycles deposition. Thus, IrO_2-BDD-E was used for further study. For comparison, the previous study on CO_2 electrochemical reduction on bare BDD (B/C 1%) required a higher potential around -2.3 V to produce HCOOH with faradaic efficiency around 50% [22]. This work was successfully reducing the applied potential to -1.7 V to possibly produce the product efficiency around that value.

(A)

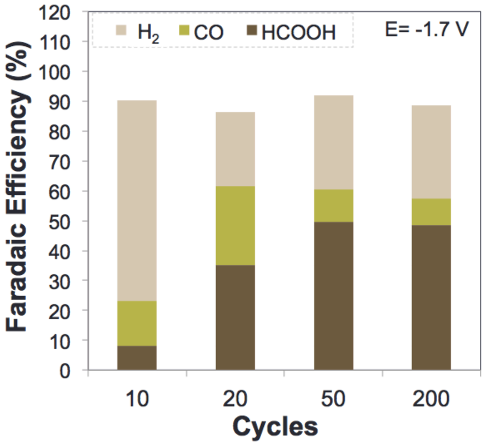

(B)

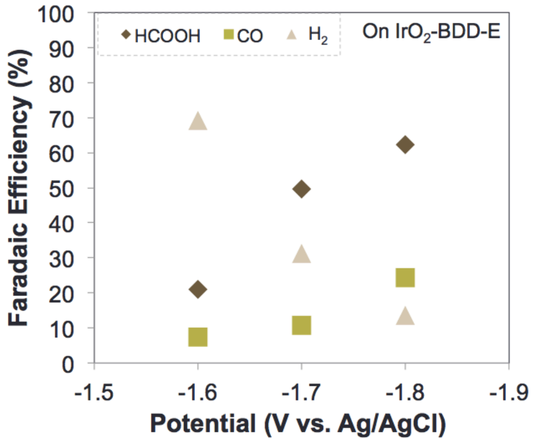

Figure 9. Faradaic efficiency of products on IrO_2-BDD with different (A) number of CV cycles and (B) potential reduction

The CO_2 electrochemical reduction was also carried out on IrO_2-BDD-E at potential -1.6 V and -1.8 V to show the dependence of applied potential clearly toward the product efficiency (Figure 9B). At the potential -1.6 V, the H_2 production was dominant than CO_2 reduction. This result is vise-versa to the result at potential -1.8 V, in which, the efficiency of CO_2 reduction is higher compare to H_2 production. The efficiency of HCOOH is increases as the potential increased.

In addition, the repeatability of the HCOOH production at potential -1.7 V on IrO_2-BDD-E was evaluated (Figure 10A). The production of HCOOH was produced in the range of 42% to 52%. Beside the stability of the modified electrode is also an important part to be considered for practical application. The SEM image shows that the deposited IrO_2 still remained on the surface of BDD electrode after electrolysis. Thus, the stability of the modified electrode was achieved (Figure 10B).

(A)

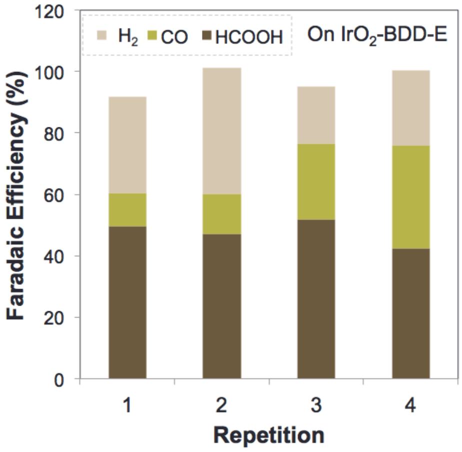

(B)

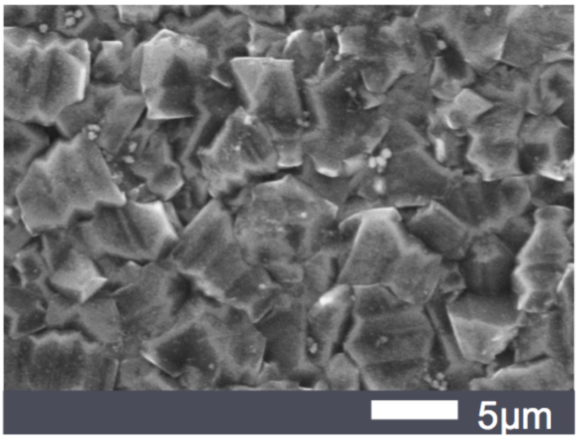

Figure 10. (A) The repeatability of HCOOH production at potential -1.7 V on IrO$_2$-BDD-E electrode. (B) The SEM image of IrO$_2$-BDD-E electrode after one hour reduction at potential -1.7 V

4. Conclusions

1. The electrochemical reductions of CO$_2$ on as deposited and annealed nickel modified BDD electrode were carried out at various potential reduction. The annealed electrode activity was poor, suggesting that the electrode activation is needed after the annealing treatment. Moreover, as deposited Ni-BDD was active for hydrogen production rather than the CO$_2$ reduction. Thus, for future experiment, it is not suggested to use the single metal, nickel modified BDD, however combining with other metal will improve the activity for CO$_2$ reduction itself.
2. Various IrO$_2$-BDD electrodes with different CV cycles for electrode preparation have been successfully fabricated. The CO$_2$ electrochemical reduction products were HCOOH and CO. The faradaic efficiency of HCOOH could be improved by

the lower applied potential compare to the previous results on bare BDD (B/C 1%) electrode. Finally, stability test for longer electrolysis and also improving the CO_2 reduction efficiency on metal modified BDD electrode is worth more studies as one of the effort to reduce the overpotential of CO_2 reduction on bare BDD electrode.

5. References

[1] S. Willie, L.B. Sallie, B.R. Arthur, W.R. Zachary, Environmental effects of increased atmospheric carbon dioxide, Clim. Res. 13 (1999) 149–164.

[2] T. Adit Maark, B.R.K. Nanda, CO and CO_2 Electrochemical Reduction to Methane on Cu, Ni, and Cu3Ni (211) Surfaces, J. Phys. Chem. C. 120 (2016) 8781–8789.

[3] G. Keerthiga, R. Chetty, Electrochemical Reduction of Carbon Dioxide on Zinc-Modified Copper Electrodes, J. Electrochem. Soc. 164 (2017) H164–H169.

[4] Y. Lum, J.W. Ager III, Sequential catalysis controls selectivity in electrochemical CO_2 reduction on Cu, Energy Environ. Sci. 11 (2018) 2935–2944.

[5] T.A. Ivandini, J. Ariani, P.K. Jiwanti, J. Gunlazuardi, E. Saepudin, Y. Einaga, Electrochemical Detection of Neuraminidase Based on Zanamivir Inhibition Reaction at Platinum and Platinum-Modified Boron-Doped Diamond Electrodes, Makara J. Sci. 21 (2017) 34–42.

[6] T.A. Ivandini, Y. Einaga, Polycrystalline boron-doped diamond electrodes for electrocatalytic and electrosynthetic applications, Chem. Commun. 53 (2017) 1338–1347.

[7] P.K. Jiwanti, K. Natsui, Y. Einaga, The Utilization of Boron-doped Diamond Electrodes for the Electrochemical Reduction of CO_2: Toward the Production Compounds with a High Number of Carbon Atoms, Electrochemistry 2 (2019) 109–113.

[8] K. Natsui, H. Iwakawa, N. Ikemiya, K. Nakata, Y. Einaga, Stable and Highly Efficient Electrochemical Production of Formic Acid from Carbon Dioxide Using Diamond Electrodes, Angew. Chemie - Int. Ed. 57 (2018) 2639–2643.

[9] K. Nakata, T. Ozaki, C. Terashima, A. Fujishima, Y. Einaga, High-yield electrochemical production of formaldehyde from CO_2 and seawater, Angew. Chemie - Int. Ed. 53 (2014) 871–874.

[10] P.K. Jiwanti, K. Natsui, K. Nakata, Y. Einaga, The electrochemical production of C_2/C_3 species from carbon dioxide on copper-modified boron-doped

diamond electrodes, Electrochim. Acta. 266 (2018) 414–419.

[11] N. Roy, N. Suzuki, Y. Nakabayashi, Y. Hirano, K. Katsumata, K. Nakata, A. Fujishima, C. Terashima, H. Ikari, Facile Deposition of Cu-SnOx Hybrid Nanostructures on the Lightly Boron-Doped Diamond Electrodes for CO_2 Reduction, ChemElectroChem. 5 (2018) 2542–2550.

[12] E. Tayyebi, J. Hussain, Y. Abghoui, E. Skúlason, Trends of Electrochemical CO_2 Reduction Reaction on Transition Metal Oxide Catalysts, J. Phys. Chem. C. 122 (2018) 10078–10087.

[13] A. Bandi, J. Schwarz, C.U. Maier, Adsorption of CO_2 on Transition Metals and Metal Oxides, J. Electrochem. Soc. 140 (1993) 1006.

[14] P. Kang, C. Cheng, Z. Chen, C.K. Schauer, T.J. Meyer, M. Brookhart, Selective electrocatalytic reduction of CO_2 to formate by water-stable iridium dihydride pincer complexes, J. Am. Chem. Soc. 134 (2012) 5500–5503.

[15] I. Osadchuk, T. Tamm, M.S.G. Ahlquist, Reduced State of Iridium PCP Pincer Complexes in Electrochemical CO_2 Hydrogenation, ACS Catal. 6 (2016) 3834–3839.

[16] M. Khalil, S. Wang, J. Yu, R.L. Lee, N. Liu, Electrodeposition of Iridium Oxide Nanoparticles for pH Sensing Electrodes, J. Electrochem. Soc. 163 (2016) B485–B490.

[17] T.A. Ivandini, R. Sato, Y. Makide, A. Fujishima, Y. Einaga, Electrochemical detection of arsenic(III) using indium-implanted boron-doped diamond electrodes, Anal. Chem. 78 (2006) 6291–6298.

[18] A. Salimi, M.E. Hyde, C.E. Banks, R.G. Compton, Boron doped diamond electrode modified with iridium oxide for amperometric detection of ultra trace amounts of arsenic(III), Analyst. 129 (2004) 9–14.

[19] T. Yano, D.A. Tryk, K. Hashimoto, A. Fujishima, Electrochemical Behavior of Highly Conductive Boron-Doped Diamond Electrodes for Oxygen Reduction in Alkaline Solution, J. Electrochem. Soc. 145 (1998) 1870–1876.

[20] J.E. Baur, T.W. Spaine, Electrochemical deposition of iridium (IV) oxide from alkaline solutions of iridium(III) oxide, J. Electroanal. Chem. 443 (1998) 208–216.

[21] F. Gao, N. Yang, C.E. Nebel, Highly stable platinum nanoparticles on diamond, Electrochim. Acta. 112 (2013) 493–499.

[22] J. Xu, K. Natsui, S. Naoi, K. Nakata, Y. Einaga, Effect of doping level on the electrochemical reduction of CO_2 on boron-doped diamond electrodes, Diam. Relat. Mater. 86 (2018) 167–172.

6

Chapter

Summary and Future Perspective

1. Summary

The increasing of CO_2 emission from the combustion of fossil fuels has attracted high attention due to its negative impact. Attempts have been made to reduce emission or the emitted-CO_2 gas itself in atmosphere, by using carbon capture and storage technology, or else, by converting to added-value chemicals incorporation to the renewable energy system. One of the efforts is utilizing the electricity to convert CO_2 to more valuable compound, through electrochemistry system. As in electrochemistry, a suitable electrodes and an adequate whole system is needed. This thesis is focusing on the utilization of so called boron-doped diamond (BDD) electrode, as the new material studied in CO_2 reduction area.

First of all, in chapter 1, the broad perspective and current condition of greenhouse gas and carbon cycle is briefly discussed. The effort of reducing CO_2 emission and the motivation of using BDD electrode as an electrode for the designed electrochemistry system is explained.

In chapter 2, we present the first study on CO_2 reduction on bare BDD electrode using aqueous ammonia solution. Methanol has been successfully produced. The attempt to improve the product efficiency is discussed. Finally, the use of aqueous ammonia solution is mandatory to improve the production of methanol, compare to the use of other electrolytes. The pH of the solution is also one of the important parts to be considered to possibly producing methanol.

In chapter 3, we shifted the focus on improving the electrocatalytic activity of bare BDD electrode and focusing on the production of higher number of carbon atom compounds. Metal modification on surface of BDD electrode, especially using copper, was carried out and successfully producing C_2/C_3 species with quite satisfying efficiency compare to the use of only bare copper metal.

Whereas in chapter 4, the study on metal modified BDD electrode was continued. Palladium was chosen to be the metal that was deposited, since it is a well-known metal catalyst, other than its ability to be active for CO_2 reduction. The result shows the improvement of CO production that used to be a side product on bare BDD electrode. The appropriate amount of deposited palladium particles, and also the applied potentials are needed to optimize the efficiency of CO production.

The last chapter is discussing about the CO_2 electrochemical reduction on other metal particles modified on BDD electrode. Ni and Ir, including its oxide formed were researched. It has been known that the oxide form of the metal will have different behavior, or else, improving the efficiency and selectivity. However, some negative result was also observed using nickel, since H_2 evolution dominates the overall reaction. Meanwhile, the oxide form of iridium modified on BDD electrode may improve the production of formic acid.

Finally, the summary of CO_2 reduction on the metal modified BDD electrode from this work, in comparison to metal electrode [1,2] is presented in Table 1.

Table 1. CO_2 reduction products faradaic efficiency on various metal modified BDD and metal electrodes

	Potential (V vs. Ag/AgCl)	**Products Faradaic Efficiencies (%)**							
		CH_4	C_2H_4	Ethanol	Acetal-dehyde	Acetone	CO	HCOOH	H_2
Cu	-1.64	33.3	25.5	5.7	1.1	-	1.3	9.4	20.5
CuBDD	-1.0	-	-	42.4	14.7	7	-	-	-
Pd	-1.4	2.9	-	-	-	-	28.4	2.8	26.2
PdBDD	-1.6	-	-	-	-	-	53.3	9.3	39.9
Ni	-1.68	1.8	0.1	-	-	-	-	1.4	88.9
NiBDD	-1.5	1.54	-	-	-	-	3.21	4.90	90.22
Ir	-								~100
IrBDD*	-1.7	-	-	-	-	-	24.5	52	18.69

2. Future Perspective

Along the story of many efforts that has been addressed for CO_2 reduction to value-added chemicals, the improvement of the design system and a finding of new catalytic system are still widely researched. Electrochemical method is one of the methods that taken into account as the way to overcome the unstable classic renewable energy system. In which, this method uses electrical energy with possibly the customizable condition, including potential dependence and an ambient temperature and pressure. Therefore, it is assumed that this method still becomes a promising method, specifically for designing a CO_2 reduction with a desired product efficiency and selectivity.

However, through many years research activity on CO_2 electrochemical reduction, a wide commercial industrial application is still not existed. In this point, BDD electrode might become a good material due to its inner nature, wide potential window and high mechanical and chemical stability. The challenge is its high over-potential to produce quantifiable amount of products, in which, it has a high correlation with the production cost. Therefore, a modification should be applied for BDD electrode, with the provision of maintaining the activity of BDD itself. A small modification of metal thus may promote a higher activity of BDD electrode. Beside, a modification with active functional group might also be able to be applied in the future. Despite of its exceptional ability as a support electrode, a very stable and inert BDD surface remains a challenge for a stable metal modification. Thus, the improvement of modification technique is highly suggested to study. In addition, a focus on the mechanism of CO_2 electrochemical reduction using bare or modified BDD electrode is not yet understood. Therefore, a surface study on the electrode during CO_2 reduction is also need.

3. References

[1] Y. Hori, H. Wakebe, T. Tsukamoto, O. Koga, Electrocatalytic process of CO selectivity in electrochemical reduction of CO_2 at metal electrodes in aqueous media, Electrochem. Commun. 39 (1994) 1833–1839.

[2] J. L. White, M.F. Baruch, J.E. Pander, Y. Hu, I.C. Fortmeyer, J.E. Park, T. Zhang, K. Liao, J. Gu, Y. Yan, T.W. Shaw, E. Abelev, A.B. Bocarsly, Light-Driven Heterogeneous Reduction of Carbon Dioxide: Photocatalysts and Photoelectrodes, Chem. Rev. 115 (2015) 12888–12935.

List of Publications and Conferences

Published paper presented in this thesis

Selective production of methanol by the electrochemical reduction of CO_2 on boron doped diamond electrodes in aqueous ammonia solution
P.K. Jiwanti, K. Natsui, K. Nakata, Y. Einaga, *RSC Adv.* **2016**, 6, 102214.

The electrochemical production of C_2/C_3 species from carbon dioxide on copper-modified boron-doped diamond electrodes
P.K. Jiwanti, K. Natsui, K. Nakata, Y. Einaga, *Electrochimica Acta.* **2018**, 266, 414.

Electrochemical reduction of CO_2 using palladium modified boron doped diamond electrode: enhancing the production of CO
P.K. Jiwanti, Y. Einaga, *Phys. Chem. Chem. Phys,* **2019**, DOI: 10.1039/C9CP01409H. **[HEADLINE IN BACK COVER]**

Other publications

The Utilization of boron-doped diamond electrodes for the electrochemical reduction of CO_2: toward the production compounds with a high number of carbon atoms
P.K. Jiwanti, K. Natsui, Y. Einaga, *Electrochemistry*, **2019**, 87, 109. **[HEADLINE PAPER]**

Electrochemical detection of neuraminidase based on zanamivir inhibition reaction at platinum modified boron doped diamond electrode
T.A. Ivandini, J. Ariani, P.K. Jiwanti, J. Gunlazuardi, E. Saepudin, Y. Einaga, *Makara J Sci,* **2017**, DOI: 10.7454/mss.v21i1.7535.

Electrochemical behavior of Zanamivir at gold-modified boron-doped diamond electrodes for an application in neuraminidase sensing
W.T. Wahyuni, T.A. Ivandini, P.K. Jiwanti, E. Saepudin, J. Gunlazuardi, Y. Einaga, *Electrochemistry*, **2015**, 83, 357-362.

Electrochemical oxidation of palmitic acid solution using boron-doped diamond electrodes
S. Muharam, P.K. Jiwanti, Irkham, J. Gunlazuardi, Y. Einaga, T.A. Ivandini, *Diam. Relat. Mater,* **2019** (Accepted)

Conferences

1. CO_2 reduction on boron-doped diamond electrode in aqueous ammonium hydroxide solution.
   P.K. Jiwanti, K. Natsui, K. Nakata, Y. Einaga
   PRiME on electrochemical and solid state science, Honolulu Hawaii, 2016, *oral presentation*
2. Selective production of methanol by the electrochemical reduction of CO_2 on boorn doped diamond electrodes in aqueous ammonia solution
   P.K. Jiwanti, K. Natsui, K. Nakata, Y. Einaga
   Diamond symposium, Japan, 2016, *oral presentation*
3. The production of C_2/C_3 species from CO_2 electrochemical reduction on copper modified boron doped diamond electrode
   P.K. Jiwanti, K. Natsui, K. Nakata, Y. Einaga
   27th international conferences on researches in science and technology (ICRST), Bangkok Thailand, 2017, *oral presentation*
4. The electrochemical production of C_2/C_3 species from carbon dioxide on copper-modified boron-doped diamond
   P.K. Jiwanti, K. Natsui, K. Nakata, Y. Einaga
   Diamond symposium, Japan, 2017, *oral presentation*
5. CO_2 electrochemical reduction on metal modified boron doped diamond electrode
   P.K. Jiwanti, K. Natsui, K. Nakata, Y. Einaga
   The 3rd international symposium on current progress in functional materials (ISCPFM), Indonesia, 2018, *oral presentation*
6. The electrochemical production of C_2/C_3 species from carbon dioxide on copper-modified boron-doped diamond
   P.K. Jiwanti, K. Natsui, K. Nakata, Y. Einaga
   Green and sustainable chemistry (JACI/GSC), Japan, 2018, *poster presentation*
7. Electrochemical deposition of palladium o BDD electrode for CO_2 electrochemical reduction to CO
   P.K. Jiwanti, Y. Einaga
   International symposium on diamond electrochemistry, Japan, 2019, *poster presentation*
8. CO_2 electrochemical reduction on palladium modified BDD electrode
   P.K. Jiwanti, Y. Einaga
   The 86th annual meeting on the electrochemical society of Japan, Japan, 2019, *oral presentation*
9. Copper-Nickel modified boron doped diamond electrode for CO_2 electrochemical reduction application: a preliminary study
   P.K. Jiwanti, R.P. Aritonang, I. Abdullah, Y. Einaga, T.A. Ivandini
   Makara International colloquium of science, Indonesia, 2019, *oral presentation*

Curriculum Vitae

Prastika Krisma Jiwanti was born in Trenggalek, Indonesia, in 1991. She finished her high school study in this city with satisfying result, that bring her to get a full-funded scholarship to pursue bachelor study in Department of Chemistry, Universitas Indonesia. To finish her bachelor study, she was supported by her supervisor to do a short research in Keio University, under the supervision of Prof. Einaga in 2013. Then, she could graduate with *cumlaude* predicate for 3.5 years, on February 2014, after presented her research result about Neuraminidase electrochemical sensing using gold modified BDD electrode.

After obtaining her bachelor degree in science, she decided to continue master study. While waiting for a master study, she worked in bioelectrochemistry research group in Universitas Indonesia and also became a teaching assistant for physical chemistry and electrochemistry classes. Finally, she was promoted by her previous scholarship for a full-funded Indonesia endowment fund for education (LPDP) scholarship, provided by the ministry of finance Republic of Indonesia, and continued her study to Keio University in September 2014. She did a research about CO_2 electrochemical reduction using BDD electrode in Prof. Einaga laboratory, and presented her results in several conferences. She was awarded as an excellent presenter in ICSREE South Korea in 2016.

Due to her interest in research, she continued directly for doctoral study in the same laboratory, supported by the same full-funded LPDP scholarship. She has been working in CO_2 electrochemical reduction especially on metal modified BDD electrode. During her study in doctoral degree, she produced several publications from research collaboration and also her own research topic for doctoral study. She also presented her results in national and International conferences.

Acknowledgment

All the glory and the highest gratitude to Jesus Christ, for all His blessings and grace. I would like to dedicate my works in this thesis to my beloved parent that always give me a mindset about what the important of education is, since I was young. I know that it must be difficult to take a part and let me flight far away to other country to pursue higher education. Thank you for the financial, emotional, and spiritual support through all the process I have passed until this moment. (*saya dedikasikan disertasi ini kepada kedua orang tua saya yang sejak dari saya kecil telah menanamkan pentingnya sebuah pendidikan. Saya memahami bahwa tidak mudah untuk berpisah dan melepas saya keluar negeri untuk menempuh pendidikan tinggi. Terimakasih untuk dukungan secara finansial, emosional dan spiritual dalam menjalani proses pendidikan dasar sampai dengan saat ini*). To my beloved sister, never give up, and always do your best.

To my advisor, Prof. Yasuaki Einaga, thank you very much for having me as your student in your laboratory for up to 5 years since I was in master course. Thank you for all the fruitful discussions, support, and motivation on dealing with difficulties in research. I always appreciated your patience and optimistic attitude that made me stronger during my study. I also thank you for Einaga's laboratory members and all the staffs. All the helps and togetherness are very important and meaningful for me personally. Thank you also for the friendship, I hope to be able to keep in touch with you all.

In addition, I would like to thank you to all the reviewers, Prof. Hiroshi Kondoh, Prof. Taku Hasobe, and Prof. Yuya Oaki for all the useful questions and comments, that I would be able to also see the other point of view of my research. I thank you for the revision of this PhD thesis that make it even better.

Outside the laboratory activity, I would like to say thank you for the people from GIII Tokyo. I am lucky and very happy to find a Church that could support me spiritually. Not only that, I could find friendship and learn many things about life in here. Moreover, thank you very much for the fellowship from Indonesian friends in Keio University. Moreover, thank you to a lovely person, Johannes, who personally keeps me positive and feel grateful in life.

I also thank you for Indonesia Endowment Fund for Education (LPDP) Scholarship that support my study for 5 years since I was in master course. I may not be able to finish my study until the highest degree without LPDP financial support. I believe, this is a very good program from the government of Indonesia for education, as one of the way for realizing Indonesia to be a developed country in the future.

At last, I hope that all the works written in this thesis gives a useful information for research generally and especially for the development of CO_2 electrochemical reduction study using BDD electrode.

Japan, July 2019

Prastika Krisma Jiwanti